Genome editing reveals reproductive and developmental dependencies on specific types of vitellogenin in zebrafish (Danio rerio)

Ozlem Yilmaz, Amélie Patinote, Thuy Thao Vi Nguyen, Emmanuelle Com, Charles Pineau, Julien Bobe

Title: Genome editing reveals reproductive and developmental dependencies on specific types of vitellogenin in zebrafish (*Danio rerio*)

Ozlem Yilmaz[1,3]*, Amelie Patinote[1], Thaovi Nguyen[1], Emmanuelle Com[2], Charles Pineau[2], Julien Bobe[1].

[1]INRA, UR1037, Laboratory of Fish Physiology and Genomics, Campus de Beaulieu, 35042 Rennes Cedex, France.

[2]Protim, Inserm U1085, Irset, Campus de Beaulieu, 35042 Rennes Cedex, France.

[3]Present address: Institute of Marine Research, Austevoll Research Station, 5392, Storebø, Norway

ozlem.yilmaz@hi.no.

ABSTRACT

Oviparous vertebrates produce multiple forms of vitellogenin (Vtg), the major source of yolk nutrients, but little is known about their individual contributions to reproduction and development. This study utilized CRISPR/Cas9 genome editing to assess essentiality and functionality of zebrafish (*Danio rerio*) type-I and -III Vtgs. A multiple CRISPR approach was employed to knock out (KO) all genes encoding type-I *vtgs* (*vtg1, 4, 5, 6, and 7*) simultaneously (*vtg1*-KO), and the type-III *vtg* (*vtg3*) individually (*vtg3*-KO). Results of PCR genotyping and sequencing, qPCR, LC-MS/MS and Western blotting showed that only *vtg6* and *vtg7* escaped Cas9 editing. In fish whose remaining type-I *vtgs* were incapacitated (*vtg1*-KO), and in *vtg3*-KO fish, significant increases in Vtg7 transcript and protein levels occurred in liver and eggs, revealing a heretofore-unknown mechanism of genetic compensation regulating Vtg homeostasis. Egg numbers per spawn were elevated >2-fold in *vtg1*-KO females, and egg fertility was ~halved in *vtg3*-KO females. Substantial mortality was evident in *vtg3*-KO eggs/embryos after only 8h of incubation and in *vtg1*-KO embryos after 5d. Hatching rate and timing were markedly impaired in embryos from *vtg* mutant mothers and pericardial and yolk sac/abdominal edema and spinal lordosis were evident in the larvae, with feeding and motor activities also being absent in *vtg1*-KO larvae.

By late larval stages, *vtg* mutations were either completely lethal (*vtg1*-KO) or nearly so (*vtg3*-KO). These novel findings offer the first experimental evidence that different types of vertebrate Vtg are essential and have disparate requisite functions at different times during both reproduction and development.

Keywords; *CRISPR/Cas9, knock out, vitellogenins, zebrafish*

1. INTRODUCTION

In oviparous animals, maternally supplied vitellogenins (Vtgs) are the major source of yolk nutrients supporting early development. Vertebrate Vtgs are specialized members of a superfamily of large lipid transfer proteins that are preferentially produced by the liver and transported via the bloodstream to the ovary (Babin et al., 2007). The Vtgs are taken up into growing oocytes via receptor-mediated endocytosis (Opresko and Wiley, 1987), where they are processed by the lysosomal endopeptidase, cathepsin D, into product yolk proteins that are stored in the ooplasm (Carnevali et al., 1999a,b, 2006). Jawed vertebrates produce three major forms of Vtg arising from a *vtg* gene cluster that was present in the ancestor of tetrapods and ray-finned fish (Babin, 2008; Finn et al., 2009). During vertebrate evolution these ancestral *vtg* genes were subject to whole genome duplications, loss of paralogs and lineage-specific tandem duplications, giving rise to substantial variation in the repertoire and number of *vtg* genes present in an individual species, especially among teleost fish (Andersen et al., 2017). The linear yolk protein domain structure of complete teleost Vtgs is: NH_2-lipovitellin heavy chain (LvH)-phosvitin (Pv)-lipovitellin light chain (LvL)-beta component (β'c)-C-terminal component (Ct)-COOH (Patiño and Sullivan, 2002; Hiramatsu et al., 2005). Most teleosts possess from two to several forms of A-type Vtg (VtgA), which may be complete or incomplete, as well an incomplete C-type Vtg (VtgC) lacking both Pv and the two small C-terminal yolk protein domains (β'c and Ct). For example, the complex zebrafish (*Danio rerio*) Vtg repertoire includes five type-I Vtgs (Vtg 1, 4, 5, 6 and 7) that are

incomplete, lacking β′-c and Ct domains (=ostariophysan VtgAo1), two type-II Vtgs (Vtg2 and Vtg8) that are complete (=VtgAo2), and one type-III Vtg (Vtg3), which is a typical VtgC (Yilmaz et al., 2018).

The multiplicity of teleost Vtgs and the roles that different types of Vtg play in oocyte growth and maturation and in embryonic and larval development have been targets of attention for decades (Hiramatsu et al., 2005; Reading and Sullivan, 2011; Sullivan and Yilmaz, 2018). The most diverse group of fishes, the spiny-rayed teleosts (Acanthomorpha) generally possess two paralogous complete forms of VtgA (VtgAa, and VtgAb) in addition to VtgC, and these are orthologs of the zebrafish type-I, type-II and type-III Vtgs, respectively (Finn et al., 2009). In some marine species spawning pelagic eggs, the VtgAa has become neofunctionalized so that its product yolk proteins are highly susceptible to proteolytic degradation by cathepsins during oocyte maturation, yielding a pool of free amino acids (FAA) that osmotically assist oocyte hydration and acquisition of proper egg buoyancy (Matsubara et al., 1999; Finn and Kristoffersen, 2007) and that also serve as critical nutrients during early embryogenesis (Thorsen and Fyhn, 1996; Finn and Fyhn, 2010). The major yolk protein derived from the corresponding VtgAb (LvHAb) is less susceptible to maturational proteolysis. Based on its limited degradation during oocyte growth and maturation, and its utilization late in larval life in some species, it has been proposed that the VtgC may be specialized to deliver large lipoprotein nutrients to late stage larvae without affecting the osmotically active FAA pool (Reading et al., 2009; Reading and Sullivan, 2011). Aside from these few examples, very little is known about specific contributions of the different types of Vtg to developmental processes in acanthomorphs, virtually nothing is known about specialized functions of individual types of Vtg in other vertebrates, and no individual form of Vtg has been proven to be required for the developmental competence of eggs or offspring.

The zebrafish has become an established biomedical model for research on reproduction and developmental biology because they are small, easily bred in the laboratory with short generation time, and lay clutches of numerous large eggs every few days, with external fertilization of the transparent eggs in which embryonic development is easily observed (Ribas and Piferrer, 2013). A reference genome sequence is available, providing the needed databases and bioinformatics tools to conduct genomic and

proteomic research on Vtgs in this species. Details on the genomic and protein domain structure of each individual zebrafish Vtg and on their transcript expression and protein abundance profiles were recently made available by Yilmaz et al. (2018). Coupled with these advantages, the presence of multiple genes encoding the three classical major types of Vtg in zebrafish offers a unique opportunity to investigate their essentiality and functionality via application of CRISPR/Cas9 (clustered regularly interspaced short palindromic repeats (CRISPR)/CRISPR-associated protein 9) technology (Doudna and Charpentier, 2014), a powerful gene-editing tool that provides a reliable process for making precise, targeted changes to the genome of living cells.

In any given species we would like to know which forms of Vtg are essential, at what specific time(s) during development they may be required, and what specific functions they may perform. This study was conducted to address these questions employing zebrafish as the model species. The extensive multiplicity of genes encoding type-I Vtgs, the major contributors to yolk proteins in zebrafish eggs, and the high degree of sequence identity among these genes are matters of interest, especially considering their lack of β'c and Ct domains, which contain 14 highly conserved cysteine residues known to engage in disulfide linkages required for complex folding of the Vtg polypeptide and possibly for the dimerization of native Vtg thought to be required for binding to its oocyte receptor (Reading et al., 2009; Reading and Sullivan 2011). Additionally, the type-III Vtg (VtgC), lacking all but Lv domains and usually being the least abundant form of Vtg, but one universally present in teleosts, begs investigation regarding its contributions to early development.

The main objectives of this study were to discover whether type-I Vtgs and/or type-III Vtg (VtgC) are required for zebrafish reproduction, and to identify specific developmental periods and processes to which they significantly contribute, by investigating the effects of knock out (KO) of their respective genes using the CRISPR/Cas9 gene-editing tool. In this context, KO refers to the process of rendering genes incapable of producing mRNA transcripts or their respective functional proteins. The high sequence identity among zebrafish type-I *vtgs* precluded single-gene loss of function studies and compelled us to employ a gene family editing design, which is now common practice in CRISPR/Cas9

experiments (cf Hyams et al. 2018). This approach is based upon utilization of pooled sets of guide RNAs expected to target most or all gene family members. In this study, we sought to individually but simultaneously incapacitate all genes encoding type-I *vtgs* (*vtg1, 4, 5, 6,* and *7*) by employing three target sites common to all five genes, and to also incapacitate *vtg3* by employing three gene-specific targets.

2. RESULTS

The syntenic organization of *vtg* genes in the zebrafish genome is illustrated in **Fig 1**, along with the general strategy employed in the present study for CRISPR target design to KO the respective type-I and type-III *vtg* genes. Large deletion mutations of 1281 bp and 1181 bp of gDNA were introduced in zebrafish type-I *vtgs* (*vtg1*-KO) and in *vtg3* (*vtg3*-KO), respectively, via CRISPR/Cas9 genome editing (**S1 Fig A-B**). The 1181 bp deletion in *vtg3* was closely matched in size and position to the sequence between two of the three single guide (sg) RNAs (sg32 and sg33). However, the 1281 bp deletion in *vtg1*, which overlapped sg12, was much smaller than would result from a perfect excision between sg11 and sg13 (**S1 Fig A**).

The genomic deletion leads to a loss of 703 bp and 714 bp within the respective *vtg1* and *vtg3* mRNA transcripts (**S1 Fig C-D**; see **S1 Fig E-F** for cDNAs). The deletion mutation created in the *vtg1*-KO study involves a frameshift that, after 10 additional residues, leads to a premature stop codon, which would terminate the polypeptide at residue 529 so that it includes only the forward half of the LvH domain (**Fig 2A**; see also **S2 Fig A**), eliminating the remaining part of the LvH domain as well as the Pv and LvL domains of Vtg1 (see also **S1 Fig G**). The deletion created in the *vtg3*-KO study results in mutation of residue 239 from arginine (R) to leucine (L), with a clean (in-frame) deletion of the following 238 aa located at the end of the critical Vtg receptor-binding domain of LvH3 (**Fig 2B**; see also **S2 Fig B**) that does not otherwise alter the Vtg3 polypeptide (see also **S1 Fig H**). The introduced mutations were subjected to PCR screening (of gDNA) to genotype each zebrafish generation using combinations of

primers flanking the altered target sites (**Fig 3**). F0 generation individuals exhibiting a heterozygous mutant double banding pattern were retained as founders for production of stable mutant lines (**Fig 3**).

Microinjection efficiency was 20% and 80% positive as determined in embryos at 24h screening, for *vtg1*-KO and *vtg3*-KO, respectively. This efficiency was confirmed by finclip genotyping when siblings of these embryos reached adulthood. However, mutation transmission to F1 offspring was as low as 0.010% for *vtg1*-KO and 0.025% for *vtg3*-KO, and only 2 heterozygous (Ht: *vtg1*-/+ and *vtg3*-/+) adult males were available to continue reproductive crosses with non-related wild type (Wt: *vtg1*+/+ and *vtg3*+/+) females for production of F2 generations. The rate of mutation transmission to the F2 generation produced from F1 Ht males and Wt females was 55% and 70% for *vtg1*-KO and *vtg3*-KO, respectively. Reproductive crosses of Ht males and Ht females revealed a Mendelian inheritance pattern with 25% wild type (wt: sibling wild type; *vtg1*+/+ and *vtg3*+/+), 52% heterozygous and 22% homozygous (Hm: *vtg1*-/- and *vtg3*-/-) individuals at the F3 generation. Hm F3 females and males were crossed to produce the F4 generation yielding 100% homozygous offspring carrying only the mutated allele (**Fig 3**). As these Hm individuals are generally inviable (*see below*), production of subsequent generations of mutants requires crossbreeding of heterozygotes.

For both *vtg* KO lines, the relative level of expression of each individual *vtg* transcript in livers of Hm, Ht, and wt F3 generation females were compared to those obtained for Wt female liver. KO of type-I *vtgs* resulted in the absence of *vtg1*, *vtg4*, and *vtg5* transcripts in F3 Hm *vtg1*-KO female liver, representing a significant decrease in levels of these transcripts compared to Ht, wt and Wt females ($p<0.05$). Levels of *vtg6* and *vtg7* transcripts were still detectable, with *vtg7* transcript levels being significantly higher (~3-fold) in Hm *vtg1*-KO female liver as compared to Wt female liver ($p<0.05$). The *vtg1*-KO had no significant effect on *vtg2* and *vtg3* expression (**Fig 4A**). No *vtg3* transcripts were detected in F3 Hm *vtg*3-KO female livers, this representing a significant decrease in *vtg3* transcript levels compared to Ht, wt and Wt females ($p<0.05$). The F3 Hm *vtg*3-KO females showed a statistically significant ~3-fold increase in hepatic *vtg7* transcript levels relative to Wt fish ($p<0.05$). No significant effect of *vtg3*-KO on expression of other *vtg* genes was observed (**Fig 4B**).

155 The relative abundances of individual Vtgs or of their product yolk proteins were evaluated in
156 liver and eggs, respectively, of F3 Hm *vtg1*-KO females as normalized spectral counts (N-SC) from LC-
157 MS/MS. These measurements revealed no detectable amount of Vtg1, 4 or 5 protein ($p<0.05$) (**Fig 5A**).
158 Similar to gene expression levels in these same samples, Vtg6 and 7 proteins were still detectable, with
159 Vtg7 protein levels being significantly higher in Hm *vtg1*-KO female liver and eggs than in corresponding
160 samples from Wt females. ($p<0.05$). The relative abundance of Vtg7 protein was ~4-fold and ~3-fold
161 higher in Hm *vtg1*-KO liver and eggs, respectively, than in Wt females. Additionally, even though they
162 were uniformly low, Vtg3 protein levels were also significantly higher (~2-fold) in Hm *vtg1*-KO eggs
163 than in Wt eggs ($p<0.05$) (**Fig 5A**).
164 The *vtg3*-KO resulted in the absence of detectable Vtg3 protein in both liver and eggs of F3 Hm
165 *vtg3*-KO females ($p<0.05$) but it did not seem to influence the relative abundances of Vtg1, 2, 4, 5, and 6,
166 or of their yolk protein products, in these samples (**Fig 5B**). However, Vtg7 protein levels were
167 significantly higher (~1.5-fold) in *vtg3*-KO eggs than in Wt eggs ($p<0.05$), but *vtg3*-KO did not
168 significantly alter the relative abundance of Vtg7 protein in the liver of the egg donors, although average
169 levels were higher in the *vtg3*-KO fish (**Fig 5B**). In *vtg1*-KO, *vtg3*-KO and Wt females, relative protein
170 abundances for all detected Vtgs were generally lower in liver in comparison to eggs. Among the various
171 forms of Vtg protein, their relative abundance in eggs from Wt females ranged from 15 to 31 times higher
172 than in livers of the same fish.
173 Domain-specific, affinity purified polyclonal antibodies were developed in rabbits against
174 zebrafish (zf) Vtg type-specific epitopes (Type-I Vtg: NEDPKANHIIVTKS on LvH1; Type-III Vtg:
175 AQKDDIEMIVSEVG on LvL3. See **Fig 2**). The antibodies were used to detect these proteins by Western
176 blotting in the respective Hm *vtg*-KO, Ht and Wt female livers, ovaries and eggs. The rabbit anti-zfLvH1
177 antibody revealed the presence of high molecular weight bands corresponding in mass to LvH1 in all
178 tested individuals and tissues (*data not shown*), consistent with the reported escape of the *vtg6* and *vtg7*
179 from Cas9 editing and the presence of Vtg6 and Vtg7 protein in liver, ovary and eggs from all groups of
180 fish in the *vtg1*-KO experiment (Hm, Ht and Wt). In Western blots performed using anti-zfLvL3 in the

vtg3-KO experiment, the antibody detected mainly a bold ~24 kDa band in samples of both ovary and eggs from Ht and Wt fish, but not from Hm fish, very close to the deduced mass of the LvL3 polypeptide (21.3 kDa) (Yilmaz et al., 2018) (**Fig 6**). Zebrafish LvLs were previously shown to migrate to this position in SDS-PAGE (Yilmaz et al., 2017). The distinct absence of the ~24 kDa band only in samples of Hm ovary and eggs is considered to be evidence of successful *vtg3*-KO in this experiment. The very bold ~68 kDa band also present in samples of ovary and eggs from Ht and Wt females, but absent in samples from Hm *vtg3*-KO fish, which have a faint band in this position, may represent a degradation product of intact, covalently linked LvH-LvL conjugate (Vtg3) persisting after maturational proteolysis, as has been described for several species (Reading et al., 2009). Faint high molecular weight bands mainly $\geq$ 68 kDa were also evident for samples of liver, ovary and eggs from all individuals and from all groups of fish in the *vtg3*-KO experiment (Hm, Ht and Wt). These bands are taken to indicate slight non-specific binding of the antibody with yolk proteins under the experimental conditions employed. For Ht and Wt fish, some of these bands may represent high molecular weight Vtg3 products bearing intact or partially degraded LvL3, as noted above. No bands specific to Ht and Wt fish were detected in Western blots of liver performed using this antibody, consistent with absence of significant quantities of Vtg3 protein detectable in Wt liver by LC-MS/MS (**Fig 5B**), a commonly observed phenomenon (see Yilmaz et al., 2016) suggesting that Vtg3 is rapidly released into the bloodstream after synthesis.

Phenotypic parameters including number of eggs per spawn, egg fertilization, hatching and survival rates, and egg diameter (embryo and chorion diameter) as well as larval size at 8 days post fertilization (dpf), were measured to detect potential effects of *vtg* KO on zebrafish reproductive performance and development. There were no significant differences between Hm *vtg1*-KO and Wt eggs or offspring in fertilization rate, embryo size or larval size, respectively (**Fig 7**). However, F3 Hm *vtg1*-KO females produced significantly more eggs per spawn (593 ± 40.06, mean ± SEM) than did Wt females (280 ± 28.97) ($p<0.05$), although the final hatching rate of these embryos at 10 dpf (64.9 ± 6.45 %) was significantly lower than for embryos from Wt females (99.6 ± 0.24 %) ($p<0.05$). Embryos from F3 Hm *vtg1*-KO females also were strikingly delayed in hatching, completing hatching at 9 dpf versus 5

dpf for control fish (**Fig 7**). It was noted that the Hm *vtg1*-KO embryos appeared to have weaker heartbeats and body movements during incubation antecedent to hatching as compared to *vtg3*-KO embryos, which, even with malformations, exhibited apparently normal heartbeat rhythms and body movements comparable to those seen in Wt embryos. Embryo and larval survival rates of Hm *vtg1*-KO offspring were also significantly lower than for Wt offspring, beginning from 5 dpf when their mean survival rate was 57.14 ± 7.34 % compared to 79.40 ± 5.75 % for Wt fish. The survival rate of Wt offspring changed little thereafter, whereas the survival rate of Hm *vtg1*-KO offspring continued to decline, with *vtg1*-KO being completely lethal to the larvae by 16 dpf (**Fig 8**).

There were no significant differences between Hm *vtg3*-KO fish and Wt fish in number of eggs per spawn, embryo size or larval size (**Fig 7**). However, the fertility, hatching rate and overall survival of Hm *vtg3*-KO eggs and offspring, respectively, were significantly less than seen in Wt fish ($p<0.05$) (**Fig 7**). The fertilization rate of eggs from F3 Hm *vtg3*-KO females (35.5 ± 7.7 %) was substantially lower than for Wt eggs (81.6 ± 7.0 %), although hatching of eggs from these females was only slightly delayed, and to a much lesser extent than was observed for eggs from the F3 Hm *vtg1*-KO females (*see below*). The final hatching rate for eggs obtained from F3 Hm *vtg3*-KO females was 74.3 ± 7.7 % at 10 dpf compared to 99.6 ± 0.24 % for Wt eggs (**Fig 7**). Embryo and larval survival rates of Hm *vtg3*-KO offspring were significantly less than for Wt offspring ($p<0.05$), beginning from 8 hours post fertilization (hpf), with the difference from Wt fish increasing throughout the 22 days experiment (**Fig 8**). As previously reported (Yilmaz et al., 2017), at 2–4 hpf eggs from low fertility spawns have a high incidence of abnormal embryos with asymmetric cell cleavage and/or developmental arrest at early cleavage stages. Such embryos may survive to 8 hpf but not to 24 hpf. The larval survival rate for Hm *vtg3*-KO offspring was only 6.25 ± 1.6 % at 22 dpf compared to 69.2 ± 3.8 % for Wt offspring (**Fig 8**).

Separate panels in **Fig 9** illustrate morphological disorders observed during development of F4 Hm *vtg1*-KO and Hm *vtg3*-KO fish in comparison to offspring from Wt females at 4 and 8 dpf. In Hm *vtg*-KO fish, these phenotypic disorders mainly involved pericardial and yolk sac/abdominal edema accompanied by spinal lordosis evidenced as curved or bent back deformities. The severity of these

malformations, mainly the pericardial and yolk sac edema, appeared to be relatively lower in Hm *vtg1*-KO fish than in Hm *vtg3*-KO fish. However, the prevalence of deformity was much greater for Hm *vtg1*-KO fish, with nearly all larvae exhibiting some degree of deformity versus approximately 30 % of Hm *vtg3*-KO larvae. Finally, the Hm *vtg1*-KO larvae exhibited no feeding activity or motor activities comparable to those seen in Hm *vtg3*-KO and Wt fish at the same times.

3. DISCUSSION

Vitellogenins are the 'mother proteins' that supply most yolk nutrients supporting early vertebrate development, and most species have evolved multiple forms of Vtg. However, little is known about specific functions of these different forms of Vtg and it is uncertain which forms are essential for successful development or at what stage(s) of development they are required. The present research was undertaken to address these questions using a zebrafish CRISPR/Cas9 *vtg* gene KO model. Three out of five type-I zebrafish *vtg* genes (*vtg1*, *4* and *5*) were knocked out simultaneously (*vtg1*-KO experiment), and the type-III *vtg* gene (*vtg3*) was knocked out individually (*vtg3*-KO experiment), and the effects on maternal reproductive physiology and offspring development and survival were evaluated. To the best of our knowledge, these findings constitute the first reports of *vtg* gene KO and its consequences in any animal.

The efficacy of CRISPR/Cas9, which is reported to be the most practical and efficient tool available for genome editing, was lower in the *vtg1*-KO experiment (20 %), where five genes were targeted concomitantly, than in the *vtg3*-KO experiment (80 %) where only a single gene was targeted. Since the site-specific cleavage efficiency is mostly dependent on the concentrations of single guide (sg) RNAs and Cas9 endonuclease, Liu et al. (2018) related the low efficiency of simultaneous knockout of multiple homologous genes to the fact that more sgRNAs and gene target sites share the same Cas9 enzyme. In addition to low efficiencies in the *vtg1*-KO experiment, the escape of the type-I *vtg6* and *vtg7* from Cas9 editing might be simply an outcome of an insufficient amount of administered Cas9 RNA.

Attempts at optimization of sgRNA/Cas9 concentrations may be useful in future studies. Taking into account the syntenic organization and close proximity of type-I *vtg* genes in zebrafish (Yilmaz et al., 2018, **Fig 1**), and the identity (100 %) of the common target sites for these genes, it is difficult to postulate criteria upon which any preference of Cas9 activity might be directed. No matter which gene-editing tool is used, low efficiency of germline mutant transmission has been a commonly faced problem among researchers, usually leading to labor intensive and time consuming screening work to acquire high-throughputs (Xie et al., 2016). The low ratios of mutation transmission to next generations in the present study (0.01 % - 0.025 %) emphasize the need for further research to improve germline transmission efficiencies in genome editing. Production of stable mutant lines was delayed an extra generation in both the *vtg1*-KO and *vtg3*-KO experiments since no mutation-positive female founders were obtained at the F1 generation for performing subsequent reproductive crosses.

The incapacitation of *vtg1*, *vtg4*, and *vtg5* in the *vtg1*-KO experiment, and of *vtg3* in the *vtg3*-KO experiment, was confirmed by conventional PCR, agarose gel electrophoresis and sequencing of gDNA and also by relative quantification of corresponding *vtg* transcript and Vtg protein abundances via qPCR and LC-MS/MS, respectively, with the absence of Vtg3 protein in Hm *vtg3*-KO ovary and eggs being additionally confirmed by Western blotting. The absence of transcripts for *vtg1*, *vtg4* and *vtg5* in liver of F3-generation homozygous mutant females and lack of the respective Vtg proteins in both liver and eggs collected from these females, proven by the results of qPCR and LC-MS/MS, provided strong evidence of concomitant incapacitation of *vtg1*, *4* and *5* in this study. Therefore, and furthermore to avoid complications due to high sequence identities among type-I *vtg* genes, detailed genotyping by sequencing was conducted for *vtg1* only as a representative of type-I *vtgs*, and also for *vtg3*. The specific alterations made to *vtg4* and *vtg5* gDNA during CRISPR/Cas9 editing were not otherwise visualized.

The introduced mutations were large deletions achieved by administration of multiple sgRNAs. The 1181 bp deletion confirmed in *vtg3* mutants closely matched the sequence bounded by flanking guide RNAs sg32 and sg33. However, the 1281 bp deletion overlapping sg12 in *vtg1* mutants was much smaller than would result from excision between the flanking sg11 and sg13 (**S1 Fig A**). It is possible that

285 homologous recombination initiated in the heterozygous F0 mutant after Cas9 editing, combined with any
286 other non-homologous and/or homology-directed repairs, may have contributed to restoration of much of
287 the sequence between sg11 and sg12, as well as the short sequence between the 1281 bp deletion and
288 sg13. In the end, we pursued this unexpected *vtg1* mutant because the annotated deletion was predicted to
289 incapacitate the gene (**S1 Fig G,** see also **S2 Fig**), an expectation later verified by the absence of *vtg1*
290 transcripts and of Vtg1 protein, and because early generational screening indicated that it was heritable.

291 In gene family editing experiments where family members are closely arrayed in tandem on the
292 same chromosome, as are the zebrafish type-I *vtgs* (see **Fig 1**), the use of pooled guide RNAs common to
293 all genes creates the possibility of deletions spanning several genes. In this study, while the deletion in
294 *vtg1* was localized to a specific position via genotyping by sequencing, the corresponding deletions in
295 *vtg4* and *vtg5* mutants were not, although their KO status was confirmed by the lack of relevant
296 transcripts and proteins. Expression of both mRNA and protein were clearly detected for *vtg7*, which is
297 located in the middle of the type-I *vtg* cluster and is flanked by *vtg4* and *vtg5* (**Fig 1**). Therefore, no large
298 deletion spanning these three *vtgs* could have occurred. The *vtg6* is located at the far end of the cluster
299 separated from *vtg5* only by *si:rp71-23d18.4*, a gene lacking targets for any sgRNAs employed in this
300 study whose predicted transcript encodes an uncharacterized non-Vtg protein. A deletion spanning *vtg5,*
301 *si:rp71-23d18.4* and *vtg6* did not occur, as *vtg6* transcripts and their encoded proteins were also detected.
302 Therefore, we surmise that our *vtg4* and *vtg5* mutants did not arise from deletions spanning several genes.
303 It appears that our experimental design effectively targeted 3 of 5 type-I *vtg* genes for incapacitation (KO)
304 and this action was apparently restricted to the individual genes.

305 By disturbing the structure of the LvH chain in both the *vtg1*-KO and *vtg3*-KO experiments via
306 the creation of large gaps in the respective LvH polypeptides, it was expected that the mutant proteins
307 would not fold properly, or be able to bind to their receptor in the case of Vtg3, even if they were
308 produced and partly expressed by the liver. However, there were no signs of hepatic synthesis of Vtg1, 4
309 or 5 in Hm *vtg1*-KO individuals or of Vtg3 in Hm *vtg3*-KO liver. We surmise that the predicted deletions
310 in the sequences encoding Vtg1 and Vtg3 led to premature termination of transcription and rapid

311 transcript degradation without translation. The affected regions of the transcripts encoding LvH including,
312 in the case of LvH3, its Vtg receptor-binding domain, may be essential for production and translation of
313 stable transcripts.

314 While detection of the *vtg6* and *vtg7* transcripts and their product proteins was expected in the
315 *vtg1*-KO experiment, since these two type-I *vtg* genes escaped Cas9 editing, the strikingly high abundance
316 of Vtg7 (but not Vtg6) at both transcript and protein levels in both Hm *vtg1*-KO and Hm *vtg3*-KO
317 individuals (**Figs 4 and 5**) was unexpected. These observations suggest an attempt of the organism to
318 compensate for the loss of other types of Vtgs by augmentation of Vtg7 levels, and they imply the
319 existence of heretofore-unknown mechanisms for regulating Vtg homeostasis.

320 The lack of a mutant phenotype in Hm mutant individuals due to compensatory gene expression
321 triggered upstream of protein function is known as 'genetic compensation' and this phenomenon has been
322 encountered in gene editing studies of a wide range of model organisms. As examples, Marschang et al.
323 (2004) related the normal development and lack of mutant phenotypes in LDL receptor-related protein 1b
324 (*LRP1b*)-deficient mutant mice to functional compensation by *LRP1,* and Sztal et al. (2018) found that a
325 genetic *actin1b* (*actc1b*) zebrafish mutant exhibits only mild muscle defects and is unaffected by injection
326 of an *actc1b*-targeting morpholino due to compensatory transcriptional upregulation of an *actin* paralog in
327 the same fish. In the present study, compensatory increases in relative levels of total Vtg protein
328 attributable to upregulation of Vtg7 protein in F4 Hm *vtg1*-KO eggs offset only about half of the decrease
329 in total Vtg protein attributable to KO of *vtg1*, *4* and *5* (**Fig 5A**). Therefore, these eggs/offspring were still
330 deficient of type-I Vtg protein and they uniformly exhibited mutant and ultimately lethal phenotypes,
331 perhaps due to the insufficient compensation. In contrast, the compensatory increase in total Vtg protein
332 attributable to upregulation of Vtg7 in Hm *vtg3*-KO eggs was several-fold greater than the loss of Vtg
333 protein attributable to *vtg3* KO (**Fig 5B**), yet many of these eggs/offspring still exhibited mutant
334 phenotypes, with egg fertility being very low (*see below*) and most offspring not surviving for 22 d of
335 development. Nonetheless, the incidence of mutant phenotypes in Hm *vtg3*-KO larvae (30 %) was far less
336 than in Hm *vtg1*-KO larvae, all of which were malformed, and a low percentage (6.25 %) of Hm *vtg3*-KO

larvae did survive for 22 d post fertilization, whereas no Hm *vtg1*-KO larvae did. These observations indicate that, while it is possible that upregulation of Vtg7 may have mitigated to some extent the effects *vtg3* KO owing to decreased total Vtg protein, Vtg7 cannot fully substitute for Vtg3 or eliminate the adverse effects of *vtg3* KO on egg fertility and offspring development. Therefore, Vtg3 must have functional properties distinct from Vtg7 and perhaps other type-I Vtgs.

Transcription of *vtg* genes is initiated when estrogen (E2)/estrogen receptor (Esr) complexes bind to estrogen response elements (ERE) located in the gene promoter regions (Babin, 2008; Nelson and Habibi, 2013). E2-Esr complexes can also be tethered to transcription factor complexes targeting binding sites distinct from EREs, and several transcription factors other than Esrs have binding sites located in promoter regions of zebrafish *vtg* genes (reviewed by Lubzens et al., 2017). There is evidence that the multiple *vtg* genes in zebrafish exhibit differential sensitivities to estrogen induction as well as disparate patterns of ERE and other transcription factor binding sites in their promoter regions (Levi et al., 2009, 2012). Bioinformatics analyses indicated that the promoter region of *vtg7* is comparatively rich in binding sites for transcription factors involved in retinoic acid signaling such as retinoic acid response elements (RAREs) and peroxisome proliferator-activated receptors (PPARs)/retinoid X receptor (RXR), while having only a single ERE (most other *vtgs* having 2-3) (see Levi et al., 2012 Table 3). These types of differences between *vtg* promoters could underpin selective upregulation of Vtg7 in response to ablation of other forms of Vtg (other type-I Vtgs, Vtg3) via gene KO. Conspecific Vtg (type not specified) has been shown to downregulate plasma levels of E2 *in vivo* when injected into vitellogenic rainbow trout (*Oncorhynchus mykiss*) (Reis-Henriques et al., 1997) and to inhibit steroidogenesis leading to E2 production *in vitro* by ovarian follicles of rainbow trout (Reis-Henriques et al., 1997, 2000) and greenback flounder, *Rhombosolea tapirina* (Sun and Pankhurst, 2006). Partial release from such inhibition in *vtg*-KO fish would increase vitellogenic signaling to the liver, activating estrogen responsive genes including those encoding Vtgs, Esr (Esrs) and PPARs.

Whether Vtg7 itself has vitellogenic properties remains to be determined. Certain conspecific Vtgs have been shown to upregulate vitellogenesis in Indian walking catfish (*Clarias batrachus*) (Juin et

al., 2017; Bhattacharya et al., 2018) and comparisons of the available deduced catfish Vtg polypeptide sequences (85 and 152 residues; Juin et al., 2017, Fig. 3) to Vtgs from zebrafish and other teleosts using CLUSTAL W and BLASTP (*data not shown*) indicate that they are forms of VtgAo1 showing a high identity to type-I zebrafish Vtgs (up to 80% in the case of Vtg7). The specific mechanism(s) by which Vtg7 is preferentially upregulated in *vtg*-KO zebrafish, and special properties of Vtg7 for regulation of Vtg homeostasis, are meaningful subjects for future research. Levels of Vtg3 protein were also upregulated in eggs from F3 Hm *vtg1*-KO females (**Fig 5A**) but the significance of this increase is difficult to interpret as it was too slight to have much impact on total Vtg levels, and because hepatic levels of *vtg3* transcripts and of Vtg3 protein were not elevated in these same fish (**Figs 4A and 5A**). Transcripts of *vtg3* are reported to be the most intensely upregulated transcripts in vitellogenic female and estrogenized male zebrafish (Levi et al., 2009) and there may not have been scope for further increases in the *vtg1*-KO fish. In this case, post-transcriptional mechanisms for upregulating Vtg3 could have been at play (Flouriot et al., 1996; Ren et al., 1996). As noted above, Vtg3 may be released into the bloodstream immediately after synthesis, which would explain the lack of significant quantities of this protein in livers of Hm *vtg1*-KO and Wt fish (**Fig 5A**).

Neither *vtg1*-KO nor *vtg3*-KO influenced egg, embryo or larval size in spawns producing F4 offspring of the stable mutant lines (**Fig 7**), and there were no apparent differences in ovary structure among the different groups of maternal F3 females (Hm, Ht, wt and Wt) sampled after spawning (*data not shown*). However, F3 Hm *vtg1*-KO females exhibited a 2-fold increase in number of produced eggs relative to Wt females, with normal egg fertility equivalent to that of Wt females (**Fig 7**). This response to elimination of three type-I Vtgs (including the most abundant one, Vtg1) implies that one or more of these Vtgs are normally involved in restriction of fecundity, perhaps via the aforementioned inhibition of follicular estrogenesis. It is also possible that Vtg7, which was highly elevated in Hm *vtg1*-KO females, might somehow positively modulate fecundity. The referenced VtgAo1 of walking catfish, when pelleted and implanted into pre-vitellogenic females, has been shown to stimulate vitellogenesis and complete oocyte growth all the way through the transition to final maturation (Bhattacharya et al., 2018). In the

final analysis, any 'compensation' by Vtg7 for loss of other type-I Vtgs must be deemed ineffectual, as the resulting embryos unconditionally exhibited serious and lethal developmental abnormalities (*see below*).

The *vtg*-KO zebrafish larvae exhibited major phenotypic disorders, mainly pericardial and yolk sac/abdominal edemas and spinal lordosis associated with curved or arched back deformities. These abnormalities were observed to be much less prevalent, albeit usually more severe, in *vtg3*-KO larvae, but present to some extent in all *vtg1*-KO larvae along with the noted behavioral differences. Skeletal axis malformations and pericardial and yolk sac/abdominal edema are among the most common deformities observed in cultured teleosts and they form an interrelated cluster of abnormalities that tend to be observed together (Alix et al., 2017). For example, pericardial edema tends to precede development of yolk sac edema in zebrafish, which when severe leads to notochord deformation (see Hanke et al., 2013, Fig. 1). These abnormalities have been associated with a broad variety of conditions including, as examples, rearing systems for Eurasian perch, *Perca fluviatilis* (Alix et al., 2017), larval rearing temperatures for Atlantic halibut, *Hippoglossus hippoglossus L.* (Ottesen and Bolla, 1998), embryo cryopreservation practices for streaked prochilod, *Prochilodus lineatus* (Costa et al., 2017), and, in zebrafish, phenanthroline toxicity (Ellis and Crawford, 2016), influenza A virus infection (Gabor et al., 2014), knockdown or KO of genes related to kidney function or development, respectively (Hanke et al., 2013; Zhang et al., 2018), knockdown of the *wwox* tumor suppressor gene (Tsuruwaka et al., 2015), deletion of a gene (*pr130*) encoding a protein essential for myocardium formation and cardiac contractile function (Yang et al., 2016), and mutagenesis of genes involved in thyroid morphogenesis and function (Trubiroha et al., 2018), among others. The edemas may ultimately result from many different proximal causes such as cardiac, kidney, liver or osmoregulatory failure, and researchers are just beginning to develop screens to differentiate between them (Hanke et al., 2013). Although they can occur under many different conditions and arise via several possible mechanisms, these major mutant phenotypes observed in the present study were not encountered in control Wt offspring and, therefore, they are clearly related to deficiencies of type-I Vtgs (Vtg1, 4 and 5) and of Vtg3. The question of whether these phenotypes

result from loss of Vtg1 alone or are an effect of ablation of Vtg1 in combination with Vtg4 and/or Vtg5 will need to be addressed in future research.

Embryo and larval survival rates were severely diminished by *vtg* gene KO, but the magnitude, type and timing of losses differed between *vtg1*-KO and *vtg3*-KO fish (**Fig 8**). The fertility of Hm *vtg3*-KO eggs was only half that observed in Wt eggs (**Fig 7**), indicating that Vtg3 is an important contributor to fertility in zebrafish. Among the Vtgs examined, this dependency was specific to Vtg3, since fertility was not 'rescued' by the increase in Vtg7 levels in Hm *vtg3*-KO eggs, which was far greater than normal Vtg3 levels in Wt fish (**Fig 5B**), and this adverse effect on fertility was not seen in Hm *vtg1*-KO eggs. The substantial losses of Hm *vtg3*-KO eggs began early, at only 8 hpf, and less than 30% survived to 24 hpf (**Fig 8**). Both *vtg1*-KO and Wt eggs showed significant but much fewer losses ($p<0.05$) during this same interval. In this study, fertility was estimated conservatively, based on numbers of viable embryos showing normal cell division and subsequently developing to ~24 hpf. It is uncertain whether the high mortality of Hm *vtg3*-KO eggs between 8 and 24 hpf (**Fig 8**) resulted from a failure to be fertilized or from defects in early development involving zygotes that fail to initiate cell division or that briefly undergo abnormal cell divisions and then die. In future studies, some Hm mutant and Wt females should be bred with males bearing a unique germline marker gene, such as *vasa*::*egfp* (Krøvel and Olsen, 2002), that can be genotyped in resulting eggs and embryos to resolve this question.

The mechanism(s) whereby Vtg3 deficiency impairs fertility and/or early development of zebrafish are unknown. A recent study examining the proteomics of egg/embryo developmental competence in zebrafish identified disruption of normal oocyte maturation, including maturational proteolysis of Vtgs, as a likely cause of poor egg quality (Yilmaz et al., 2017). The proteolysis of Vtgs by cathepsins during oocyte maturation, a phenomenon that has been observed in zebrafish eggs undergoing maturation *in vitro* (Carnevali et al., 2006), releases FAA that steepen the osmotic gradient driving water influx through aquaporins on the cell surface, leading to oocyte hydration (Cerdà et al., 2007, 2013). These FAA are also major substrates for aerobic energy metabolism during early embryogenesis (Thorsen and Fyhn, 1996; Finn and Fyhn, 2010). In some species, Vtg3 (VtgC) is subjected to maturational

proteolysis (see Yilmaz et al., 2016) and it is possible that zebrafish Vtg3 contributes to these critical processes ongoing during oocyte maturation, which are required for production of viable eggs. However, mass balance considerations seem to exclude the possibility that the early mortality of Hm *vtg3*-KO embryos results substantially from nutritional deficiencies. In this and prior studies of zebrafish, Vtg3 has been shown to be a very minor form of Vtg making only a miniscule contribution to stores of Vtg-derived yolk proteins in eggs (**Fig 5**; see also Yilmaz et al., 2018). Nonetheless, Vtg3 is clearly an important, if not essential, contributor to fertility and/or early development in zebrafish. The continuous mortality of Hm *vtg3*-KO embryos after 24 hpf, leading to only ~6% survival at 22 dpf, suggests that Vtg3 also contributes to late embryonic and larval development, as suggested in several prior studies (see below).

Survival of embryos emanating from Hm *vtg1*-KO females remained relatively high at 24 hpf (~70%) but decreased continuously thereafter, becoming significantly less than survival of Wt embryos by 5 dpf, and then decreasing to zero by 16 dpf (**Fig 8**). The collective absence of Vtg1, 4 and 5 in zebrafish is lethal to offspring, and this effect could not be rescued via genetic compensation by Vtg7 or offset by the remaining intact Vtgs. This finding is not surprising as, collectively, these 3 type-I Vtgs account for the vast majority of Vtg-derived protein in Wt zebrafish eggs (**Fig 5**; see also Yilmaz et al., 2018). Since most mortality of *vtg1*-KO offspring occurred relatively late in larval development, with mortality rate increasing after 10 dpf when yolk sac absorption was being completed (**Fig 8**), the collective contributions of Vtg1, 4 and 5 to survival could be largely nutritional, although this remains to be verified.

It is evermore apparent that the different types of vertebrate Vtg can have dissimilar effects on reproductive processes. As noted above (see also Introduction), in marine acanthomorphs spawning pelagic eggs in seawater the different types of Vtg can play disparate roles in oocyte hydration, acquisition of egg buoyancy, and early versus late embryonic and larval nutrition (Matsubara and Koya, 1997; Matsubara et al., 1999, 2003; Reith et al., 2001; Sawaguchi et al., 2005, 2006a, 2006b; Finn, 2007). The type-specific ratios of circulating Vtgs (e.g. VtgAa:VtgAb:VtgC) may vary considerably during oocyte growth, but ratios of their derived yolk protein products present in eggs tend to be fixed and

characteristic of species (Hiramatsu et al., 2015; Reading et al., 2017). This is also the case in zebrafish as evidenced by the similarity of Vtg profiles by type (and subtype) in Wt fish in the *vtg1*-KO and *vtg3*-KO experiments, and also in comparison to Wt fish in an earlier study (Yilmaz et al., 2018). It is thought that Vtg type-specific ratios of yolk proteins in eggs are maintained via activity of selective receptors for each type of Vtg, which target their specific ligand(s) into different compartments where their yolk protein products undergo disparate degrees of proteolysis during oocyte maturation. The initial abundance and degree of proteolysis of the yolk proteins determines their relative contribution(s) to oocyte hydration, egg buoyancy, FAA nutrition of early embryos and lipoprotein nutrition for late stage larvae (Hiramatsu et al., 2015; Reading et al., 2017). The collective findings of the present study introduce a new point of view on the roles that multiple vitellogenins can play in vertebrate reproduction. Distinctively from what has been reported previously, the present study presents a mixed model of Vtg functionality covering both maternal reproductive physiology and early development of offspring, where type-I Vtgs regulate fecundity and make essential contributions to embryonic morphogenesis, hatching and larval kinesics and survival (Vtg1, 4 and 5), and also provide some homeostatic regulation of total Vtg levels (Vtg7), while Vtg3 (a typical VtgC) is critically important to fertility and early embryogenesis and also influences later development.

The forgoing discussion identifies potential reproductive and developmental actions of certain type-I Vtgs (Vtg1, Vtg4, and Vtg5) and of Vtg3 based upon the results of incapacitation of their respective genes, as evidenced by elimination of their product transcripts and proteins. While such observations provide powerful evidence for these many actions, some novel, we cannot exclude involvement of the remaining Vtgs in regulation of the same physiological processes. Undetected effects of genome editing on *vtg6* and *vtg7*, short of wholesale elimination of their transcripts or product proteins, could have contributed to development of the noted '*vtg1*-KO phenotypes'.

In summary, the present study, for the first time, targeted multiple forms of Vtgs for KO at family level using CRISPR/Cas9 technology in the zebrafish, a well-established biomedical model. The collective knock out of *vtg1*, *4*, and *5* and the individual knock out of *vtg3* were achieved successfully. A

493 compensatory increase in *vtg7* at both transcript and protein levels was observed in both types of *vtg* KO
494 mutants. However, this compensation was not effective in rescuing the serious developmental
495 impairments and high mortalities resulting from ablation of three other type-I Vtgs or of Vtg3. Whether
496 the detected phenotypes result from the absence of a single type-I *vtg* or is a result of collective
497 incapacitation of *vtg1*, *vtg4* and *vtg5*, needs further research. However, by far the most abundant forms of
498 Vtg in zebrafish, the type-I Vtgs appear to have essential developmental and nutritional functions in both
499 embryos and larvae. In spite of being a very minor form of Vtg in zebrafish and most other species, and
500 also the most divergent form, Vtg3 contributes importantly to the developmental potential of zygotes
501 and/or early embryos. Finally, Vtgs appear to have previously unreported regulatory effects on the
502 physiology of maternal females, including limitation of fecundity (type-I Vtgs) and maintenance of
503 fertility (Vtg3). These novel findings represent the first steps toward discovery of the specific functions of
504 multiple vertebrate Vtgs via genome editing. Further physiological studies are necessary to pinpoint the
505 exact molecular mechanisms disturbed in the *vtg* mutants.
506
507
508 **4. MATERIAL AND METHODS**
509
510 **4.1. Animal care, spawning and phenotypic observations**
511 Zebrafish of the Tübingen strain originally emanating from the Nüsslein-Volhard Laboratory
512 (Germany) were obtained from our zebrafish facility (INRA UR1037 LPGP, Rennes, France). The fish
513 were ~15 months of age and of average length ~5.0 cm and average weight ~1.4 g. The zebrafish were
514 housed under standard conditions of photoperiod (14 hours light and 10 hours dark) and temperature (28
515 °C) in 10 L aquaria and were fed three times a day *ad libitum* with a commercial diet (GEMMA,
516 Skretting, Wincham, Northwich, UK). Females were bred at weekly intervals to obtain egg batches for
517 CRISPR sgRNA microinjection (MI). The night before spawning, paired males and females bred from
518 different parents were separated by an opaque divider in individual aquaria equipped with marbles at the

519 bottom as the spawning substrate. The divider was removed in the morning, with the fish left undisturbed
520 to spawn. Egg batches in majority containing intact, clean looking, well defined, activated eggs at the 1-
521 cell stage were immediately transferred to microinjection facilities.

522 For phenotyping observations five couples formed from F3 Hm males and females and five Wt
523 couples were spawned from 3 to 8 times and embryonic development, survival rate, hatching rate, and
524 larval development were subsequently observed until 22 dpf. Survival, fecundity and fertilization rate
525 data was collected from 21, 24 and 5 spawns from *vtg1*-KO, *vtg3*-KO and Wt couples, respectively.
526 Hatching rate was calculated based on the number of surviving embryos at 24h and only spawns with > 5
527 % survival rates were considered, therefore, hatching rate data was collected from 21, 16, and 5 spawns
528 from *vtg1*-KO, *vtg3*-KO and Wt couples, respectively, in this study. Fecundity (number of eggs per
529 spawn) was recorded immediately after spawning and collected eggs were incubated in 100 mm Petri
530 dishes filled with embryo medium (17.1 mM NaCl, 0.4 mM KCl, 0.65 mM $MgSO_4$, 0.27 mM $CaCl_2$, 0.01
531 mg/L methylene blue) to assess embryonic development and phenotyping parameters. Incubated
532 eggs/embryos were periodically observed at the early blastula (~256 cell) stage (~2-3 h post fertilization
533 hpf), at mid-blastula transition stage (~4 hpf), at the shield to 75% epiboly stages (~8 hpf), at the early
534 pharyngula stage (~24 hpf), and during the hatching period at 48 and 72 hpf (long-pec to protruding-
535 mouth stages) following standard developmental staging (Kimmel et al., 1995). Fertilization rate was
536 calculated based on viable embryos showing normal cell division and subsequent development to ~24 hpf
537 since zygotes failing to initiate cell division, and embryos showing asymmetrical cell cleavage or early
538 developmental arrest were dead by then. As noted above (see Discussion) it is uncertain whether these
539 aberrant eggs/embryos result from infertility or developmental defects. The number of surviving
540 eggs/embryos was recorded, those not surviving were removed and the number of abnormal embryos was
541 recorded at each observation point. Hatched embryos were transferred into larger volume containers (1 L)
542 filled with standard 28°C culture water and were fed *ad libitum* with artemia and GEMMA weaning diet
543 mix after yolk sac absorption (at around 10 dpf). At the time of feeding, larvae were also observed for
544 motor and feeding activities. Observations were made daily up to 22 dpf. Subsamples of 10-12 embryos

and larvae from each clutch were taken for measurements of embryo and chorion diameter, and larval size at 2-3 hpf and 8 dpf, respectively. Egg diameter refers to diameter of the chorion for each measured egg and embryo diameter refers to the embryo within the egg envelope. Larval size measurements were taken along the anteroposterior axis basis and all measurements were made using an ocular micrometer under a Zeiss Stemi 2000-C stereomicroscope connected to a ToupCam 3,1 M pixels camera employing the Toupview software.

4.2. Single guide RNA (sgRNA) design, synthesis and microinjection

Genomic DNA sequences from all five type-I zebrafish *vtgs* were aligned and three target sites common to all five genes were designed using CRISPR MultiTargeter (Prykhozhij et al., 2015) available online at http://www.multicrispr.net. Among proposed candidates, three target regions located on exons 4, 14 and 17, corresponding to the LvH yolk protein domain were chosen for the *vtg1*-KO experiment. The *vtg3* genomic region was separately submitted to online available target designer tool at http://zifit.partners.org/ZiFiT/ChoiceMenu.aspx (Sander et al., 2007, 2010) and of proposed candidates, three gene specific target regions located on exons 4, 6 and 11, corresponding to the LvH yolk protein domain, were chosen. All chosen target sites were additionally tested for their off target potential using the same tools. A schematic representation of the general strategy followed for CRISPR target design is presented in **Fig 1**. Forward and reverse oligonucleotides matching the chosen target sequences (given in **S1 Table)** were annealed and ligated to the pDR274 expression vector (Addgene). The vector was subsequently linearized by the DraI restriction digestion enzyme (Promega) and *in vitro* transcribed using mMessage mMachine T7 Transcription Kit (Ambion) according instructions from the manufacturer. The pCS2-nCas9n plasmid (Addgene Plasmid 47929) was digested with NotI restriction digestion enzyme (Promega) and transcribed using mMessage mMachine SP6 Transcription Kit (Ambion) according instructions from the manufacturer. The sgRNA concentration was measured on a Nanodrop 1000 Spectrophotometer (Thermo Scientific, USA) and integrity was tested before use using an Agilent RNA 6000 Nano Kit (Agilent) on an Agilent 2100 Bioanalyzer.

Approximately 100 eggs per batch were injected with sgRNA mix containing sgRNAs for three target sites (at ~30 ng/µl (=30 mM) in 20µl of the final mix each) and nCas9n RNA (at ~200 ng/µl (=200 mM) in the final mix) at the one-cell stage in both the *vtg1*-KO and *vtg3*-KO experiments. A total of 120 pg sgRNA mix and ~800 pg Cas9 RNA was injected per embryo. Injected embryos were kept in 100 mm petri dishes filled with embryo medium (17.1 mM NaCl, 0.4 mM KCl, 0.65 mM $MgSO_4$, 0.27 mM $CaCl_2$, 0.01 mg/L methylene blue) to assess microinjection efficiency, embryo survival and development post injection.

4.3. Genotyping by conventional PCR

As representatives of their generation, ten embryos were sampled randomly and gDNA was extracted individually and used as a template in targeted conventional PCR reactions to screen for introduced mutations in the targeted *vtg* genes. For this purpose, embryos surviving for 24 hours post-injection were incubated in 100 µl of 5 % Chelex® 100 Molecular Biology Grade Resin (BioRad) and 50 µl of Proteinase K Solution (20 mg/ml, Ambion) initially for 2 hours at 55 ºC and subsequently for 10 minutes at 99 ºC with constant agitation at 12000 rpm. Extracts were then centrifuged at 5000 xg for 10 minutes and supernatant containing gDNA was transferred into new tubes and stored at -20 ºC until use.

To evaluate generational transfer of introduced mutations, genotyping of ~2-month-old offspring was conducted after extraction of gDNA from finclips. For this purpose, fish were anaesthetized in 2-phenoxyethanol (0.5 ml/L) and part of their caudal fin was excised with a sterile scalpel. Genomic DNA from fin tissues were then extracted using Chelex 5 % as described above.

One µl (~ 100 ng) of extracted gDNA was used in 20 µl PCR reactions using AccuPrime™ Taq DNA Polymerase, High Fidelity (Invitrogen) and 10x AccuPrime™ PCR Buffer II in combination with gene specific primer pairs (10 µM per primer) anchoring target sites on the genomic sequence of targeted genes (**Fig 3**). In cases where one primer of the pair was highly identical to sequences common to more than one form of type-I *vtg*, it was ensured that the other primer was completely specific to *vtg1*.

PCR cycling conditions were as follows; 1 cycle of initial denaturation at 94 °C for 2 minutes, 35 cycles of denaturation at 94 °C for 15–30 seconds, annealing at 52–64 °C for 15–30 seconds and extension at 68 °C for 1 minute per kb plus 1 cycle of final extension at 68 °C for 5 minutes. Non-purified PCR products or gel purified DNA were sequenced using gene specific primers indicated in **S1 Table** by the Eurofins Genomics sequencing service (https://www.eurofinsgenomics.eu/). Obtained sequences were aligned to corresponding zebrafish genomic sequence using Clustal Omega (Sievers et al., 2011) for characterization and localization of introduced mutations, and then were blasted against all sequences available online using NCBI nucleotide Blast (Blastn) (Altschul et al., 1990) for confirmation of the consistency, accuracy and type of the mutations created at the target sites.

4.4. Generation of pure zebrafish lines carrying the introduced mutations

In both the *vtg1*-KO and *vtg3*-KO experiments, embryos carrying introduced mutations were raised to adulthood, fin clipped and re-genotyped to confirm mutation of their type-I or III *vtgs,* and then heterozygous (Ht; *vtg1*+/- and *vtg3*+/-) males with the mutation on a single allele were outcrossed with non-related wild type (Wt; *vtg1*+/+ and *vtg3*+/+) females with no genomic disturbance to produce the F1 generation. Embryos from F1 generation were genotyped as stated above and remaining embryos were raised to adulthood. F1 offspring were screened again at ~2 months of age and, since mutation transmission occurred in two males only per group, these Ht males were crossed with Wt females to produce the F2 generation. Following the same genotyping strategy, F2 Ht males were crossed with Ht females to produce the F3 generation. Finally, F3 homozygous (Hm; *vtg1*-/- and *vtg3*-/-) males and Hm females with both alleles carrying the desired mutation were crossed to produce the F4 *vtg* mutants.

4.5. Tissue sampling and analyses

Liver and ovary samples from *vtg1*-KO and *vtg3*-KO F3 Hm, Ht, wt and Wt female zebrafish were excised within 2-3 hours after egg collection at the end of phenotyping experiment and after the fish were euthanized with a lethal dose of 2-phenoxyethanol (0.5 ml/L). Ovary samples were aliquoted into

four pieces and stored according to subsequent analytical procedures; snap frozen for RNA and protein extraction or placed in Bouin's solution for histological analyses. Liver samples were aliquoted in two pieces and snap frozen until being used for LC-MS/MS or Western blotting.

4.6. Quantitative real time PCR

Total RNA was extracted from frozen liver using TriReagent (SIGMA) and cDNA was synthesized using SuperScript III reverse transcriptase (Invitrogen, USA) from 1 µg of total RNA according to the manufacturer's instructions. Relative expression levels for all zebrafish *vtgs* (*vtg1, 2, 3, 4, 5, 6* and *7*) in *vtg1*-KO female liver were measured using TaqMan real-time quantitative PCR (RT-qPCR) using gene specific primers and dual-labeled probes (FAM, 6-carboxyfluorescein and a BHQ-1, Black Hole Quencher 1 on 5' and 3´ terminus, respectively). Sequences of these primers and probes used in this experiment are given in **S1 Table**. Each qPCR was performed in 10 µl reactions containing cDNA (diluted at 1:25), 600 nM of each primer, 400 nM of hydrolysis probe and 1× TaqMan Fast Advanced Master Mix (Applied Biosystems) according the manufacturer's instructions on a StepOnePlus real time PCR instrument (Applied Biosystems). PCR cycling conditions were as follows: 95°C for 20 seconds, 40 cycles at 95°C for 1 second followed by an annealing-extension at 60°C for 20 seconds. The relative abundance of the target cDNA within a sample set was calculated from a serial dilution curve made from the cDNA pool, using StepOne software (Applied Biosystems). The $2^{-\Delta\Delta CT}$ mean relative quantification of gene expression method with zebrafish *18S* as a reference gene was employed in this study. Relative expression levels of all zebrafish *vtgs* in *vtg3*-KO female liver were measured using SYBR GREEN qPCR Master Mix (SYBR Green Master Mix kit; Applied Biosystems) as indicated by the manufacturer in a total volume of 10 µl, containing RT products diluted at 1:1000 and 400 nM of each primer in order to obtain PCR efficiency between 95 and 100 %. Sequences of primers used in this experiment are given in **S1 Table**. The RT-qPCR cycling protocol included 3 minutes initial denaturation at 95 ºC followed by 40 cycles of 95 ºC for 3 seconds and 60 ºC for 30 seconds on a StepOnePlus thermocycler (Applied Biosystem). The relative abundance of target cDNA within a sample set was calculated from a serially

649 diluted cDNA pool (standard curve) using Applied Biosystem StepOne V.2.0 software. Similarly, the $2^{-\Delta\Delta CT}$
650 mean relative quantification of gene expression method with the mean expression value of zebrafish
651 elongation factor 1a (*eif1a*), ribosomal protein 13a (*rpl13a*) and *18S* as reference were employed in this
652 study. Primer sequences and properties for these genes are also given in **S1 Table**. Obtained data was
653 subjected to independent samples Kruskal-Wallis nonparametric test ($p<0.05$) followed by Benjamini
654 Hochberg correction for multiple tests ($p<0.1$) (IBM SPSS Statistics Version 19.0.0, Armonk, NY).
655
656 **4.7. Western Blotting**
657 Samples of zebrafish liver, ovary and eggs were homogenized in 100 µl of protein binding buffer
658 containing 1 mM AEBSF, 10 mM Leupeptin, 1 mM EDTA and 0.5 mM DTT as indicated by Hiramatsu
659 et al. (2002) using a Procellys tissue homogenizer (Bertin Instruments, France). Protein extracts were
660 separated from homogenates with centrifugation at 13 000 rpm +4 ºC for 30 minutes to generate
661 supernatant samples for SDS-PAGE. Protein concentrations of the samples were estimated by Bradford
662 Assay (Bradford, 1976) (Bio-Rad, Marnes-la-Coquette, France) and they were diluted to 4 µg protein μl^{-1}
663 in ultrapure water, mixed 1:1 v/v with Laemmli sample buffer (Laemmli, 1970) containing 2-
664 mercaptoethanol, and boiled for 5 minuntes before electrophoresis. A total of 10 µg of sample protein was
665 loaded onto a precast 4–15 % acrylamide gradient Tris–HCl Ready Gel® (BioRad, Hercules, CA) with 4
666 % acrylamide stacking gel and electrophoresed at 150 V for 45 minutes using a Tris–glycine buffer
667 system (Laemmli, 1970). Biotinylated protein molecular weight markers (Vector Laboratories, USA)
668 were used to estimate the mass of separated proteins.
669 Proteins in the gels were transferred to PVDF membranes using a Trans-Blot® Turbo™ Transfer
670 Starter System (BioRad) at 25 mA for 15 minutes. Blots were blocked for 2 hours with Casein solution in
671 tris buffered saline (10 mM Tris HCl containing 15 mM NaCl) and 0.05% Tween 20 (TBST) to reduce
672 non-specific reactions. Affinity purified polyclonal primary antibody raised against a specific peptide
673 epitope on lipovitellin light chain of zebrafish Vtg3 (anti-zfLvL3, GeneScript Custom Antibody
674 production Service, USA) was employed to detect Vtg3 or its product yolk proteins in liver, ovary and

675 eggs from F3 *vtg3*-KO zebrafish. For this purpose, blots were incubated for 2 h at room temperature with
676 the anti-zfLvL3 at a 1:000 dilution in phosphate buffered saline (10 mM Na_2HPO_4, pH 7.5, 150 mM
677 NaCl). Membranes were washed three times for 5 minutes in TBST solution and incubated in biotinylated
678 goat anti-rabbit IgG affinity purified secondary antibody diluted 1:8000 in casein solution for 30 minutes
679 at room temperature. Membranes were washed in TBST solution three times for 5 minutes each and
680 incubated in VECTASTAIN® ABC-AmP™ reagent (VECTASTAIN ABC-AmP Kit, for Rabbit IgG,
681 Chemiluminescent Western Blot Detection, Vector Laboratories) for 10 minutes at room temperature.
682 Following three washes of 5 minutes in TBST, membranes were equilibrated in 0.1 M Tris buffer, pH 9.5
683 before development in DuoLuX™ Substrate (Vector Laboratories) and exposure to chemiluminescent
684 signal detection on FUSION-FX7 advanced chemiluminescence/fluorescence system (Vilber Lourmat,
685 Germany). In preliminary experiments performed to optimize concentrations of the second antibody
686 employing ovary samples from Wt fish, 'no primary antibody' control blots did not produce any signal,
687 verifying that detected immunoreactivity was due to the primary antibody (*data not shown*).
688
689 **4.8. Liquid Chromatography Tandem Mass Spectrometry**
690 Protein extraction of liver and egg samples from *vtg1*-KO, *vtg3*-KO and Wt female zebrafish
691 were done as described by Yilmaz et al. (2017). Briefly, samples were subjected to sonication in 20 mM,
692 pH 7.4, HEPES buffer on ice, soluble protein extracts were recovered following centrifugation (15 000 x
693 g) at +4 ºC for 30 minutes and the remaining pellet was re-sonicated in 30 mM Tris / 8 M Urea / 4 %
694 CHAPS buffer on ice. Ultracentrifugation (105,000 xg) of the pooled protein extracts for 1 hour at 4 ºC
695 was followed by supernatant recovery and determination of the protein concentration by Bradford Assay
696 (Bradford, 1976) (Bio-Rad, Marnes-la-Coquette, France). Samples of extracts were mixed with sample
697 buffer and DTT and denatured at 70 ºC for 10 minute before being subjected to SDS-PAGE (60 µg
698 protein/sample lane). When protein samples had completely penetrated the stacking gel (~2 minutes at
699 200 V-400 mA (~23 W)), electropohoresis was stopped and gels were briefly rinsed in MilliQ ultrapure
700 water (Millipore S.A.S., Alsace, France) and then incubated in fixation solution containing 30 % EtOH /

10 % acetic acid / 60 % MilliQ water for 15 minutes in order to fix proteins on the gel. Gels were then washed in MilliQ water three times for 5 min each and incubated in EZBlue™ Gel Staining Reagent (Sigma-Aldrich, Saint-Quentin Fallavier, France) at room temperature with slight agitation for 2 hours, and de-stained in MilliQ water at room temperature overnight. Subsequently, protein bands were excised from the gel and the excised gel pieces were processed for tryptic digestion and peptide extraction as indicated by Yilmaz et al. (2017). Once peptide extraction was completed, pellets containing digested peptides were resolubilized in 30 µl of 95 % H_2O : 5 % formic acid by vortex mixing for 10 minutes and diluted 10 times before being subjected to LC-MS/MS.

Peptide mixtures were analyzed using a nanoflow high-performance liquid chromatography (HPLC) system (LC Packings Ultimate 3000, Thermo Fisher Scientific, Courtaboeuf, France) connected to a hybrid LTQ-OrbiTrap XL spectrometer (Thermo Fisher Scientific) equipped with a nanoelectrospray ion source (New Objective), as previously described (Lavigne et al., 2012; Yilmaz et al., 2017). The spectra search, protein identification, quantification by spectral counts, and spectral count normalization were conducted as described by Yilmaz et al. (2017). To detect significant differences between group mean N-SC values (*vtg1*-KO vs Wt or *vtg3*-KO vs Wt) for different zebrafish Vtgs from liver and eggs, an independent samples Kruskal-Wallis nonparametric test ($p<0.05$) followed by Benjamini Hochberg correction for multiple tests ($p<0.1$) was used (IBM SPSS Statistics Version 19.0.0, Armonk, NY).

4.9. Ethical Statement

All experiments complied with French & European regulations ensuring ‘animal welfare' and that 'Animals will be held in the INRA UR1037 LPGP fish facility (DDCSPP approval # B35-238-6).’ Experimental protocols involving animals were approved by the Comité Rennais d'éthique pour l'expérimentation animale (CREEA).

5. COMPETING INTERESTS

Authors declare no competing interests.

6. FUNDING

This study was supported by the Region Bretagne in France (SAD-2013)-FishEgg (8210); Project #13009218), the EC-Marie Skłodowska-Curie Actions within the frame of the IEF program (FP7-PEOPLE-2013-IEF; FISHEGG: Project # 626272) and Maternal Legacy (ANR-13-BSV7-0015).

7. ACKNOWLEDGMENTS

Authors would like to thank Dr. Amaury Herpin and Dr. Amine Bouchareb for their advice in development of methodological strategies, and Dr. Craig V. Sullivan for his valuable contribution in reviewing and evaluating the manuscript.

8. REFERENCES

Alix, M., Zarski, D., Chardard, D., Fontaine, P., Schaerlinger, B. (2017). Deformities in newly hatched embryos of Eurasian perch populations originating from two different rearing systems. *Journal of Zoology*, 302,126-137.

Altschul, S.F., Gish, W., Miller, W., Myers, E.W., Lipman, D.J. (1990). Basic local alignment search tool. *Journal of Molecular Biology*, 215, 403-410.

Andersen, Ø., Xu, C., Timmerhaus, G., Kirste, K.H., Naeve, I., Mommens, M., Tveiten, H. (2017). Resolving the complexity of vitellogenins and their receptors in the tetraploid Atlantic salmon (Salmo salar): ancient origin of the phosvitin-less VtgC in chondrichthyean fishes. *Molecular Reproduction and Development*, 84(11), 1191–1202.

752 Babin, P.J., Carnevali, O., Lubzens, E., Schneider, W.J. (2007). Molecular aspects of oocyte
753 vitellogenesis in fish. In: Babin, P.J., Cerdà, J., Lubzens, E. (Eds.), The Fish Oocyte: From Basic
754 Studies to Biotechnological Applications. Springer, Dordrecht, pp. 39–76.
755 Babin, P.J. (2008). Conservation of a vitellogenin gene cluster in oviparous vertebrates and identification
756 of its traces in the platypus genome. *Gene*, 413, 76–82.
757 Bhattacharya, D., Sarkar, S., Juim, S.K., Nath, P. (2018). Induction of fertilizable eggs by conspecific
758 vitellogenin implantation in captive female walking catfish, *Clarias batrachus*. *Aquaculture Research*,
759 49, 3167-3175.
760 Bradford, M.M. (1976). A rapid and sensitive method for the quantitation of microgram quantities of
761 protein utilizing the principle of protein-dye binding. *Analytical Biochemistry*, 72, 248-254.
762 Carnevali, O., Centonze, F., Brooks, S., Marota, I., Sumpter, J.P. (1999a) Molecular cloning and
763 expression of ovarian cathepsin D in seabream, *Sparus aurata*. *Biology of Reproduction,* 66, 785–791.
764 Carnevali, O., Carletta, R., Cambi, A., Vita, A., Bromage, N. (1999b). Yolk formation and degradation
765 during oocyte maturation in seabream, *Sparus aurata*: involvement of two lysosomal proteinases.
766 *Biology of Reproduction,* 60, 140–146.
767 Carnevali, O., Cionna, C., Tosti, L., Lubzens, E., Maradonna, F. (2006). Role of cathepsins in ovarian
768 follicle growth and maturation. *General and Comparative Endocrinology,* 146, 195–203.
769 Cerdà, J., Fabra, M., Raldúa, D. (2007). Physiological and molecular basis of fish oocyte hydration. In:
770 Babin, P.J., Cerdà, J., Lubzens, E. (Eds.), The Fish Oocyte: From Basic Studies to Biotechnological
771 Applications. Springer, Dordrecht, pp. 349–396.
772 Cerdà, J., Zapater, C., Chauvigné, F., Finn, R.N. (2013). Water homeostasis in the fish oocyte: new
773 insights into the role and molecular regulation of a teleost-specific aquaporin. *Fish Physiology and*
774 *Biochemistry*, 39, 19–27.
775 Costa, R.S., de Souza, F.M.S., Senhorini, J.A., Veríssimo-Silveira, R., Ninhaus-Silveira, A. (2017).
776 Effects of cryoprotectants and low temperatures on hatching and abnormal embryo development of
777 Prochilodus lineatus (Characiformes: Prochilodontidae). *Neotropical Ichthyology*, 15, e170043.

778 Doudna, J.A., Charpentier, E. (2014). The new frontier of genome engineering with CRISPR-Cas9.
779 *Science* 346, 6213; DOI: 10.1126/science.1258096.
780 Ellis, T.R., Crawford, B.D. (2016). Experimental dissection of metalloproteinase inhibition-mediated and
781 toxic effects of phenanthroline on zebrafish development. *International Journal of Molecular*
782 *Sciences*, 17, 1503 DOI:10.3390/ijms17091503.
783 Finn, R.N. (2007). The maturational disassembly and differential proteolysis of paralogous vitellogenins
784 in a marine pelagophil teleost: A conserved mechanism of oocyte hydration. *Biology of Reproduction*,
785 76, 936-948.
786 Finn, R.N., Kristoffersen, B.A. (2007). Vertebrate vitellogenin gene duplication in relation to the "3R
787 hypothesis": correlation to the pelagic egg and the oceanic radiation of teleosts. *PLoS One*, 2(1):e169.
788 Finn, R.N., Kolarevic, J., Kongshaug, H., Nilsen, F. (2009). Evolution and differential expression of a
789 vertebrate vitellogenin gene cluster. *BMC Evolutionary Biology*, 9:2.
790 Finn, R.N., Fyhn, H.J. (2010). Requirement for amino acids in ontogeny of fish. *Aquaculture Research*,
791 41, 684-716.
792 Flouriot, G., Pakdel, F., Valotaire, Y. (1996). Transcriptional and post-transcriptional regulation of
793 rainbow trout estrogen receptor and vitellogenin gene expression. *Molecular and Cellular*
794 *Endocrinology*, 124, 173-183.
795 Gabor, K.A., Goody, M.F., Mowel, W.K., Breitbach, M.E., Gratacap, R.L. Witten, P.E., Kim, C.H.
796 (2014). Influenza A virus infection in zebrafish recapitulates mammalian infection and sensitivity to
797 anti-influenza drug treatment. *Disease Models and Mechanisms*, 7, 1227-1237.
798 Hanke, N., Staggs, L., Schroder, P., Litteral, J., Fleig, S., Kaufeld, J., Pauli, C., Haller, H., Schiffer, M.
799 (2013). ''Zebrafishing'' for Novel Genes Relevant to the Glomerular Filtration Barrier. *BioMed*
800 *Research International,* 658270; http://dx.doi.org/10.1155/2013/658270.
801 Hiramatsu, N., Hara, A., Hiramatsu, K., Fukada, H., Weber G.M., Denslow, N.D., Sullivan, C.V. (2002).
802 Vitellogenin-derived yolk proteins of white perch, *Morone americana*: Purification, characterization,
803 and vitellogenin-receptor binding. *Biology of Reproduction*, 67, 655-667.

804 Hiramatsu, N., Cheek, A.O., Sullivan, C.V., Matsubara, T., Hara, A. (2005). Vitellogenesis and endocrine
805 disruption. In: Mommsen, T.P., Moon, T. (Eds.), Biochemistry and Molecular Biology of Fishes,
806 Environmental Toxicology Vol. 6. 2005; Elsevier Science Press, Amsterdam, The Netherlands, pp.
807 431–471 (Chapter 16, 562 pp).
808 Hiramatsu, N., Todo, T., Sullivan, C.V., Schilling, J., Reading, B., Matsubara, T., Ryu, Y-W., Mizuta, H.,
809 Luo, W., Nishimiya, O., Wu, M., Mushirobira, Y., Yilmaz, O., Hara, A. (2015). Ovarian yolk
810 formation in fishes: molecular mechanisms underlying formation of lipid droplets and vitellogenin-
811 derived yolk proteins. *General and Comparative Endocrinology*, 221, 9-15.
812 Hyams, G., Abadi, S., Lahav, S., Avni, A., Halperin, E., Shani, E., Mayrose, I. (2018). CRISPys: Optimal
813 sgRNA design for editing multiple members of a gene family using the CRISPR system. Journal of
814 Molecular Biology, 430, 2184-2195.
815 Juin, S.K., Mukhopadhyay, B.C., Biswas, S.R., Nath, P. (2017). Conspecific vitellogenin induces the
816 expression of vg gene in the Indian male walking catfish, *Clarias batrachus* (Linn.). *Aquaculture*
817 *Reports*, 6, 61-67.
818 Kimmel, C.B., Ballard, W.W., Kimmel, S.R., Ullmann, B., Schilling, T. (1995). Stages of embryonic
819 development of the zebrafish. *Developmental Dynamics*, 203, 253-310.
820 Krøvel, A.V., Olsen, L.C. (2002). Expression of a vas::EGFP transgene in primordial germ cells of the
821 zebrafish. *Mechanisms of Development*, 116, 141-150.
822 Laemmli, U.K. (1970). Cleavage of structural proteins during the assembly of the head of bacteriophage
823 T4. *Nature*, 227, 680–685.
824 Lavigne, R., Becker, E., Liu, Y., Evrard, B., Lardenois, A., Primig, M., Pineau, C. (2012). Direct iterative
825 protein profiling (DIPP)-an innovative method for large-scale protein detection applied to budding
826 yeast mitosis. *Molecular and Cellular Proteomics*, 11, M111-012682.
827 Levi, L., Pekarski, I., Gutman, E., Fortina, P., Hyslop, T., Biran, J., Levavi-Sivan, B., Lubzens, E. (2009).
828 Revealing genes associated with vitellogenesis in the liver of the zebrafish (*Danio rerio*) by
829 transcriptome profiling. *BMC Genomics*, 10:141. http://dx. doi.org/10.1186/1471-2164-10-141.

Levi, L., Ziv, T., Admon, A., Levavi-Sivan, B., Lubzens, E. (2012). Insight into molecular pathways of retinal metabolism, associated with vitellogenesis in zebrafish. *American Journal of Physiology-Endocrinology and Metabolism*, 302, E626–E644.

Li, A., Sadasivam, M., Ding, J.L. (2003). Receptor–ligand interaction between vitellogenin receptor (VtgR) and vitellogenin (Vtg), implications on low density lipoprotein receptor and apolipoprotein B/E. The first three ligand binding repeats of VtgR interact with the amino-terminal region of Vtg. *The Journal of Biological Chemistry*, 278, 2799–2806.

Liu, H., Sui, T., Liu, D., Liu, T., Chen, M., Deng, J., Xu, Y., Li, Z. (2018). Multiple homologous genes knockout (KO) by CRISPR/Cas9 system in rabbit. *Gene*, 647, 261–267.

Lubzens, E., Bobe, J., Young, G., Sullivan, C.V. (2017). Maternal investment in fish oocytes and eggs: The molecular cargo and its contributions to fertility and early development. *Aquaculture,* 472, 107-143.

Marschang, P., Brich, J., Weeber, E.J., Sweatt, J.D., Shelton, J.M., Richardson, J.A., Hammer, R.E., Herz, J. (2004). Normal development and fertility of knockout mice lacking the tumor suppressor gene LRP1b suggests functional compensation by LRP1. *Molecular and Cellular Biology*, 24,3782-3793.

Matsubara, T., Koya, Y. (1997). Course of proteolytic cleavage in three classes of yolk proteins during oocyte maturation in barfin flounder, *Verasper moseri*, a marine teleost spawning pelagic eggs. *Journal of Experimental Zoology*, 278, 189-200.

Matsubara, T., Ohkubo, N., Andoh, T., Sullivan, C.V., Hara, A. (1999). Two forms of vitellogenin, yielding two distinct lipovitellins, play different roles during oocyte maturation and early development of barfin flounder, *Verasper moseri*, a marine teleost spawning pelagic eggs. *Developmental Biology*, 213, 18–32.

Matsubara, T., Nagae, M., Ohkubo, N., Andoh, T., Sawaguchi, S., Hiramatsu, N., Sullivan, C.V., Hara, A. (2003). Multiple vitellogenins and their unique roles in marine teleosts. *Fish Physiology and Biochemistry*, 28, 295–29.

855 Nelson, E.R., Habibi, H.R. (2013). Estrogen receptor function and regulation in fish and other vertebrates.
856 *General and Comparative Endocrinology,* 192, 15–24. http://dx.doi.org/10.1016/j. ygcen.2013.03.032.
857 Opresko, L.K., Wiley, H.S. (1987). Receptor-mediated endocytosis in *Xenopus* oocytes: I-
858 Characterization of vitellogenin receptor system. *The Journal of Biological Chemistry,* 262, 4109-
859 4115.
860 Ottesen, O.H., Bolla, S. (1998). Combined effects of temperature and salinity on development and
861 survival of Atlantic halibut larvae. *Aquaculture International*, 6, 103-120.
862 Patiño, R., Sullivan, C.V. (2002). Ovarian follicle growth, maturation and ovulation in teleost fish. *Fish*
863 *Physiology and Biochemistry*, 26, 57–70.
864 Prykhozhij, S.V., Rajan, V., Gaston, D., Berman, J.N. (2015). CRISPR MultiTargeter: A web tool to find
865 common and unique CRISPR single guide RNA targets in a set of similar sequences. *PLoS ONE*,
866 10(3): e0119372. doi:10.1371/journal.pone.0119372.
867 Reading, B.J., Hiramatsu, N., Sawaguchi, S., Matsubara, T., Hara, A., Lively, M.O., Sullivan, C.V.
868 (2009). Conserved and variant molecular and functional features of multiple vitellogenins in white
869 perch (*Morone americana*) and other teleosts. *Marine Biotechnology*, 11, 169–187.
870 Reading, B.J., Sullivan, C.V. (2011). The Reproductive Organs and Processes - Vitellogenesis in Fishes,
871 Editor: Anthony P. Farrell, Encyclopedia of Fish Physiology, Academic Press, pp 635-646,
872 https://doi.org/10.1016/B978-0-12-374553-8.00257-4.
873 Reading, B.J., Sullivan, C.V., Schilling, J. (2017). Vitellogenesis in fishes. Reference Module in Life
874 Sciences, Elsevier, https://doi.org/10.1016/B978-0-12-809633-8.03076-4.
875 Reis-Henriques, M.A., Cruz, M.M., Periera, J.O. (1997). The modulating effect of vitellogenin on the
876 synthesis of 17□-estradiol by rainbow trout (*Oncorhynchus mykiss*) ovary. *Fish Physiology and*
877 *Biochemistry,* 16, 181-186.
878 Reis-Henriques, M.A., Ferriera, M., Silva, L., Dias, A. (2000). Evidence for an involvement of
879 vitellogenin in the steroidogenic activity of rainbow trout (*Oncorhynchus mykiss*) vitellogenic oocytes.
880 *General and Comparative Endocrinology*, 117, 260-267.

881 Reith, M., Munholland, J., Kelly, J., Finn, R.N., Fyhn, H.J. (2001). Lipovitellins derived from two forms
882 of vitellogenin are differentially processed during oocyte maturation in haddock (*Melanogrammus*
883 *aeglefinus*). *Journal of Experimental Zoology*, 291, 58–67.
884 Ren, L., Lewis, S.K., Lech, J.J. (1996). Effects of estrogen and nonylphenol on the post-transcriptional
885 regulation of vitellogenin gene expression. *Chemico-Biological Interactions*, 100, 67-76.
886 Ribas, L., Piferrer, F. (2013). The zebrafish (*Danio rerio*) as a model organism, with emphasis on
887 applications for finfish aquaculture research. *Reviews in Aquaculture*, 5, 1-32.
888 Sander, J.D., Zaback, P.Z., Joung, J.K., Voytas, D.F., Dobbs, D. (2007). Zinc Finger Targeter (ZiFiT): an
889 engineered zinc finger/target site design tool. *Nucleic Acids Research*, 35, W599-605.
890 Sander, J.D., Maeder, M.L., Reyon, D., Voytas, D.F., Joung, J.K., Dobbs, D. (2010). ZiFiT (Zinc Finger
891 Targeter): an updated zinc finger engineering tool. *Nucleic Acids Research*, 38, W462-468.
892 Sawaguchi, S., Ohkubo, N., Koya, Y., Matsubara, T. (2005). Incorporation and utilization of multiple
893 forms of vitellogenin and their derivative yolk proteins during vitellogenesis and embryonic
894 development in the mosquitofish, *Gambusia affinis*. *Zoological Sciences,* 22, 701-710.
895 Sawaguchi, S., Ohkubo, N., Matsubara, T. (2006a). Identification of two forms of vitellogenin-derived
896 phosvitin and elucidation of their fate and roles during oocyte maturation in the barfin flounder,
897 *Verasper moseri*. *Zoological Sciences*, 23, 1021-1029.
898 Sawaguchi, S., Kagawa, H., Ohkubo, N., Hiramatsu, N., Sullivan, C.V., Matsubara, T. (2006b).
899 Molecular characterization of three forms of vitellogenin and their yolk protein products during oocyte
900 growth and maturation in red seabream (*Pagrus major*), a marine teleost spawning pelagic eggs.
901 *Molecular Reproduction and Development*, 73, 719-736.
902 Sievers, F., Wilm, A., Dineen, D.G., Gibson, T.J., Karplus, K., Li, W., Lopez, R., McWilliam, H.,
903 Remmert, M., Söding, J., Thompson, J.D., Higgins, D. (2011). Fast, scalable generation of high
904 quality protein multiple sequence alignments using Clustal Omega. *Molecular Systems Biology*, 7, 5-
905 39. doi: 10.1038/msb.2011.75.

906 Sullivan, C.V., Yilmaz, O. (2018). Vitellogenesis and yolk proteins, fish. Editor: Michael K. Skinner,
907 Encyclopedia of Reproduction (Second Edition), Academic Press, pp 266-277,
908 https://doi.org/10.1016/B978-0-12-809633-8.20567-0.
909 Sun, B., Pankhurst, N.W. (2006). In vitro effect of vitellogenin on steroid production by ovarian follicles
910 of greenback flounder, *Rhombosolea tapirina*. *Comparative Biochemistry and Physiology Part A*, 144,
911 75-85.
912 Sztal, T.E., McKaige, E.A., Williams, C., Ruparelia, A.A., Bryson-Richardson, R.J. (2018). Genetic
913 compensation triggered by actin mutation prevents the muscle damage caused by loss of actin protein.
914 *PLoS Genetics*, 14: e1007212.
915 Thorsen, A., Fyhn, H.J. (1996). Final oocyte maturation in vivo and in vitro in marine fishes with pelagic
916 eggs; yolk protein hydrolysis and free amino acid content. *Journal of Fish Biology*, 48, 1195–1209.
917 Trubiroha, A., Gillotay, P., Giusti, N., Gacquer, D., Libert, F., Lefort, A., Haerlingen, B., De Deken, X.,
918 Opitz, R., Costagliola, S. (2018). A Rapid CRISPR/Cas-based Mutagenesis Assay in Zebrafish for
919 Identification of Genes Involved in Thyroid Morphogenesis and Function. *Scientific Reports*, 8, 5647
920 https://doi.org/10.1038/s41598-018-24036-4.
921 Tsuruwaka, Y., Konishi, M., Shimada, E. (2015). Loss of wwox expression in zebrafish embryos causes
922 edema and alters Ca2+ dynamics. *PeerJ,* 3: e727; DOI 10.7717/peerj.727.
923 Xie, S-L., Bian, W-P., Wang, C., Junaid, M., Zou, J-X., Pei, D-S. (2016). A novel technique based on in
924 vitro oocyte injection to improve CRISPR/Cas9 gene editing in zebrafish. *Scientific Reports*, 6, 34555;
925 doi: 10.1038/srep34555 (2016).
926 Yang, J., Li, Z., Gan, X., Zhai, G., Gao, J., Xiong, C., Qiu, X., Wang, X., Yin, Z., Zheng, F. (2016).
927 Deletion of Pr130 Interrupts Cardiac Development in Zebrafish. *International Journal of Molecular*
928 *Sciences*, 17: 1746; doi:10.3390/ijms17111746.
929 Yilmaz, O., Prat, F., Ibáñez, J.A., Koksoy, S., Amano, H., Sullivan, C.V. (2016). Multiple vitellogenins
930 and product yolk proteins in European sea bass (*Dicentrarchus labrax*): Molecular characterization,

quantification in plasma, liver and ovary, and maturational proteolysis. *Comparative Biochemistry and Physiology Part B,* 194, 71–86.

Yilmaz, O., Patinote, A., Nguyen, T., Com, E., Lavigne, R., Pineau, C., Sullivan, C.V., Bobe, J. (2017). Scrambled eggs: Proteomic portraits and novel biomarkers of egg quality in zebrafish (*Danio rerio*). *PLoS ONE*, 12: e0188084. https://doi.org/10.1371/journal.pone.0188084.

Yilmaz, O., Patinote, A., Nguyen, T., Bobe, J. (2018). Multiple vitellogenins in zebrafish (*Danio rerio*): quantitative inventory of genes, transcripts and proteins, and relation to egg quality. Fish Physiology and Biochemistry, https://doi.org/10.1007/s10695-018-0524-y (Epub ahead of print).

Zhang, X., Lin, Q., Ren, F., Zhang, J., Dawar, F.U., Mei, J. (2018). The dysregulated autophagy signaling is partially responsible for defective podocyte development in wt1a mutant zebrafish. *Aquaculture and Fisheries*, 3, 99-105.

9. FIGURE LEGENDS

Fig 1. Schematic representation of the general strategy for CRISPR target design in the zebrafish vitellogenin gene (*vtg*) knock out (KO) study. **A)** Syntenic organization of multiple *vtg* genes. The genomic locations for *vtg* genes and neighboring genes are shown. Polygons indicate individual genes and show their available transcriptional orientation, with abbreviated gene names appearing above; different colors indicate different types of zebrafish *vtg* with red, blue, and yellow indicating zebrafish type-I, type -II, and type-III vtgs, respectively (gray indicates genes other than *vtgs*). Chr, chromosome. (from Yilmaz et al., 2018). **B)** Type-I *vtg* knock out (*vtg1*-KO). **C)** Type-III *vtg* knock out (*vtg3*-KO). Schematic representations of the intron/exon structure of zebrafish type-I *vtgs* and *vtg3* in 5' to 3' direction indicated by triangles on the left pointing to the right are given in panels **B** and **C**, respectively. Horizontal line segments indicate introns and filled gold boxes indicate exons. Exons bearing CRISPR/Cas9 target

sequences (sg11, sg12, and sg13 for type-I *vtgs*; sg31, sg32, and sg33 for *vtg3*) are indicated by large blue arrowheads pointing upwards.

Fig 2. Mutations introduced by CRISPR/Cas9 in predicted polypeptide sequences of the targeted zebrafish *vtgs*. Yolk protein domain models of Vtg1 (representative of zebrafish type-I Vtgs) and Vtg3 are pictured in 5' > 3' orientation above each panel. Contiguous white horizontal bars represent lipovitellin heavy and light chain (LvH, LvL) and phosvitin (Pv) domains of the respective Vtg (Vtg3 lacks a Pv domain) that are labeled above by their abbreviations in large bold type. Sequences within these bars set in normal type represent the N-terminus of each yolk protein domain, the starting points of which are indicated, when present, by vertical bars in the predicted polypeptide sequences shown below. Sequences arising from 5' > 3' translation (frame 1) were predicted by the Expasy translate tool (available online at https://web.expasy.org/translate/). The predicted products of open reading frames are highlighted in light gray. Start codon products (methionine, **M**) are shown in bold green type and stop codons are indicated by red dashed lines (-). The locations of deletions introduced by CRISPR/Cas9 are indicated by magenta text showing the number of deleted amino acids (aa) flanked by angle brackets. Residues encoded by nucleotide sequences targeted by sgRNAs for Cas9 editing are framed in blue-shaded boxes. Short sequences that were employed as epitopes to develop Vtg domain-specific antibodies against zebrafish (zf) Vtg1-LvH (anti-zfLvH1) and Vtg3-LvL (anti-zfLvL3) are indicated by boxed text in the respective LvH and LvL sequences, with their location also highlighted by black arrows labeled with the epitope names in vertically-oriented text in the panel margins. The 85-residue Vtg receptor-binding domain (***RbD***) and the critical 8-residue Vtg receptor-binding motif (***RbM***) located within this domain, which were identified by Li et al. (2003) in the LvH domain of blue tilapia (*Orechromis aureus*) VtgAb, are shown in the polypeptide sequences in boldface italic type. The ***RbM*** sequence is additionally

underlined and also shown in the yolk protein domain map above. The location of these sequences is highlighted by black arrows labeled with **RbD/RbM** as vertically-oriented text in the panel margins. For *vtg1*-KO (panel A), the diagram below the yolk protein domain model shows the relative location of the 234 aa deletion introduced by CRISPR/Cas9 (double headed magenta arrow), the frameshift induced by this deletion (left pointing blue arrow), the first premature stop codon arising from this frameshift (single red dash), the 529 aa sequence product of the contiguous open reading frame terminating at this stop codon (right pointing black arrow), and the remaining broken sequence interrupted by multiple stop codons (right pointing red and black dashed arrow). For *vtg3*-KO (panel B), the diagram below the yolk protein domain model employs similar color coding and shows the relative position of the in-frame 238 aa deletion, the single stop codon terminating the sequence, and the 999 aa sequence product of the contiguous open reading frame.

Fig 3. Detection of CRISPR/Cas9-introduced mutations by embryo genotyping and production of F4 generation *vtg*-KO mutants. Left and middle panels illustrate genotyping of embryos at 24 hours post-fertilization (hpf) by PCR for the *vtg1*-KO (representative of zebrafish type-I *vtgs*) and *vtg3*-KO lines, respectively, from the F0 to F4 generation. Target sites are shown by blue colored arrows labeled as sg followed by 1, 2 or 3 indicating the targeted zebrafish *vtg* type and the number of the target site (i.e. sg11, sg12, and sg13: single guide RNAs (sgRNAs) for target sites 1, 2, and 3 for *vtg1*, respectively. sg31, sg32, and sg33: sgRNAs for target sites 1, 2, and 3 for *vtg3*, respectively). Arrows are oriented to indicate the sense/antisense orientation of each target. Numbers above each target site specify its exact location by nucleotide in the genomic sequence of the zebrafish *vtgs*. Primers used in screening for introduced mutations by PCR are shown as gray arrowheads outlined in black, which are oriented to indicate the sense/antisense orientation of the primer. Numbers below each primer site indicate its exact position by nucleotide in the genomic sequence of the targeted gene (see also **S1 Fig A-B**). Horizontal brackets below indicate areas screened for mutations by PCR using selected primer combinations. Text below the brackets indicates the primer pair followed by the size of the band (bp) expected for wild type

gDNA in agarose gel electrophoresis. 11Fw, *vtg1* target1 forward primer; 12Rv, *vtg1* target2 reverse primer; 13Rv, *vtg1* target3 reverse primer; 12Fw, *vtg1* target2 forward primer; 31Fw, *vtg3* target1 forward primer; 32Rv, *vtg3* target2 reverse primer; 33Rv, *vtg3* target3 reverse primer; 32Fw, *vtg3* target2 forward primer. Primer sequences are given in **S1 Table**. F0 indicates the generation reared from microinjected embryos and F1-4 represent offspring raised from each subsequent generation. The agarose gel electrophoresis results shown here represent screening of 10 randomly sampled embryos as representatives of their generations and two additional wild type embryos as controls. Bands comprised of wild type intact gDNA (*wild type:* 3642 bp and 1733 bp for *vtg1* and *vtg3*, respectively) and mutated gDNA (*mutated:* 2361 bp and 551 bp for *vtg1*-KO and *vtg3*-KO, respectively) are shown and highlighted by black arrowheads on the right side of each panel. Open circles; non-related wild type fish (Wt) carrying intact (*vtg1*+/+ or *vtg3*+/+) genomic DNA. Open diamonds; sibling wild type individuals, which do not carry the desired mutation in either allele (*vtg1*+/+ or *vtg3*+/+) of their gDNA. Open triangles; heterozygous (Ht) individuals carrying the introduced mutation on only a single allele (*vtg1*-/+ or *vtg3*-/+) in their genomic DNA. Asterisks; homozygous embryos (Hm) carrying the introduced mutation in both alleles (*vtg1*-/- or *vtg3*-/-) of their genomic DNA. The panel on the far right illustrates the general strategy followed to establish pure zebrafish lines bearing the desired Cas9 introduced mutation. This process involved stepwise reproductive crosses (indicated by X) between males (♂) and females (♀) indicated here with zebrafish icons. F0-4 represents the zebrafish generations produced in the process. Images of sub-adult fish are shown for simplicity at generation F4; all or most of these fish were actually inviable and did not survive past early developmental stages (see text for details).

Fig 4. Relative quantification of *vtg* gene expression in *vtg*-KO zebrafish female liver. A) Comparison of gene expression levels for all *vtgs* in F3 *vtg1*-KO female liver (Hm, homozygous; Ht, heterozygous; wt, sibling wild type) versus non-related wild type female liver (Wt). TaqMan qPCR-$2^{-\Delta\Delta CT}$ mean relative quantification of gene expression was employed using zebrafish 18S ribosomal RNA (*18S*) as the reference gene. Data were statistically analyzed using a Kruskal Wallis nonparametric test $p<0.05$

followed by Bejamini Hochberg corrections for multiple tests $p<0.1$. **B)** Comparison of gene expression levels for all *vtgs* in F3 *vtg3*-KO female liver (Hm, Ht and wt) versus Wt female liver. SYBR Green qPCR-$2^{-\Delta\Delta CT}$ mean relative quantification of gene expression normalized to the geometric mean expression of zebrafish elongation factor 1a (*eif1a*), ribosomal protein L13a (*rpl13a*) and *18S* was employed. Data were statistically analyzed using a Kruskal Wallis nonparametric test $p<0.05$ followed by Benjamini Hochberg corrections for multiple tests $p<0.1$. In the box plots, the centerlines indicate the median for each data set, upper boxes indicate the difference of the 3rd quartile from the median, lower boxes indicate the difference of the 1st quartile from the median. Top whiskers indicate difference of the maximum value from the 3rd quartile and the bottom whiskers indicate the difference of the minimum values from the 1st quartile in each data set. In both panels, numbers below x-axis labels indicate sample size and lowercase letters above the error bars represent significant differences between means ($p<0.05$). For box plots sharing a common letter superscript, the means are not significantly different.

Fig 5. Relative quantification of multiple vitellogenins by LC-MS/MS in *vtg*-KO zebrafish female liver and eggs. A) Comparisons of mean normalized spectral counts (N-SC) for Vtg protein levels in Wt versus Hm F3 *vtg1*-KO female zebrafish livers and in eggs obtained from these females, indicated by dark and light gray vertical bars, respectively. Vertical brackets indicate SEM. **B)** Corresponding comparison of N-SC for Vtg protein levels in Wt versus F3 Hm *vtg3*-KO female zebrafish livers and in eggs obtained from these females. Asterisks indicate statistically significant differences between group means detected by an independent samples Kruskal Wallis non-parametric test ($p<0.05$) followed by Benjamini Hochberg correction for multiple tests ($p<0.1$)

Fig 6. Detection of Vtg3 in *vtg3*-KO versus wild type female liver, ovary and eggs by Western blotting. An affinity-purified, polyclonal anti-zfLvL3 antibody was employed to detect LvL3 in this experiment. Numbers on the left of each panel indicate the mass of molecular weight marker proteins (kDa). M, marker protein ladder; Hm, homozygous; Ht, heterozygous; Wt, non-related wild type. Bands

that were detected in Ht and Wt zebrafish, but not Hm zebrafish, whose mass corresponds to LvL derived from zebrafish (zf) Vtg3 are indicated by horizontal brackets with labels immediately underneath (zf LvL3, ~24 kDa).

Fig 7. Phenotypic measurements of F3 *vtg*-KO females and their F4 progeny. Bar graphs indicate mean values (±SEM) for measurements of each parameter and labels below the x-axes indicate the groups that were compared. Egg and embryo diameter measurements were taken in fertilized eggs at 2-3 hpf, egg diameter refers to the diameter of the chorion for each measured egg and embryo diameter refers to the embryo within the egg envelope. Larval size measurements were taken along the anteroposterior axis. In the panel at the bottom right, mean hatching percentages for Hm *vtg1*-KO, Hm *vtg3*-KO, and Wt eggs are shown as circles, triangles and diamonds, respectively. Numbers on the x-axis accompanied by dashed- and solid-lined arrows represent sampling times in hours or days post spawning, respectively. In all graphs, asterisks and black stars indicate mean values that are statistically significantly different from corresponding Wt mean values based upon results of an independent samples t-test ($p<0.01$) followed by Benjamini Hochberg corrections for multiple tests in the case of hatching percentage ($p<0.05$).

Fig 8. Comparisons of survival percentages for homozygous F4 *vtg1*-KO and *vtg3*-KO zebrafish embryos and larvae versus wild type offspring. Line plots represent mean survival percentages and numbers on the x-axis accompanied by dashed- and solid-lined arrows represent sampling times in hours or days post fertilization during the observation period. Mean survival percentages for Hm *vtg1*-KO, Hm *vtg3*-KO and unrelated Wt embryos and larvae at each time point are indicated by circles, triangles and diamonds, respectively, and vertical lines indicate SEM. Asterisks and black stars indicate mean values that are statistically significantly different from corresponding mean wild type (Wt) values based upon results of an independent samples t-test ($p<0.01$) followed by Benjamini Hochberg corrections for multiple tests ($p<0.05$).

Fig 9. Observed phenotypes of F4 homozygous (Hm) *vtg*-KO offspring compared to wild type (Wt) offspring. A) Hm *vtg1*-KO unhatched embryos and hatched larvae at 4 dpf. **B)** Dorsal view of Wt larva at 4 dpf. **C)** Lateral view of Wt larvae at 4 hpf. **D)** Hm *vtg3*-KO larvae at 4 dpf. **E)** Hm *vtg1*-KO larvae at 8 dpf. **F)** Dorsal view of Wt larva at 8 dpf. **G)** Lateral view of Wt larva at 8 dpf. **H)** Hm *vtg3*-KO larvae at 8 dpf. Special features of observed phenotypes are indicated by pointed arrows (see text for details). In all images, horizontal bars indicate 1000 μm.

10. SUPPORTING INFORMATION LEGENDS

S1 Fig. Location and character of mutations introduced by CRISPR/Cas9 in zebrafish *vtgs*. A-B) Location on genomic DNA. Schematic representations of the intron/exon structure of zebrafish *vtg1* (representative of type-I *vtgs*) and *vtg3* are given at the top of panels A and B, respectively. Horizontal line segments indicate introns and filled gold boxes indicate exons. Exons bearing CRISPR/Cas9 target sequences are indicated by large blue arrowheads pointing upwards to the target name (sg11, sg12, and sg13 for *vtg1*; sg31, sg32, and sg33 for *vtg3*). Horizontal dashed lines bearing dual arrowheads indicate regions where mutations were introduced, with the size of deletions in bp given below the arrows (1281 bp and 1181 bp for *vtg1*-KO and *vtg3*-KO, respectively). The lower sections of panels A and B show Clustal Omega alignments for partial genomic sequences of the *vtg1* and *vtg3* genes, respectively, covering regions where Cas9 introduced targeted mutations. Sequences of undisturbed wild type alleles are labeled *vtg1*+/+ and *vtg3*+/+, and sequences of homozygous mutated alleles are labeled *vtg1*-/- and *vtg3*-/-, respectively. Dashes were introduced to illustrate regions where deletions occurred in the *vtg1*-/- and *vtg3*-/-sequences. Nucleotide positions are indicated by numbers on the right and asterisks indicate nucleotide identity. Target sequences are enclosed in blue-shaded boxes emphasized by blue arrowheads on the right. Intron sequences are given in dark gray font enclosed in light gray filled frames and are labeled by Intron on the right with the same formatting. Exons are shown in regular black font and labeled

on the right with exon numbers (e.g. Exon 6, 7, 8...). Exons bearing the target sites are also labeled with the target name below in parenthesis (e.g. Exon 14 (sg12)). **C-D)** Location on mRNA**.** The deleted region of mRNA is indicated in the sequence by magenta text showing the number of deleted nucleotides (703 bp *vtg1* and 714 bp for *vtg3*) enclosed by magenta angle brackets; flanking nucleotides that come together to form a new codon are underlined in magenta. **E-F)** Location on predicted cDNA. Nucleotide sequences targeted by sgRNAs for Cas9 editing and present in the predicted transcript are framed in blue-shaded boxes. The deleted region of the transcript is indicated in the sequence by magenta text showing the number of deleted nucleotides enclosed by magenta angle brackets, with flanking nucleotides that come together to form a new codon underlined in magenta (see also **S2 Fig**). The sequence encoding the Vtg receptor-binding domain (***RbD***) on the LvH of the respective Vtg (see **G-H**, below) is shown in italic typeface with the sequence encoding its critical, short receptor-binding motif (***RbM***) being additionally underlined. **G-H)** Location on predicted polypeptide sequence. Yolk protein domain models of Vtg1 (representative of zebrafish type-I Vtgs) or Vtg3 are pictured in 5' > 3' orientation above each panel. Contiguous white horizontal bars represent lipovitellin heavy and light chain (LvH, LvL) and phosvitin (Pv) domains of the respective Vtg (Vtg3 lacks a Pv domain) that are labeled with their abbreviation above in large bold type. Sequences within these bars set in normal type represent the N-terminus of each yolk protein domain, the starting points of which are indicated, when present, by vertical bars in the predicted polypeptide sequences shown below. Predicted sequences arising from three frames of 5' > 3' translation performed using the Expasy translate tool (available online at https://web.expasy.org/translate/) are shown. Predicted products of open reading frames are highlighted in light gray, start codon products (methionine, **M**) are shown in bold green type, and stop codons are indicated by red dashed lines (-). The locations of deletions are indicated by magenta text showing the number of deleted amino acids (aa) enclosed by angle brackets. Residues encoded by nucleotide sequences targeted by sgRNAs for Cas9 editing are framed in blue-shaded boxes. Short sequences that were employed as epitopes to develop Vtg domain-specific antibodies against zebrafish (zf) Vtg1-LvH (anti-zfLvH1) and Vtg3-LvL (anti-zfLvL3) are indicated by boxed text in the respective LvH and LvL

sequences, with their location also highlighted by black arrows labeled with the epitope names given by vertically-oriented text in the panel margins. The 85-residue Vtg receptor-binding domain (***RbD***) and the critical 8-residue Vtg receptor-binding motif (***RbM***) located within this domain, which were identified by Li et al. (2003) in the LvH domain of blue tilapia (*Orechromis aureus*) VtgAb, are shown in the polypeptide sequences in boldface italic type, with the ***RbM*** sequence being additionally underlined and also shown in the yolk protein domain map above. The location of these sequences is also highlighted by black arrows labeled with **RbD/RbM** as vertically-oriented text in the panel margins. For *vtg1*-KO (panel G), the diagram below the yolk protein domain model shows the relative location of the 234 aa deletion introduced by CRISPR/Cas9 (double headed magenta arrow), the 529 aa sequence product of the contiguous open reading frame 1 (right pointing black arrow), which is terminated by a premature stop codon arising from a frameshift introduced by the deletion (see **Fig 2A**), and the 609 aa sequence product of the contiguous open reading frame 3 (right pointing blue arrow), which initiates just after the deletion. For *vtg3*-KO (panel H), the diagram below the yolk protein domain model employs the same symbols and color coding and shows the relative position of the in-frame 238 aa deletion introduced by CRISPR/Cas9 (see **Fig 2B**), and the remaining 999 aa sequence product of the contiguous open reading frame 1.

S2 Fig. Location and consequence of deletion mutations introduced by CRISPR/Cas9 into zebrafish *vtgs.* A) *vtg1*-KO. The 703 bp deletion introduces a frame shift at residue 519, changing the codon without altering the encoded amino acid (isoleucine, I). This frame shift results in the appearance of a premature stop codon after 10 additional residues (not shown, see **Fig 2A** for details). **B) *vtg3*-KO.** The 714 bp deletion alters the codon encoding residue 239, resulting in the substitution of leucine (L) for arginine (R) at this position, but it does not otherwise alter the remainder of the Vtg3 polypeptide (see **Fig 2B**).

S1 Table. Targets, primers and probes utilized in *vtg1*-KO and *vtg3*-KO studies. Target oligo and screening primer names are given according Figure 1 and 3. CRISPR recognition NGG motifs are highlighted by bold

typeface on sequences. Position of primers, target sites and probes on vitellogenin (Vtg) yolk protein (YP) domains are given on the far right columns.

Fig 1

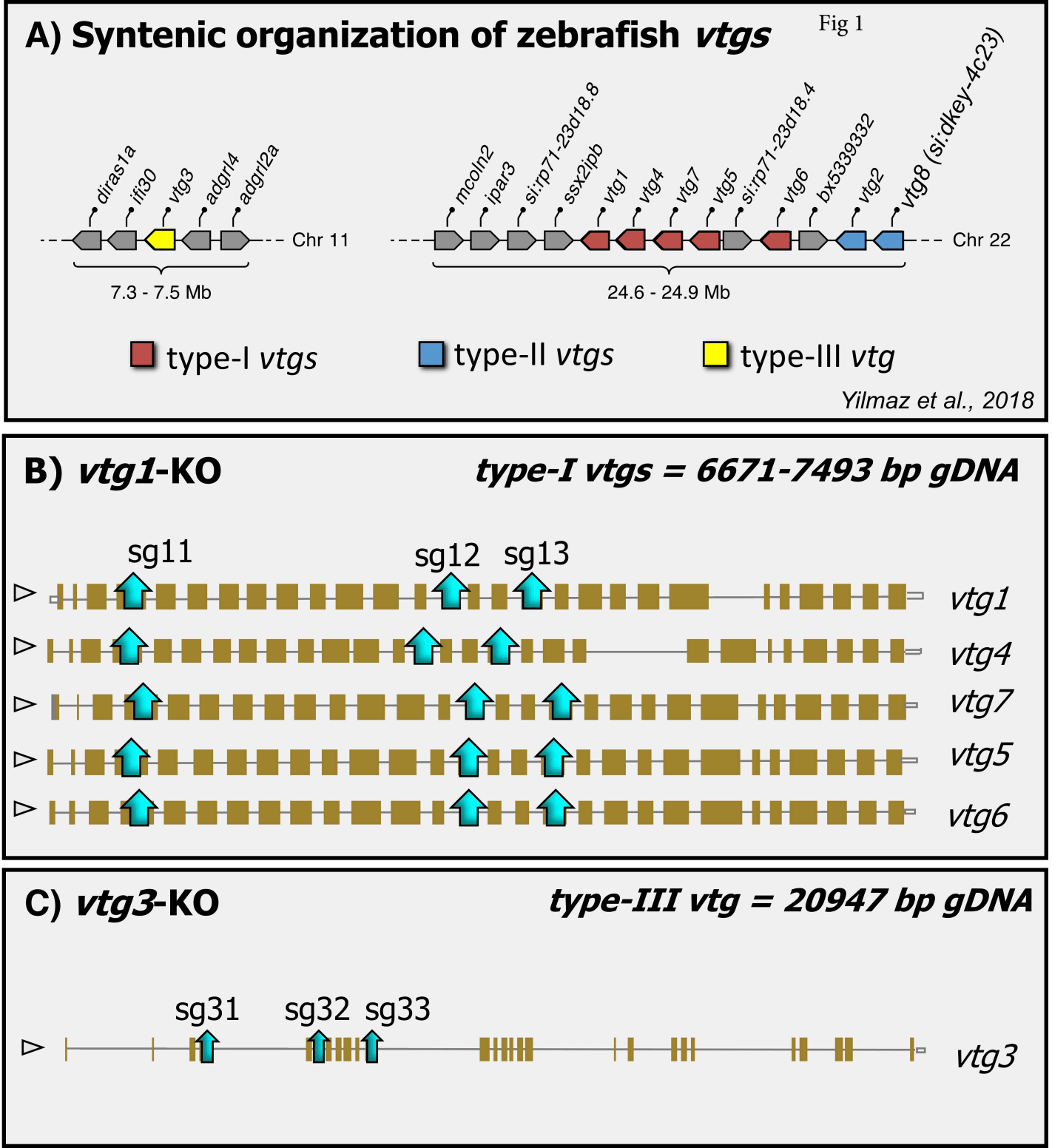
A) Syntenic organization of zebrafish vtgs
diras1a
ifi30
vtg3
adgrl4
adgrl2a
Chr 11
7.3 - 7.5 Mb
mcoln2
ipar3
si:rp71-23d18.8
ssx2ipb
vtg1
vtg4
vtg7
vtg5
si:rp71-23d18.4
vtg6
bx5339332
vtg2
vtg8 (si:dkey-4c23)
Chr 22
24.6 - 24.9 Mb
type-I vtgs
type-II vtgs
type-III vtg
Yilmaz et al., 2018
B) vtg1-KO
type-I vtgs = 6671-7493 bp gDNA
sg11
sg12
sg13
vtg1
vtg4
vtg7
vtg5
vtg6
C) vtg3-KO
type-III vtg = 20947 bp gDNA
sg31
sg32
sg33
vtg3

A) *vtg1*-KO

Frame 1 5'>3'

MRAVVLALTVALVACQQFNLVPEFAHDKTYVYKYEALLLGGLPQEGLARAGIKVSSKVLISATTENTYLMKLMD
PLLYEYAGTWPKDPFVPATKLTSALAAQLQIPIKFEYANGVVGKVFAPAGVSPTVMNLHRGILNILQLNLKKTQN
IYEMQEAGAQGVCRTHYVI*NEDPKANHIIVTKSKDLSHCQERIMKDVGLAYTERCAECTERVKSLIETATYNYIM*
*KPADNGALIAEATVEEVYQFSPFNEIHG*AAMMEAKQTLAFVEIEKTPVVPIKADYMPRGSLQYEFATEILQTPIQ
LMKISDAPAQIVEVLKHLVSNNKDMVHDDAPFKFVQLVQLLRVASLEKIEAIWSQFKDKPVYRRWLLDALPAVGT
PVIIKFIKEKFLAGEFTTPEFIQTLVIALQMVTADPETIKMTASLATHEKFATIPALREVVMLGYGSLIAKYCVA
VPTCPAELLRPIHEIATEAISKNDIPEITLALKVMGNAGHPSSLKPIMKLLPGLRTAANALPIRVQVDAI<234aa>
WLLDPNHVHC-RRLLKLCRKELPSSMLNLCLQLKCVASCQLQLVCPWSSVGTLLQLLLQVSMFRPPLHLLSLR
NWSP-LMSN-RRLMFSSKLKLDQVLLSRHLL-WELTLPSSKLLLWQEERSVQLHPEKWQQEQTFSRATTRWRLCL
LNFLNTLLLQALRLMPWSETLKITVLKGLFPWYLNCLCKTPRHLMLVICHLRCHLLLQ-ELLLHLTEPSVMLSHT
LKSRDVLRCTLTMLLLSEIPLFST-LDTTQSVLQWQELKVLQLKDWSLKFKLVLELLRGLLSKSTSLMMILQKDR
LSC-N-GKSWTLKLKMHLFLLKAAAVVTVAAAAAAAPALAPAQAQAQVQVQVQAQAPLCPALVCLRLPPSLSLSG
NSTKIGTWHTIAPQRILAVEVLQLALNKCRNRIDSLEMIFHLFLLSSPVLLELTRSFWATNWLLTLTNQLQECN-
-FPPLLKTTT-RSVLMVLC-ASTKLLASFLGVRSANSMQSLLKLKLVSWVNSLLHV-KWNGRDCQ-LSPPMPKSW
VNTSLQQLTTQDSGLNEQRTARKRLN-LQPCHLRGP-ISLLGFQRSQCQKGIFIFLSLFPSIQTELFPLRPMKTF
SPGSRNISRRN

RbD/RbM anti-zfLvH1 epitope

B) *vtg3*-KO

Frame 1 5'>3'

MANYEPFLNSKKTYEYKYEGLVQVGRELPHLVESALKLRCTFKIIGESPHTFVLQVSNVDFEDFNGIPGKSVFS
PSKNITKHLSAEISQPIIFEYSKGQITDIRTAPGVSNTVVNIVRGILGFLQVTVKTTQSFYELIELGIHGLCQSS
YTV*DEDSNAKELIVTRIVDITNCQQPASLYRGMALAPEDKLSKQRGESVVSTVKHTYTVKSTADGGQITKAFAQE*
RQYFSPFNVKGGNF<238aa> LKTLLKFLPGYSNGAEKLSTRVQGAAVQAFRLLASRASHSVQDIVLNLFVQKHL
PAEIRMLACIVLLETKPSTALISVVSEVLLEEADLQVASFSYSLLKGFAKSRTPDNQHLSIACNIAMKILTRKLG
HLSYRYSKNLHFDWFHDDFLFGTSADVYMLQNESPIPTKLMLKGKFHFIGRILQFLEFGIRADGLKDLFAGKIPE
LTKDLGISDLASILKILSNWQSLPKDKPLLTAYARVFGQEAFLMDVSRDSVQSIIKSFSPSAGKESKVWERIQDV
QKGTSWHWTKPHLVYEARFIQPTCLGLPVEISKYYSVVNAVTMKAKAEINPPPKEHLGELLSSDISMQTDGFIGV
TKDHFLFHGINTDLFQCGTELKSKVSMGLPWAFDLKINPKEQTYEMNLTPSKSVTELFSVSSNVYAVLRNIEDPT
SSKITPMMPETGESWQGVPLRMLPPLRDEQTKKSGMKFRQCAEAKIYGTALCIEAEAKRAHYLHEYPLYYLLGDT
HFSYSLEPAKDAKPIEKIQIQVSASRQHPSVMSGMVNLNQRVFKETRDENTSCEERKTSSSLPV|TQDLDVTPDP
VVTVKALSLSPQAKPLGYEGVAFYLPTAQKDDIEMIVSEVGEEANWKMCANAHFDKTHTSAKAHLRWGAECQTYD
VSMRVSAACQPESKPSISTKINWGTLPSVFTTVGQIVQEYVPGVSYIMGFYQKKEENPERQASVIVVASSPETFD
LKVKIPERTIYKKKIPSPIELLGIEAANLTMST-

RbD/RbM anti-zfLvL3 epitope

vtg1-KO Embryo Genotyping

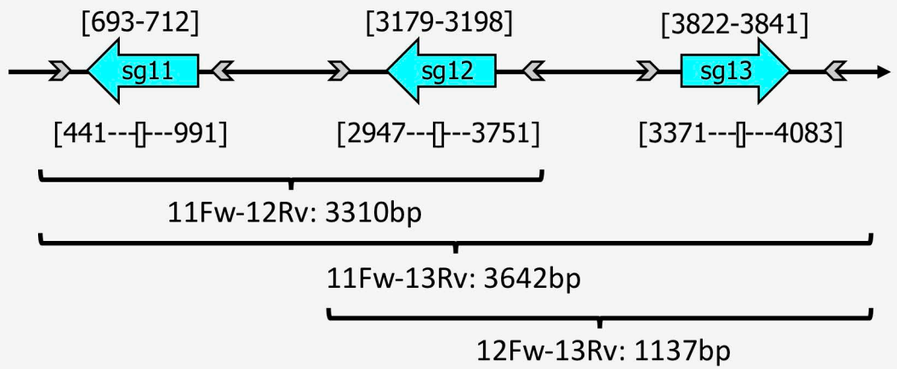

wild type : 3642 bp
mutated: 2361 bp

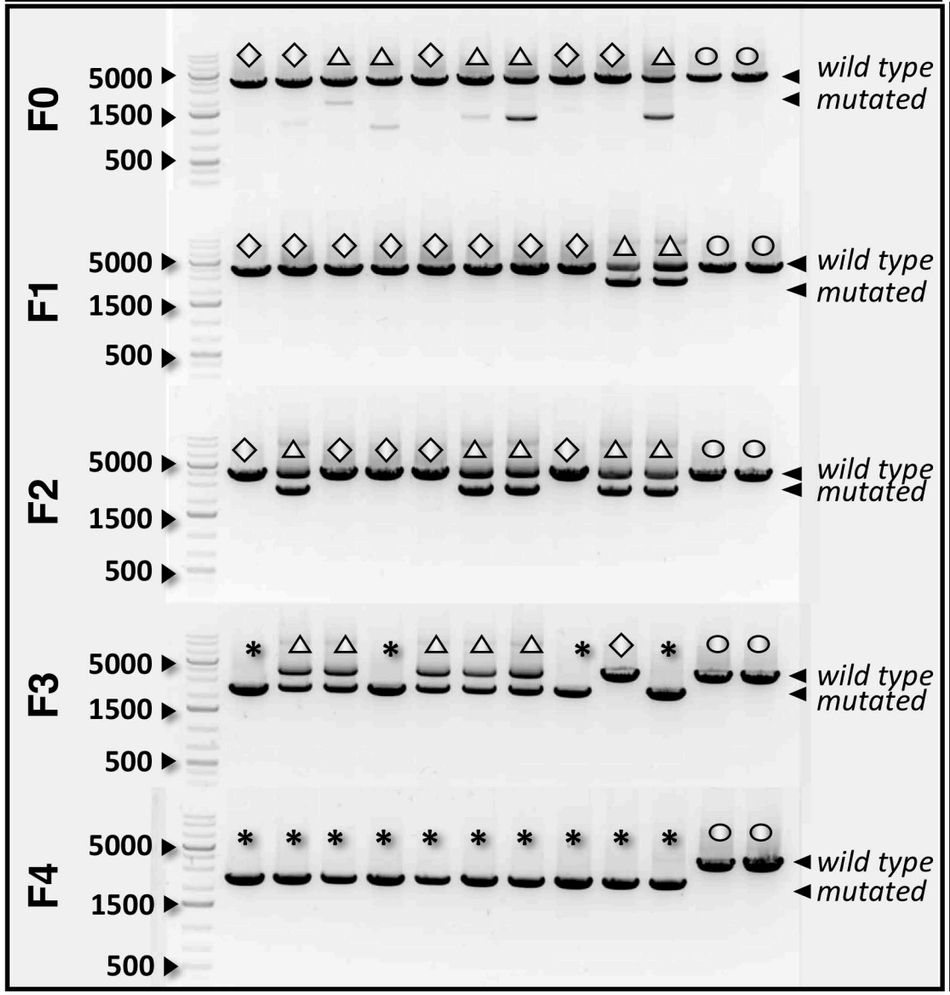

vtg3-KO Embryo Genotyping

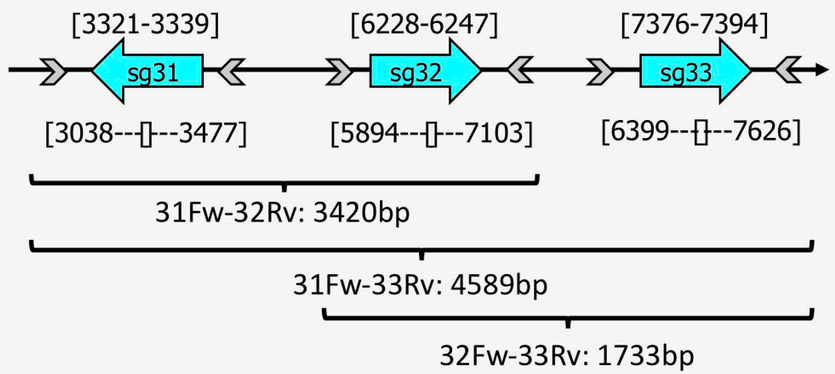

wild type : 1733 bp
mutated: 551 bp

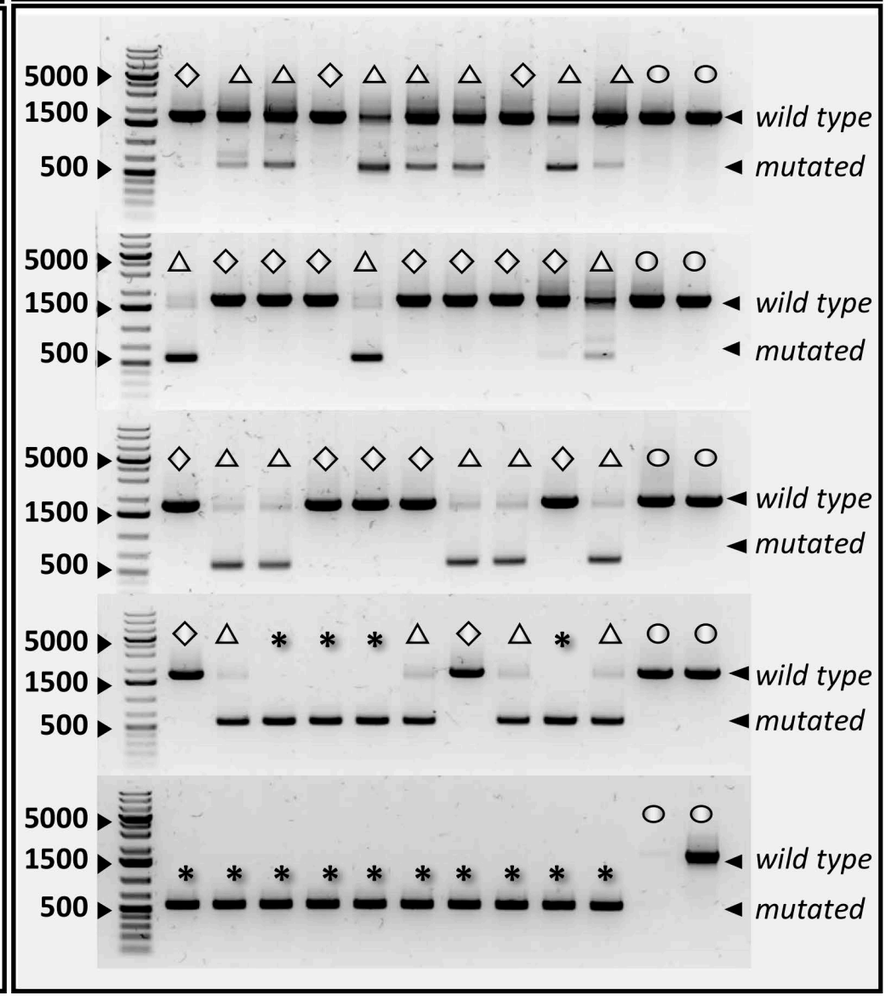

Pure Line Production

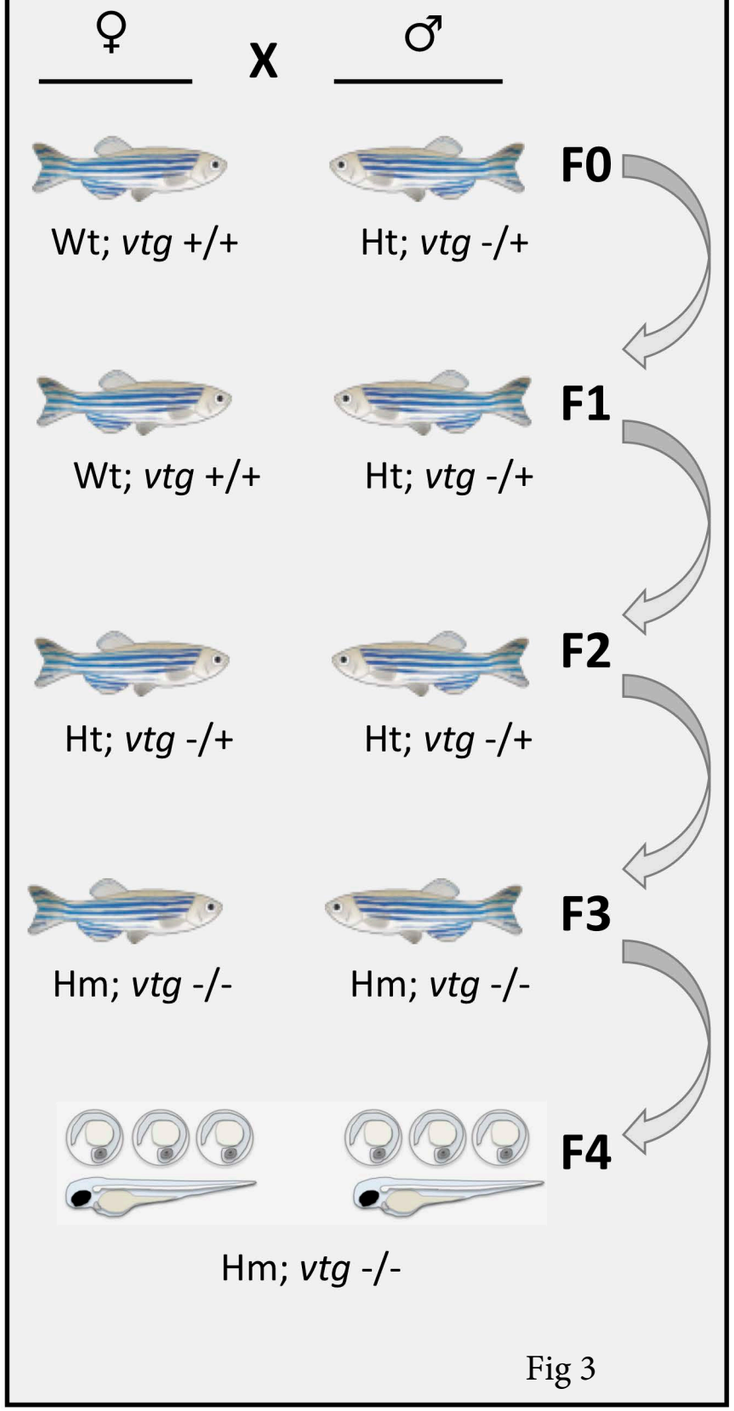

Fig 3

Fig 4

A) *vtg* expression in *vtg1*-KO liver

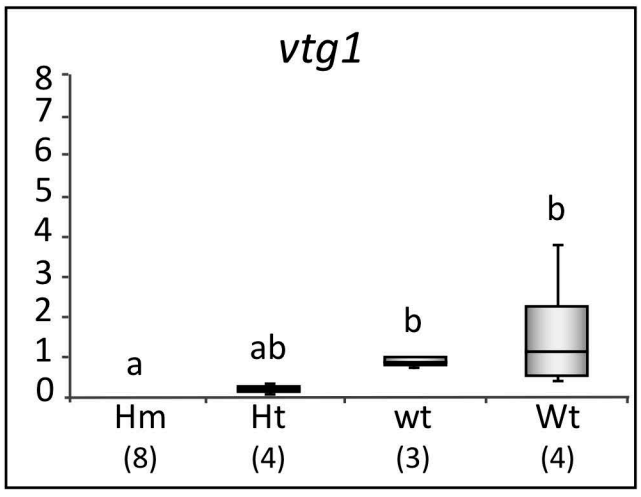

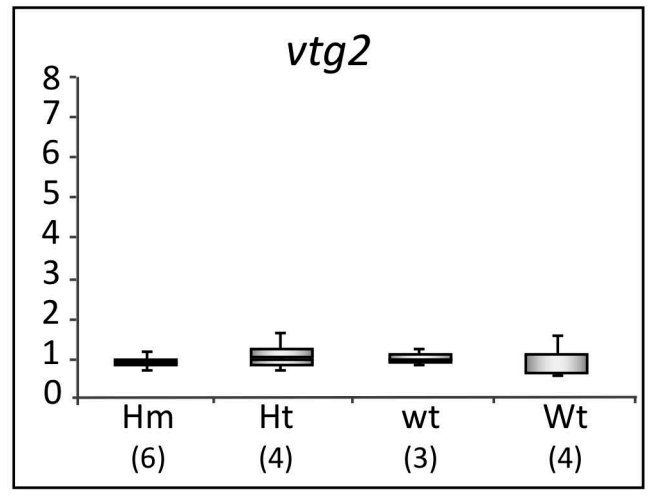

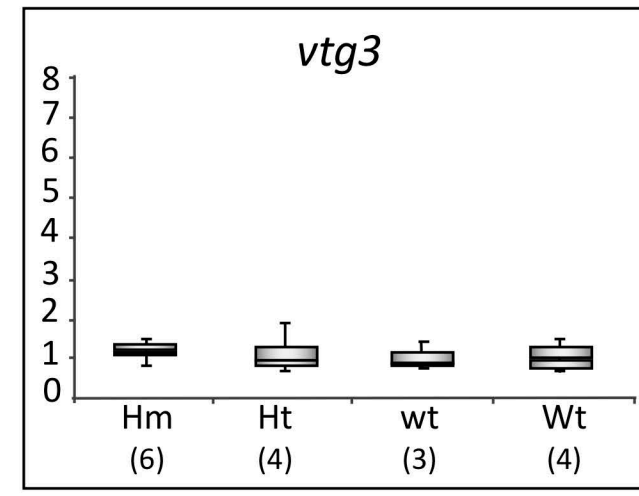

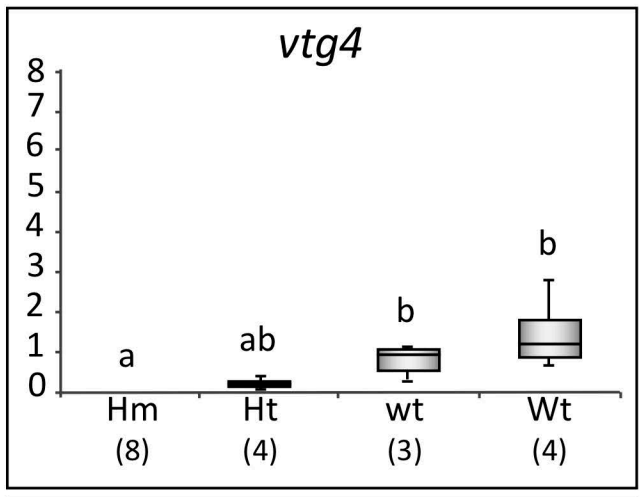

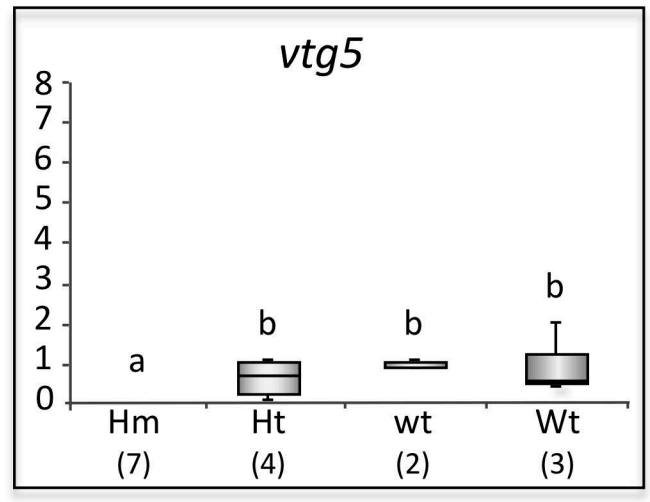

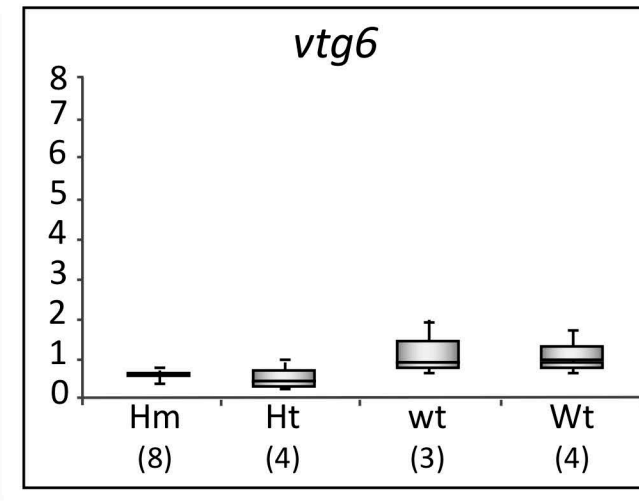

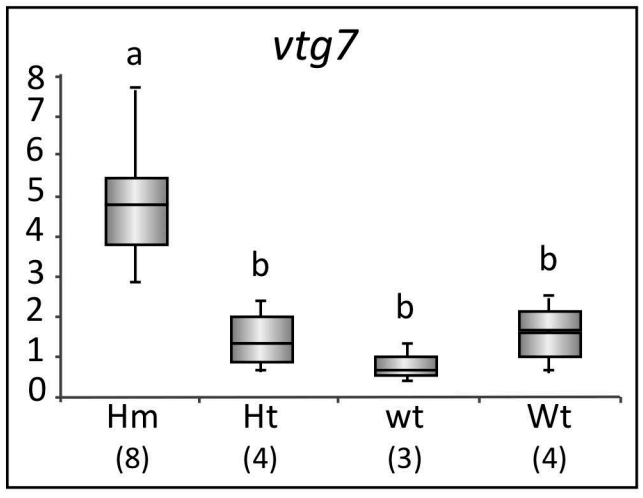

B) *vtg* expression in *vtg3*-KO liver

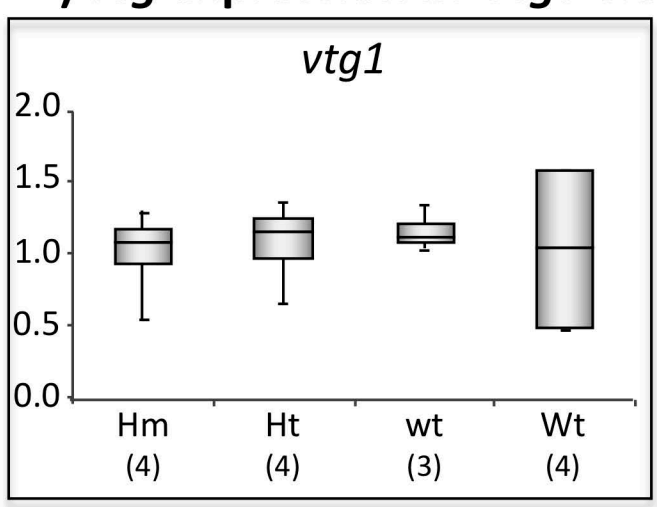

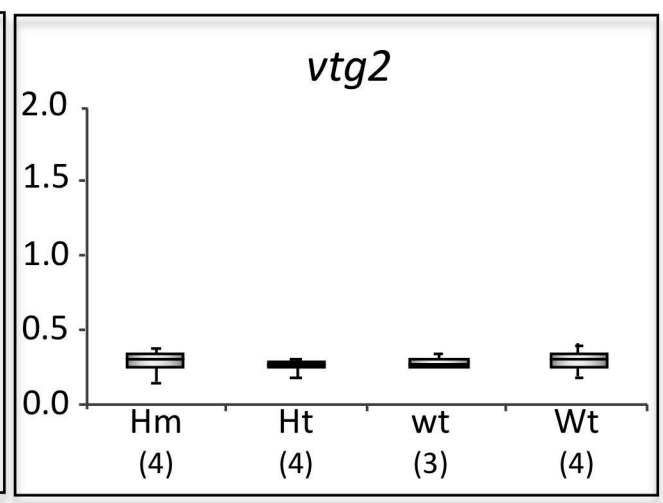

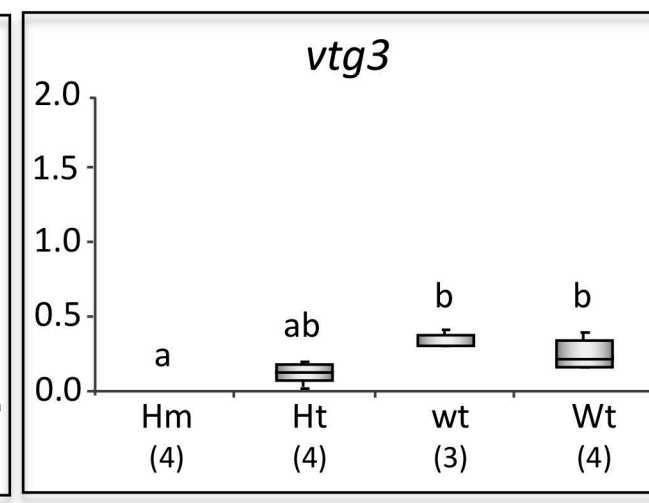

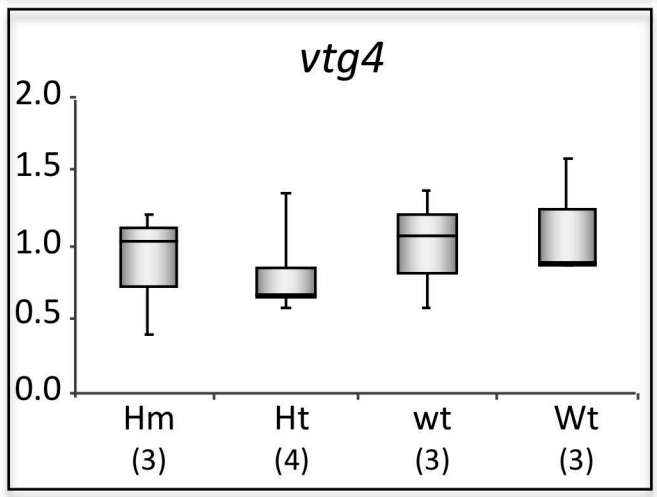

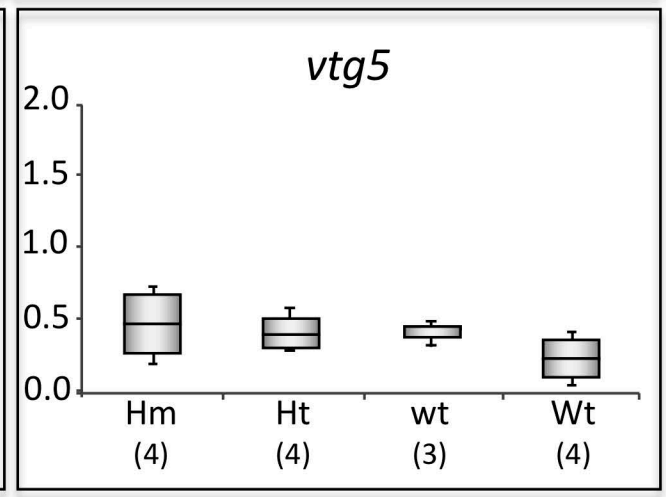

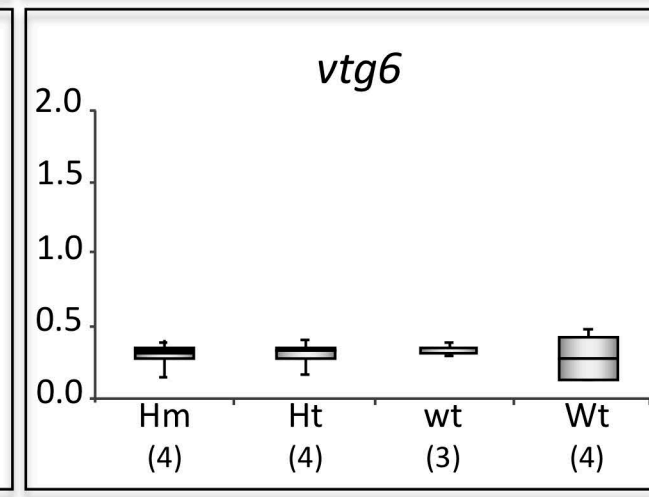

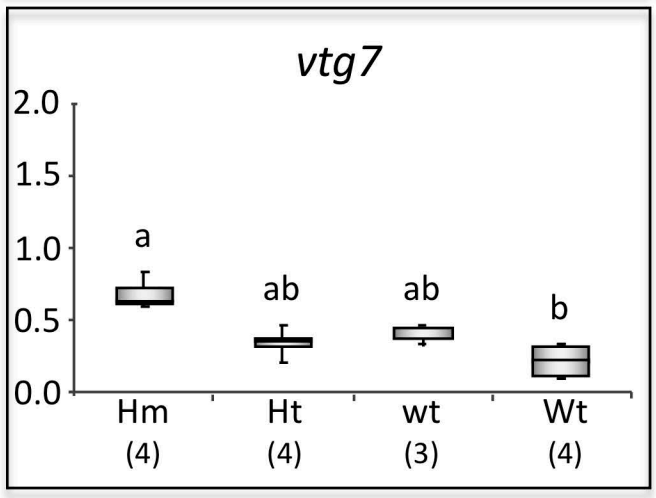

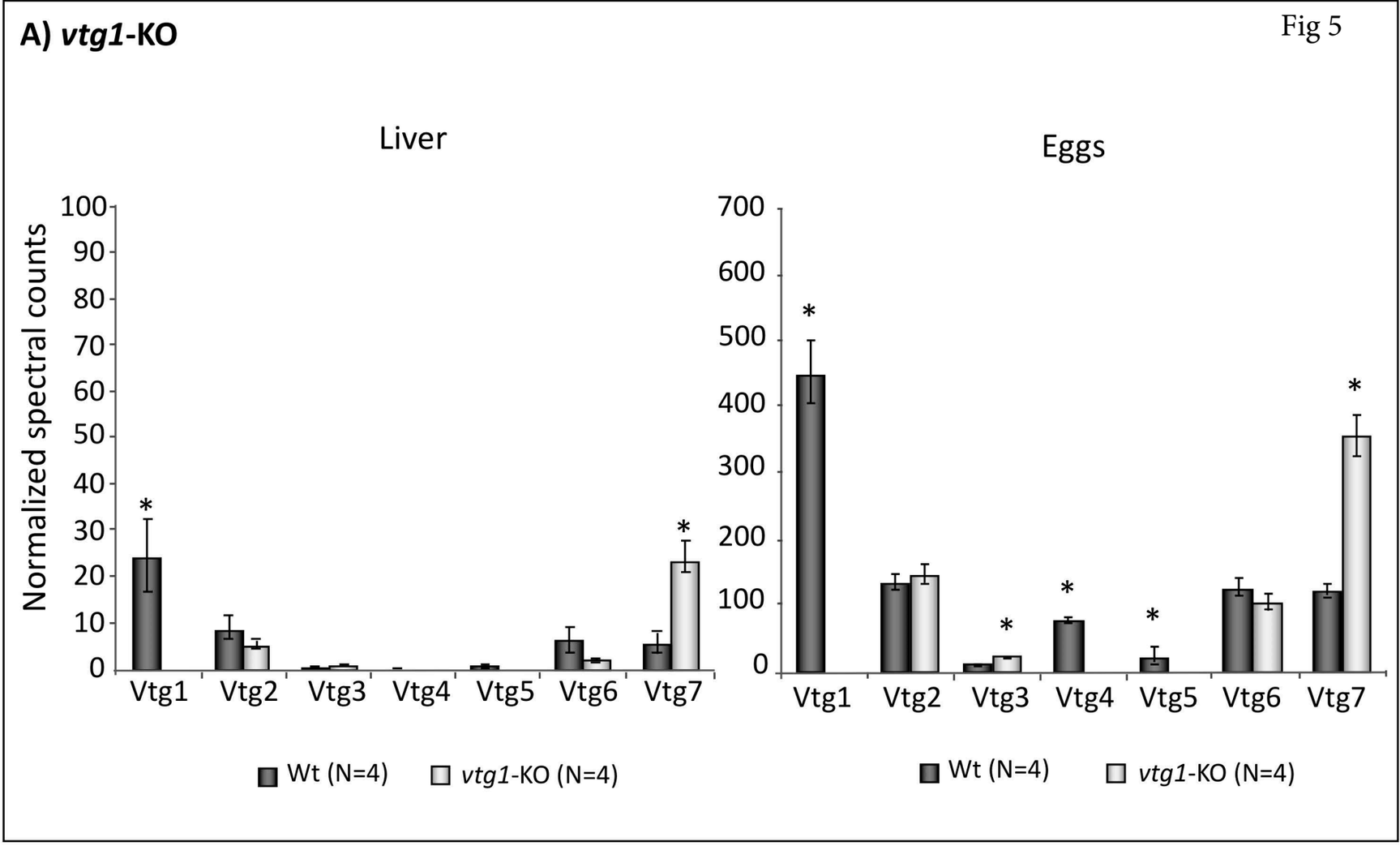
A) vtg1-KO
Liver
Eggs
Normalized spectral counts
100
90
80
70
60
50
40
30
20
10
0
700
600
500
400
300
200
100
0
*
Vtg1
Vtg2
Vtg3
Vtg4
Vtg5
Vtg6
Vtg7
Wt (N=4)
vtg1-KO (N=4)

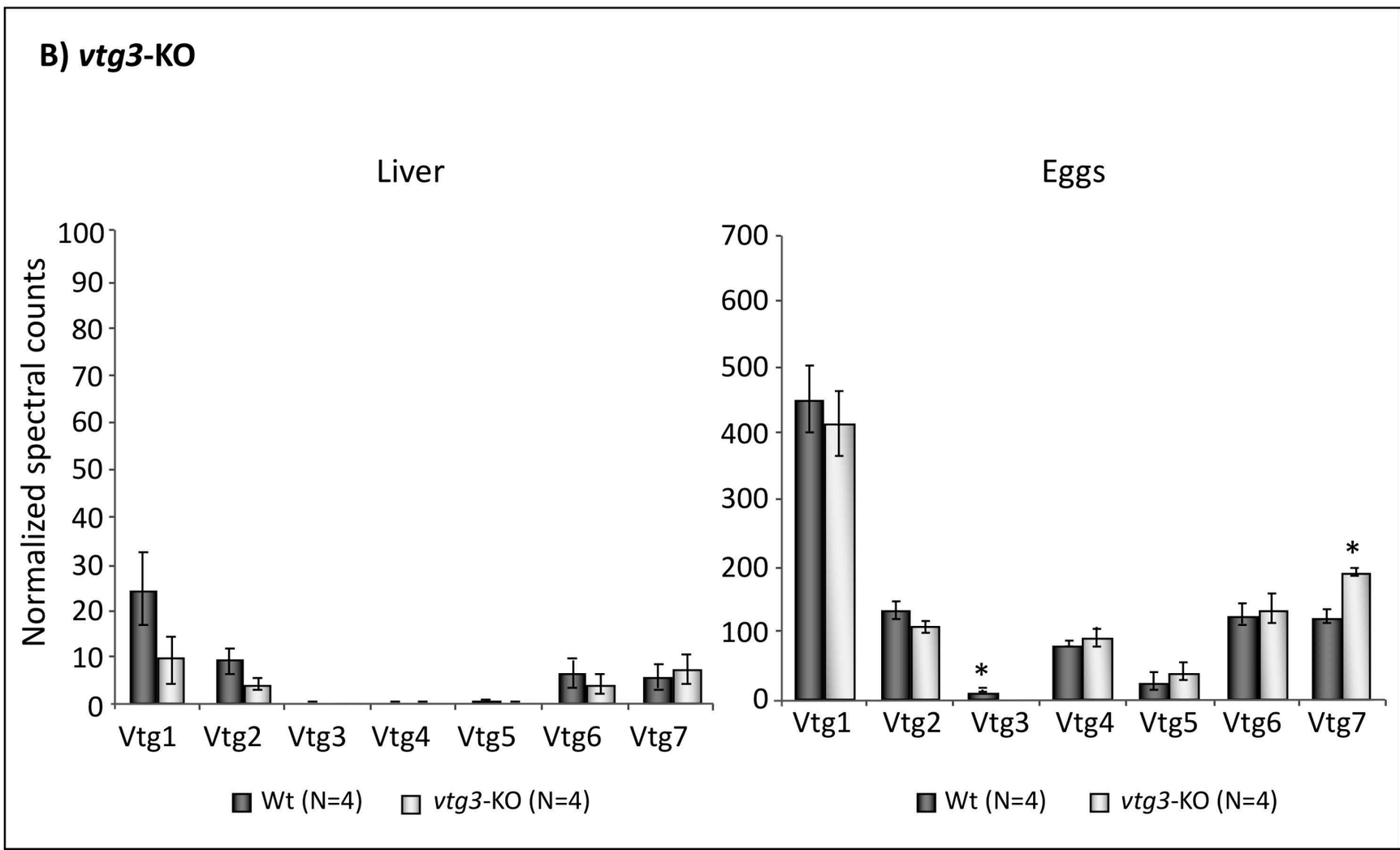
B) vtg3-KO
Liver
Eggs
Normalized spectral counts
100
90
80
70
60
50
40
30
20
10
0
700
600
500
400
300
200
100
0
*
Vtg1
Vtg2
Vtg3
Vtg4
Vtg5
Vtg6
Vtg7
Wt (N=4)
vtg3-KO (N=4)

Fig 6

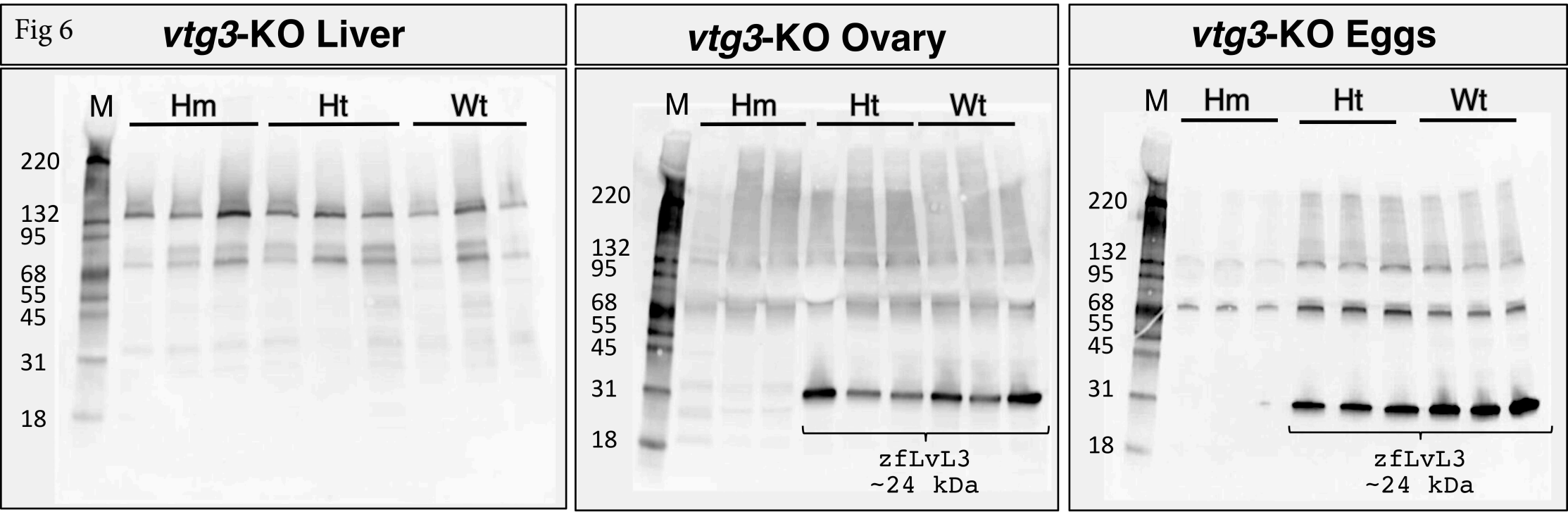
vtg3-KO Liver
M
Hm
Ht
Wt
220
132
95
68
55
45
31
18
vtg3-KO Ovary
M
Hm
Ht
Wt
220
132
95
68
55
45
31
18
zfLvL3
~24 kDa
vtg3-KO Eggs
M
Hm
Ht
Wt
220
132
95
68
55
45
31
18
zfLvL3
~24 kDa

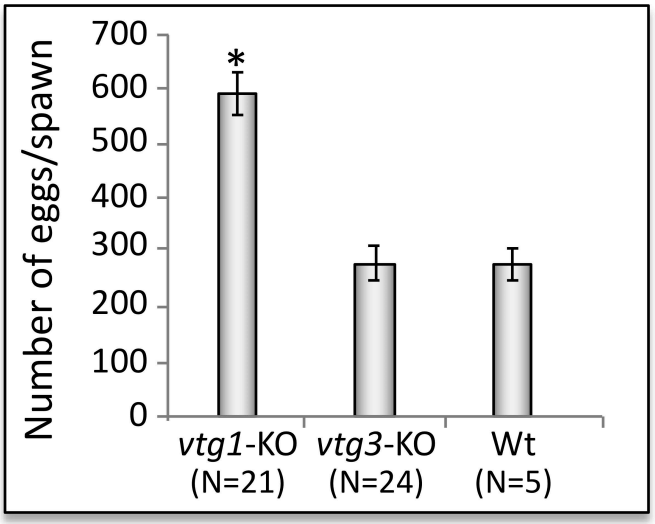
Number of eggs/spawn
700
600
500
400
300
200
100
0
*
vtg1-KO (N=21)
vtg3-KO (N=24)
Wt (N=5)

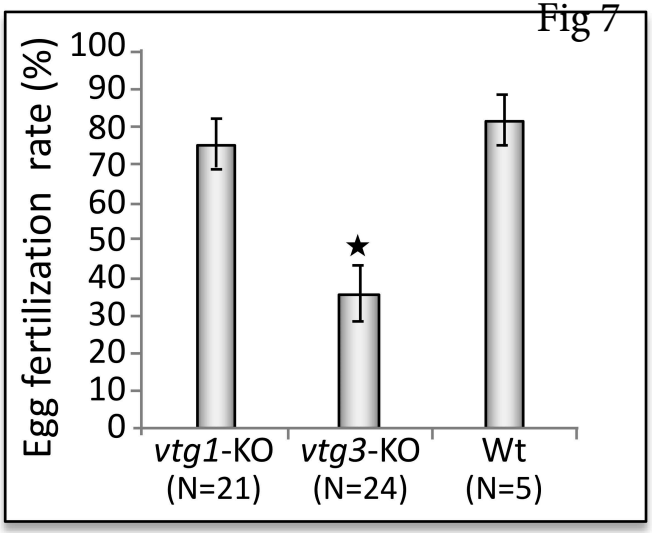
Egg fertilization rate (%)
100
90
80
70
60
50
40
30
20
10
0
★
vtg1-KO (N=21)
vtg3-KO (N=24)
Wt (N=5)

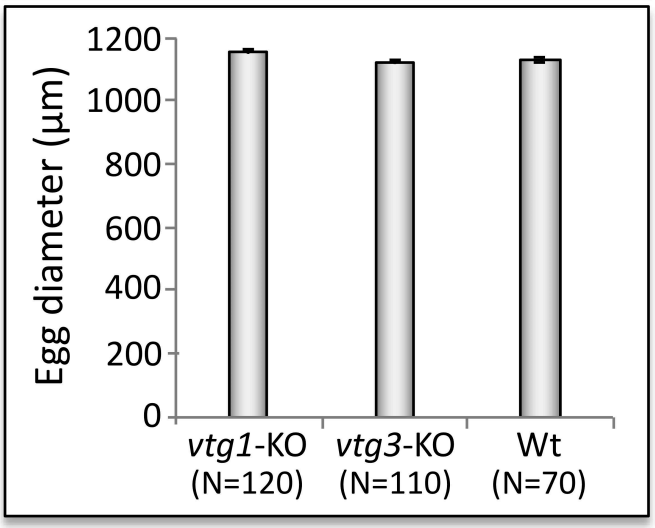
Egg diameter (µm)
1200
1000
800
600
400
200
0
vtg1-KO (N=120)
vtg3-KO (N=110)
Wt (N=70)

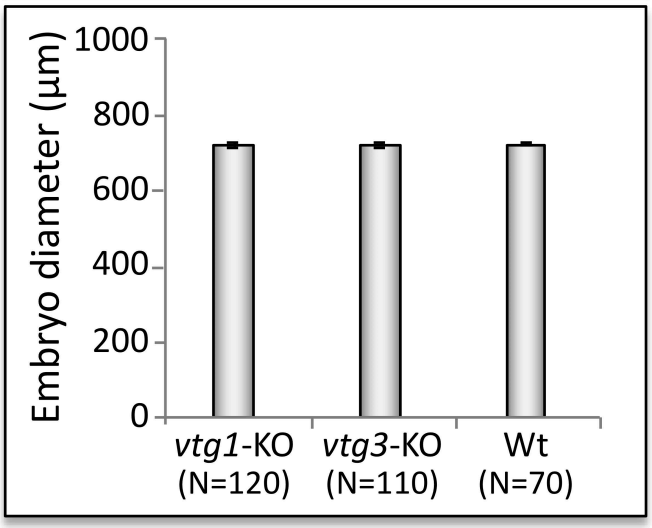
Embryo diameter (µm)
1000
800
600
400
200
0
vtg1-KO (N=120)
vtg3-KO (N=110)
Wt (N=70)

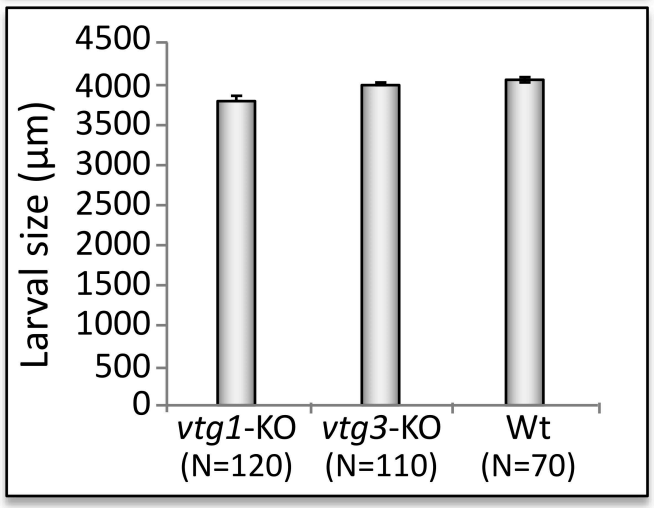
Larval size (µm)
4500
4000
3500
3000
2500
2000
1500
1000
500
0
vtg1-KO (N=120)
vtg3-KO (N=110)
Wt (N=70)

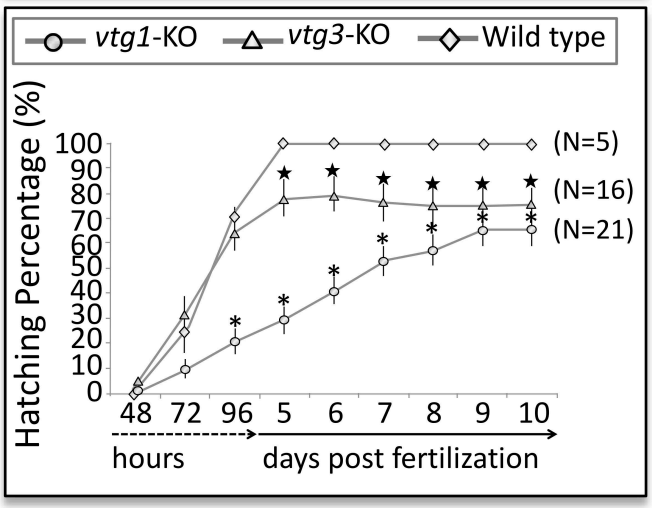
vtg1-KO
vtg3-KO
Wild type
Hatching Percentage (%)
100
90
80
70
60
50
40
30
20
10
0
(N=5)
(N=16)
(N=21)
48
72
96
5
6
7
8
9
10
hours
days post fertilization

Fig 8

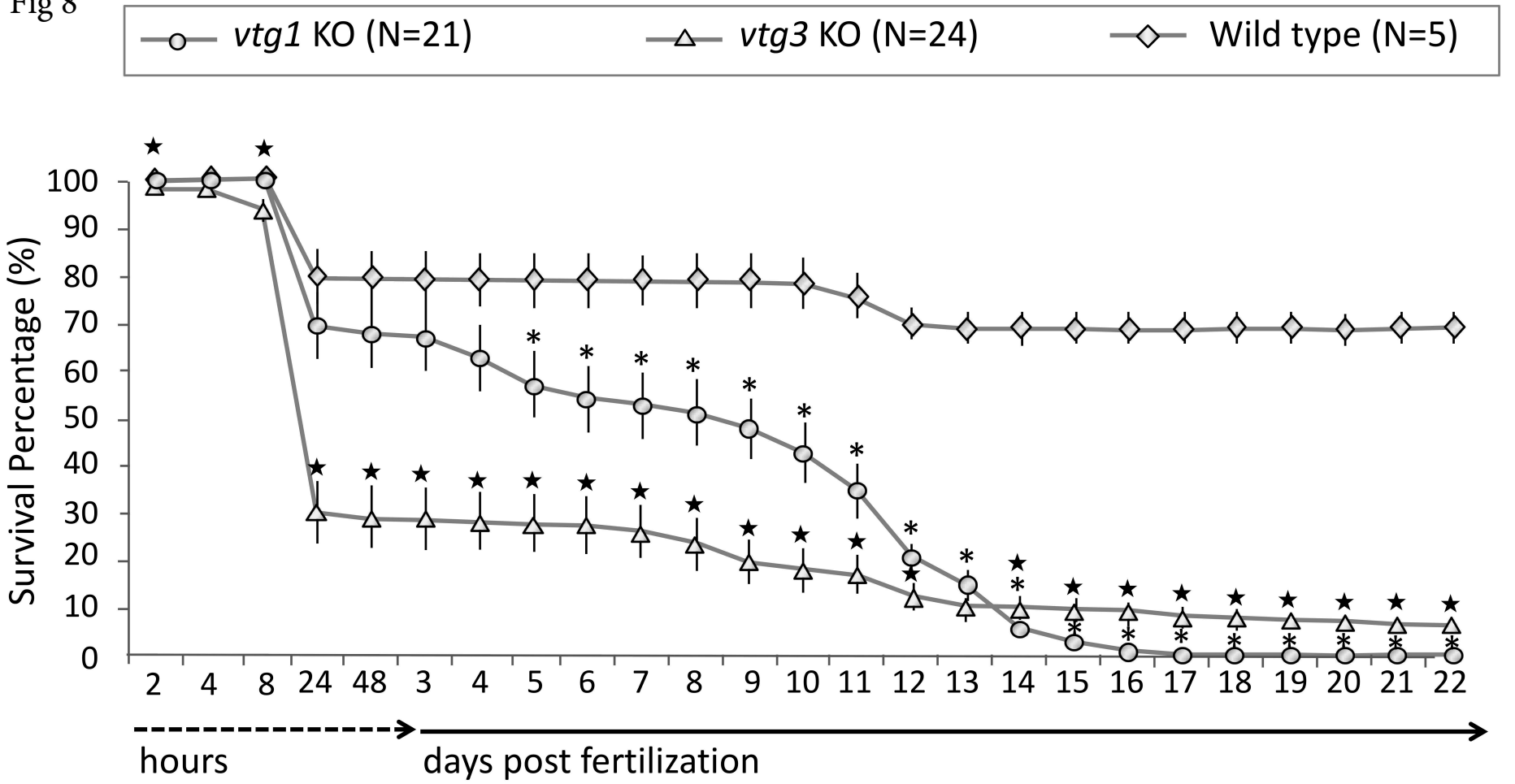
vtg1 KO (N=21)
vtg3 KO (N=24)
Wild type (N=5)
Survival Percentage (%)
100
90
80
70
60
50
40
30
20
10
0
2 4 8 24 48 3 4 5 6 7 8 9 10 11 12 13 14 15 16 17 18 19 20 21 22
hours
days post fertilization

Fig 9

4 dpf

8 dpf

vtg1-KO

Wild type

Wild type

vtg3-KO

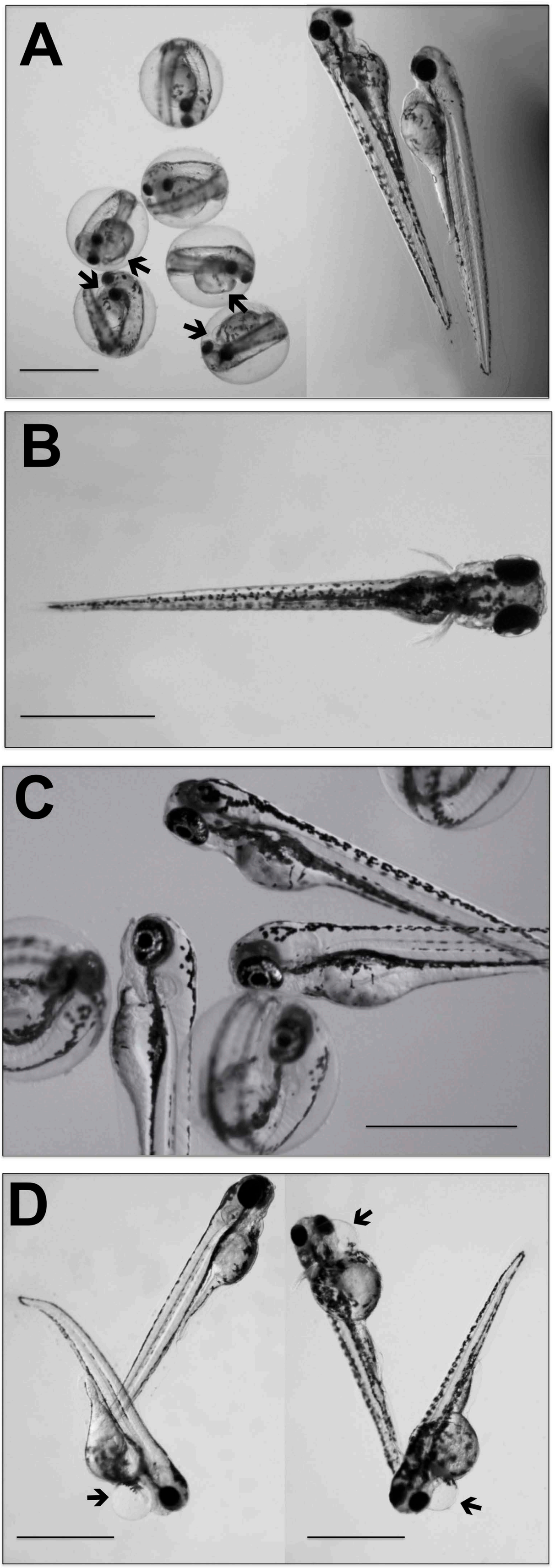

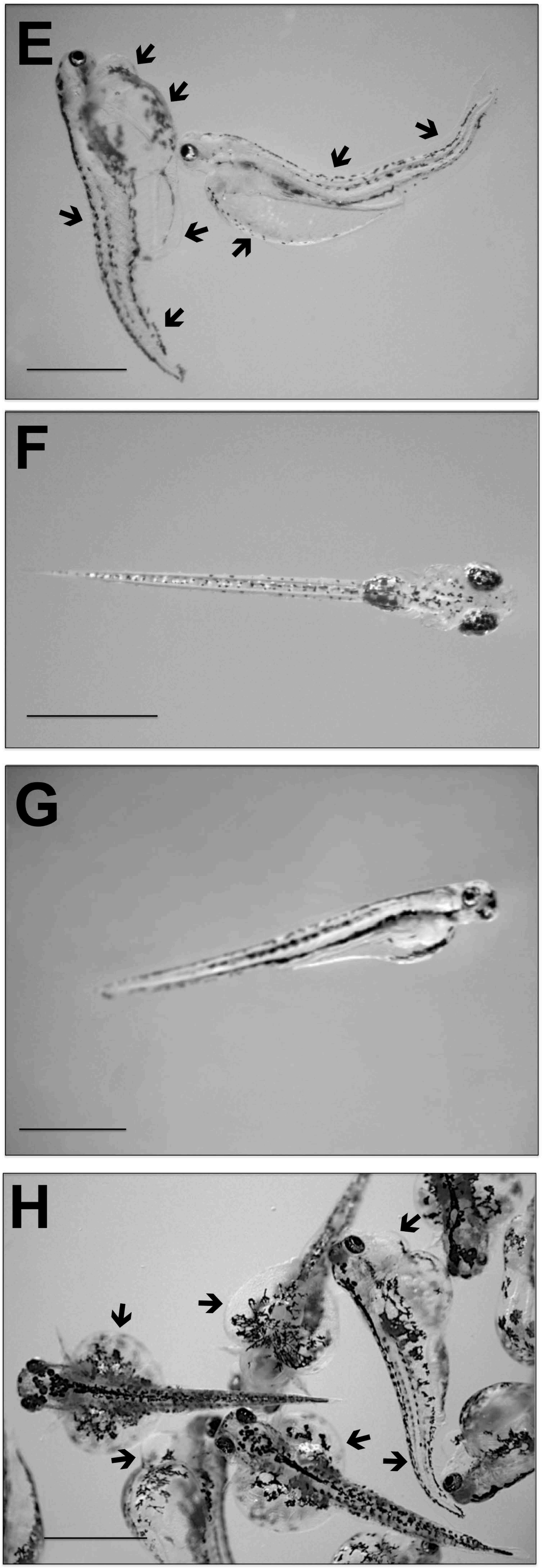

A) *vtg1*-KO


```
vtg1-/-  CTTCCTGGACTGAGAACTGCAGCTAATGCTTTGCCCATTAGAGTCCAGGTTGATGCCAT-  2458
vtg1+/+  CTTCCTGGACTGAGAACTGCAGCTAATGCTTTGCCCATTAGAGTCCAGGTTGATGCCATC  2460   Exon 11
         ************************************************************

vtg1-/-  ------------------------------------------------------------  2458
vtg1+/+  TTGGCCCTGAGAAACATTGCTAAGAAAGAGCCCAAACTGGTAAGATTCAGGTATTTTAGA  2520

vtg1-/-  ------------------------------------------------------------  2458
vtg1+/+  TATGAACTGCTGTAAATGTTATGCATGTTTTCTTCCAATGAAAAAAACTTTGTTTCCTGT  2580   Intron

vtg1-/-  ------------------------------------------------------------  2458
vtg1+/+  ATCAGGTTCAGCCTGTTGCCCTGCAGCTTGTTTTGGACAGAGCTCTCCACCCCGAGGTGC  2640

vtg1-/-  ------------------------------------------------------------  2458
vtg1+/+  GCATGGTTGCTTGTATTGTGCTGTTTGAGGCTGAGCCTTCAGTGGCACTTGTCTCTAGTC  2700   Exon 12

vtg1-/-  ------------------------------------------------------------  2458
vtg1+/+  TTGCTGGAGCTCTAAGGATTGAGCCAAACATGCATGTTGCAAGCTTTGCCTATTCCCACA  2760

vtg1-/-  ------------------------------------------------------------  2458
vtg1+/+  TCAAGTCCTTGACCAGAATCACTGCTCCTGATATGGCATCTGTGTAAGAAAAGCCAATAT  2820   Intron

vtg1-/-  ------------------------------------------------------------  2458
vtg1+/+  ATTTCAGTTTTGTGTTTTTACATTAAATTCTCCATGTTTTTCACACTTTACACATGAAAC  2880

vtg1-/-  ------------------------------------------------------------  2458
vtg1+/+  GAGTACAAGCCTAGGTAATCATGGCTATTTATTTTCAGTGCTGGTGCAGCTAATGTTGCA  2940   Exon 13

vtg1-/-  ------------------------------------------------------------  2458
vtg1+/+  ATCAAGCTTATGAGCCGCAAACTGGACAGACTTAACTACCGTTACAGCAGAGCTTTTCAG  3000

vtg1-/-  ----------------------------------------------------------    2458
vtg1+/+  ATGGACTATTATTATAGTAAGAATTTCTAATTTCTTAAGAGCTAAGAAATTATATCGGAT  3060   Intron

vtg1-/-  ------------------------------------------------------------  2458
vtg1+/+  GTTTCTTAAACTGCATTAAAATTTGTCTGACATACAGTATTGCAAATTTATTCTTTAAAT  3120

vtg1-/-  ------------------------------------------------------------  2458
vtg1+/+  GTATCTTTTAAATTTGTCCATTAAGCTCCTCTTATGATTGGAGCTGCTGGTAGTGCCTAT  3180   Exon 14 (sg12)

vtg1-/-  ------------------------------------------------------------  2458
vtg1+/+  ATGATCAATGATGCTGCCACCATCCTGCCCAGAGCTGTTGTAGCTAAAGCTCGTGCTTAC  3240

vtg1-/-  ------------------------------------------------------------  2458
vtg1+/+  CTGGCTGGAGCTGCTGCTGATGTTATTGAGGTGAACCATCTAAAATTTCCTTACTAGATA  3300   Intron

vtg1-/-  ------------------------------------------------------------  2458
vtg1+/+  TTTGACTTACTATTTAAATCAATTTTAAAATGCATCACTAAATTGTTCCTCTAAAACAGT  3360

vtg1-/-  ------------------------------------------------------------  2458
vtg1+/+  TTGGTGTGAGAACTGGAGGAATCCATGAAGCTCTCCTAAAATCTCCTGCTGCAGATGAAA  3420   Exon 15

vtg1-/-  ------------------------------------------------------------  2458
vtg1+/+  GTGCTGACCGTATCACAAAGATTAAGCGTACACTGAGAGCAGTAAGTTTTTTTTATGTCC  3480   Intron

vtg1-/-  ------------------------------------------------------------  2458
vtg1+/+  ATAGTATCTTAATTTTACACTTTAATTATAAAATTGAAAAAGAAAAAACTGACTTAAAAA  3540

vtg1-/-  ------------------------------------------------------------  2458
vtg1+/+  TGATTTGTTTCTTCAAGCTCACAAACTGGAAGGCTTTGCCAACCGATAAACCACTAGCAT  3600   Exon 16

vtg1-/-  ------------------------------------------------------------  2458
vtg1+/+  CAGCCTATCTCAAAGTATTTGGACAAGAAGTGGCTTATGTCAACTTTGACAAGACCATCA  3660

vtg1-/-  ----------------------------------------------------------    2458
vtg1+/+  TTGAAGAAGCCATACCGGTATTGTGTTGTCATTTATCTCTTCCTACCATATGCTTGAAGT  3720   Intron

vtg1-/-  ------------------TGATACTCACAATTGGAATTAAGCTTCTAATAAACACTTT    2499
vtg1+/+  CTAAGAACTTGAACTGTGACTGATACTCACAATTGGAATTAAGCTTCTAATAAACACTTT  3780
                           ****************************************

vtg1-/-  CTTCAGATGGCTACTGGACCCAAACCACGTGCACTGCTGAAGGAGGCTCTTAAAGCTTTG  2559
vtg1+/+  CTTCAGATGGCTACTGGACCCAAACCACGTGCACTGCTGAAGGAGGCTCTTAAAGCTTTG  3840   Exon 17 (sg13)
         ******************************************************************
```

B) *vtg3*-KO


```
vtg3-/-  AAAGCATTTGCTCAGGAGCGCCAATATTTCTCTCCGTTCAATGTAAAGGGAGGAAACTTC  337
vtg3+/+  AAAGCATTTGCTCAGGAGCGCCAATATTTCTCTCCGTTCAATGTAAAGGGAGGAAACTTC  6240   Exon 6 (sg32)
         **************************************************************

vtg3-/-  CG----------------------------------------------------------  339
vtg3+/+  CGAATGTTGGCATTGTAAGTGCTTCTAACTGTTATCAACTTTCAAGTGGTTGCACTCCTG  6300   Intron
         **

vtg3-/-  ------------------------------------------------------------  339
vtg3+/+  ATTAATCAATGATGTTGTGCTTCCTTTTACCAGGCGGGACATTGAACTTCTTAAAGTTTC  6360

vtg3-/-  ------------------------------------------------------------  339
vtg3+/+  AGACACAACTGACAAAGTAGTGACTGGACAGGTGCAGAGCAGAGGCAACCTGATGTATAA  6420   Exon 7

vtg3-/-  ------------------------------------------------------------  339
vtg3+/+  GACAAATAAGGACCTCAAACCAATACCTGTTGTGATGCTTAACCTGAACGACCCAGTGCC  6480

vtg3-/-  ----------------------------------------------------------    339
vtg3+/+  CAAGGCAAACTTCAAAGATTATATAAACATTTAAGCATATACAGACATGAGAATTAACTC  6540   Intron

vtg3-/-  ------------------------------------------------------------  339
vtg3+/+  ATTAATCGTTTAAATCATACTTTACTCCAACAGATTTTAGATTTAATCAAGCGCCTCGCA  6600

vtg3-/-  ------------------------------------------------------------  339
vtg3+/+  CAGGCTAATATATATCATGTGGACAGTGAAACCAGCACAGAAATTCTGGACCTAATTCAG  6660   Exon 8

vtg3-/-  ------------------------------------------------------------  339
vtg3+/+  TTGATGCGGGTAACAACACTTGATAATCTAGAGCATTTATGGAAGCAGGTCTCAGGAAAT  6720

vtg3-/-  ----------                                                    339
vtg3+/+  GATGAGCACAGGTATGTTCACCCTTCTCTAAATACTATACAATCTAATATTCAAGATGAT  6780   Intron

vtg3-/-  ------------------------------------------------------------  339
vtg3+/+  CAATTTCCCCTGTTGACTTTCTTTTTTTTTTGGTCAGGCGGTGGTTCTTGGACTTGGTTG  6840

vtg3-/-  ------------------------------------------------------------  339
vtg3+/+  TGGAGGTAACAGATGAAAGAATTCTCAAATTCCTTGAGGCCAGATACAAAGCAGGAGACA  6900   Exon 9

vtg3-/-  ------------------------------------------------------------  339
vtg3+/+  TCACAGCGAATGAGGCAGGACAAGCACTGGTAGTGGCATTTAACCACTTGTCCGCTGAGC  6960

vtg3-/-  ----------------------                                        339
vtg3+/+  CTGTGTCGGTGGCATTAGCTCAGGTGAGACAGTGACCAAGTTAAATGTATGTTAGAATCC  7020   Intron

vtg3-/-  ------------------------------------------------------------  339
vtg3+/+  TTTTTTATCTGCCGTCTGATACGCTCTTCCGCTCTCCAGGAGTTCCTGACCATTCCTTTC  7080

vtg3-/-  ------------------------------------------------------------  339
vtg3+/+  AGTAAATCCCATCCTCTCCTGTGGAACACTGTAGTTTTGGCATATGGATCTCTTGTACAC  7140   Exon 10

vg3-/-   ------------------------------------------------------------  339
vtg3+/+  AGATACTGTGTGTATACTGACCCCTGCCCTATCACTGTGGTACAGGTATCTGAGATGTCC  7200

vtg3-/-  ------------------------------------------------------------  339
vtg3+/+  TACACCTCTATGTTGATTGATTCATACACCTATCATAGTAATATTTTGCTAGTTTTATGT  7260   Intron

vtg3-/-  ------------------------------------------------------------  339
vtg3+/+  CAAACTTAGTTCTTTGATATTTACAGTACATCTCACTGCTTTTTGTACATACTATTGTTT  7320

vtg3-/-  ----------------------------------------------------------    339
vtg3+/+  AGCCATTGCTGAATATGGCTGCAAGTAGCCTAAGTAAAAACTCTGAGGATGAAATGGTCC  7380

vtg3-/-  ----------                          ----------TCAAGACTCTCCTCAAGT  357
vtg3+/+  TTGCGCTGAAGTCCTTGGGAAACGCAGCTCATCTTTCCAGCTTCAAGACTCTCCTCAAGT  7440   Exon 11 (sg33)
                                             ******************

vtg3-/-  TCCTTCCTGGATACTCCAATGGAGCTGAAAAACTTTCCACCAGAGTGCAGGGAGCTGCAG  417
vtg3+/+  TCCTTCCTGGATACTCCAATGGAGCTGAAAAACTTTCCACCAGAGTGCAGGGAGCTGCAG  7500
         ************************************************************
```

C) *vtg1*-KO

>*vtg1*-KO_mRNA

UUAUUCCUCCUUGAUAUAUUUCUGGAUCCAGGCGAGAAAGUCUUCAUAGGUCUCAAUGGAAAAAGUUCCGUCUGGAUUGA
UGGGAACAGCGACAGGAAGAUAAAUAUCCCUUUUUGACAUUGUGAUCUCUGGAAUCCUAGCAAUGAUAUUCAAGGACCUC
UGAGAUGGCAAGGCUGCAGUCAGUUCAAUCUCUUUCUCGCUGUUCGUUGCUCGUUCAAACCUGAAUCCUGUGUCGUAAGC
UGCUGUAAGGAUGUGUUUACCCAGCUUUUUGGCAUAGGUGGUGACAAUUAUUGGCAGUCUCUCCCAUUCCACUUCUAGAC
GUGCAGCAGGGAAUUCACCCAGGACACCAGCUUCAGCUUUAGCAAAGACUGCAUACUGUUUGCACUCCGCACCCCAAGAA
AACUUGCCAGUAACUUUGUGCUUGCUCAACAGAGCACCAUCAGCACAGAUCUUCAUGUUGUCGUUUUCAGCAAUGGAGGA
AACUAUCAGUUGCACUCUUGCAGUUGGUUUGUCAAAGUAAGCAGCCAGUUGGUAGCCCAGAAGCUUCUGGUCAGCUCUAA
CAGCACGGGCGAUGAUAGCAAAAACAGGUGGAAUAUCAUUUCCAAGGAAUCUAUUCUGUUUCUGCAUUUGUUCAAAGCUA
GCUGCAGCACUUCCACUGCUAGUAUCCUUUGUGGCGCUAUGGUGUGCCAAGUACCGAUCUUUGUGGAAUUUCCUGAAAGG
CUCAAUGAUGGUGGCAGUCUUAGACAUACGAGAGCUGGACAUAGAGGAGCUUGAGCUUGAACUUGAACUUGAACUUGAGC
UUGAGCUUGAGCUGGUGCUAGUGCUGGUGCUGCGGCUGCUGCUGCUGCGACUGUUACGACUGCUGCUGCUUUCAGAAGAA
ACAGGUGCAUUUUUAGCUUCAGUGUCCAGGAUUUCCCUCAGUUUCAACAAGAAAGCCUGUCCUUCUGGAGUAUCAUCAUC
AAUGAUGUUGAUUUGCUUAACAAGCCUCUCAGCAGCUCUAGGACCAACUUGAACUUCAAACUCCAGUCUUUCAACUGCAG
GACCUUCAGCUCUUGCCACUGCAGCACGGACUGAGUGGUGUCCAAUUAUGUAGAAAAGAGUGGAAUUUCUGAUAAAAGCA
GCAUUGUGAGAGUGCACCUCAACACAUCCCUUGAUUUCAAUGUAUGGGACAGCAUAACAGAGGGUUCUGUCAAAUGGAGC
AGGAGCUCUUACUGAAGCAACAGAUGACAUCUCAGAUGACAAAUCACCAGCAUAAGAUGCCUGGGAGUUUUGCAGAGACA
AUUCAGGUACCAGGGGAACAGACCUUUCAGCACUGUGAUCUUCAAUGUUUCUGACCACGGCAUAAGUCUCAAAGCUUGCA
GAAGCAAUGUGUUCAGGAAGUUCAACAGGCAGAGCCUCCACCUUGUAGUUGCCCUUGAGAAUGUCUGCUCUUGCUGCCAC
UUUUCCGGGUGCAAUUGUACGGAUCUUUCCUCUUGCCAUAACAGCAGCUUGGAUGAAGGCAGUGUUAACUCCCAUCACAG
CAAAUGUCUGGAGAGCAACACUUGGUCUAGCUUCAGCUUGGAACUGAACAUCAGUCUUCUUUAGUUGCUCAUAAGUCAUG
GACUCCAAUUUCUCAGGGAGAGCAGGUGUAAUGGUGGCCUGAACAUUGACACUUGCAGCAGCAACUGCAGCAGUGUACCA
ACUGAACUCCAUGGGCACACCAACUGCAGUUGGCAAGAUGCGACGCACUUCAGCUGCAAGCAAAGGUUUAGCAUACUGGA
AGGCAACUCCUUCCUGCAAAGCUUUAAGAGCCUCCUUCAGCAGUGCACGUGGUUUGGGUCCAGUAGCCAU <703 bp>
AUGGCAUCAACCUGGACUCUAAUGGGCAAAGCAUUAGCUGCAGUUCUCAGUCCAGGAAGGAGCUUCAUGAUUGGCUUAAG
ACUUGAAGGGUGACCAGCAUUGCCCAUAACUUUCAGAGCCAAAGUGAUUUCAGGAAUGUCAUUCUUAGAAAUGGCCUCUG
UGGCGAUCUCGUGGAUGGGCCUGAGGAGCUCAGCAGGGCAAGUGGGAACUGCAACACAGUAUUUGGCAAUCAGGGAACCA
UAUCCAAGCAUGACAACUUCACGCAGAGCUGGGAUUGUGGCAAAUUUCUCAUGAGUAGCCAAACUAGCUGUCAUUUUAAU
GGUUUCAGGAUCAGCAGUGACCAUUUGCAGAGCAAUCACAAGAGUCUGAAUGAACUCGGGAGUGGUAAAUUCACCAGCCA
GGAACUUCUCCUUGAUGAAUUUUAUAAUGACUGGUGUACCAACAGCAGGAAGAGCAUCCAGAAGCCAGCGCCUGUAAACU
GGUUUGUCCUUGAACUGAGACCAGAUAGCCUCAAUUUUCUCCAAGGAGGCAACACGCAAGAGCUGGACAAGCUGAACAAA
CUUGAAUGGAGCAUCAUCAUGGACCAUGUCUUUAUUGUUUGAAACCAAGUGCUUCAGGACCUCGACAAUCUGGGCAGGUG
CAUCACUGAUCUUCAUGAGUUGAAUGGGGGUCUGAAGAAUCUCAGUUGCAAACUCGUACUGCAGGGAUCCACGGGGCAUG
UAAUCAGCUUUGAUUGGAACGACAGGGGUCUUCUCAAUCUCAACAAAAGCCAAGGUUUGUUUUGCUUCCAUCAUUGCAGC
ACCAUGAAUCUCAUUGAAGGGUGAGAACUGAUACACUUCCUCAACUGUUGCCUCAGCGAUCAGUGCACCAUUGUCAGCUG
GUUUCAUGAUGUAGUUAUAAGUUGCAGUUUCAAUCAGACUCUUGACCCUCUCUGUGCAUUCAGCACACCUCUCAGUGUAU
GCCAAGCCAACAUCCUUCAUGAUUCUCUCCUGGCAGUGGCUCAGAUCUUUAGACUUUGUCACAAUAAUGUGGUUGGCCUU
UGGAUCCUCAUUGAUGACAUAGUGUGUUCUGCACACUCCCUGAGCUCCAGCCUCUUGCAUCUCGUAGAUGUUCUGGGUCU
UCUUGAGGUUGAGCUGAAGGAUGUUGAGGAUACCUCUGUGCAAGUUCAUGACUGUAGGAGAGACUCCUGCUGGGGCAAAA
ACCUUGCCAACCACACCAUUAGCAUACUCAAACUUGAUGGGAAUCUGAAGCUGAGCAGCCAGUGCUGAGGUGAGCUUAGU
AGCAGGAACAAAUGGAUCCUUGGGCCAAGUGCCAGCAUACUCGUAGAGUAGAGGAUCCAUAAGCUUCAUCAGGUAGGUAU
UCUCUGUCGUGGCACUGAUGAGAACCUUGCUGCUGACUUUAAUACCUGCUCUGGCCAGACCUUCUUGAGGAAGACCUCCC
AAAAGCAGAGCCUCAUACUUGUACACAUAGGUCUUAUCAUGGGCAAACUCAGGAACAAGGUUGAAUUGUUGACAUGCCAC
GAGGGCUACAGUCAAGGCAAGCACAACAGCUCUCAU

D) *vtg3*-KO

>*vtg3*_mRNA

UUAAGUUGACAUGGUGAGAUUUGCAGCUUCGAUCCCCAAAAGUUCAAUUGGUGAGGGAAUUUUCUUUUUGUAGAUAGUUCGC
UCUGGAAUUUUCACUUUCAGGUCAAAGGUCUCUGGUGAGGAUGCUACAACGAUGACAGAUGCCUGCCGUUCUGGGUUUUCCU
CCUUUUUCUGGUAGAAACCCAUAAUGUAAGACACGCCAGGUACAUACUCUUGAACUAUUUGACCAACUGUUGUGAAUACUGA
GGGCAGAGUCCCCCAGUUAAUCUUUGUGCUUAUAGAUGGUUUGGACUCUGGUUGGCACGCUGCGGACACUCUCAUAGAAACA
UCAUAUGUUUGACACUCUGCACCCCAUCUGAGAUGAGCCUUUGCUGAUGUAUGAGUCUUAUCAAAAUGUGCAUUGGCACACA
UUUUCCAGUUUGCUUCUUCACCAACUUCAGAGACGAUCAUUUCAAUGUCGUCUUUUUGGGCAGUUGGCAGAUAAAAGGCUAC
GCCUUCAUAGCCAAGGGGUUUUGCUUGUGGACUUAAACUAAGUGCUUUUACUGUGACUACCGGGUCUGGAGUGACAUCUAGA
UCCUGAGUUACUGGGAGUGAACUGGAUGUUUUGCGUUCCUCACAGGAGGUGUUCUCAUCUCUUGUCUCCUUAAAUACCCUUU
GGUUGAGAUUCACCAUUCCACUCAUUACUGAAGGAUGUUGUCUGCUGGCAGAGACCUGAAUCUGAAUUUUUUCAAUGGGUUU
UGCAUCCUUUGCUGGUUCUAAACUGUAUGAAAAGUGAGUAUCACCCAGUAAGUAAUACAGAGGAUAUUCGUGAAGAUAGUGU
GCACGUUUGGCUUCUGCCUCAAUGCAGAGUGCAGUUCCAUAAAUUUUGGCUUCAGCACAUUGCCUGAAUUUCAUUCCAGAUU
UUUUGGUCUGUUCAUCCCUUAAAGGGGGUAACAUUCUCAGAGGCACACCCUGCCAGGACUCCCCUGUCUCAGGCAUCAUGGG
UGUUAUUUUAGAUGAGGUUGGGUCUUCAAUGUUUCUCAAAACAGCAUACACAUUAGAACUGACUGAAAAUAAUUCGGUGACC
GAUUUGCUUGGAGUCAAGUUCAUUUCAUACGUUUGCUCUUUCGGAUUUAUUUUCAGGUCAAAUGCCCACGGCAGGCCCAUUG
AAACCUUACUUUUCAGCUCAGUUCCACACUGAAAAAGAUCAGUGUUGAUUCCAUGGAAGAGAAAAUGAUCCUUUGUCACGCC
GAUAAAGCCAUCUGUCUGCAUGGAAAUGUCUGAGCUUAGCAGUUCACCCAGAUGUUCCUUUGGAGGAGGAUUUAUUUCAGCU
UUUGCUUUCAUUGUAACAGCAUUUACUACGGAAUAAUAUUUGCUGAUUUCAACUGGGAGACCCAGACAUGUCGGCUGUAUGA
ACCGAGCCUCAUACACAAGAUGCGGCUUAGUCCAGUGCCAUGAAGUCCCUUUCUGAACAUCUUGAAUCCUUUCCCAAACUUU
ACUCUCCUUUCCUGCAGAAGGACUGAAAGACUUUAUGAUGCUUUGAACUGAGUCUCUGCUUACAUCCAUUAAAAAGGCUUCC
UGUCCAAAAACUCUUGCAUAAGCUGUCAAAAGAGGCUUGUCUUUUGGUAGGCUCUGCCAGUUAGAGAGAAUUUUCAAUAUGG
AAGCCAAAUCGCUGAUUCCUAAAUCUUUCGUGAGUUCUGGGAUUUUUCCAGCAAACAGAUCUUUGAGUCCAUCUGCACGGAU
ACCAAACUCAAGAAAUUGCAGUAUUCUCCCAAUGAAAUGAAAUUUUCCCUUAAGCAUAAGUUUUGUGGGGAUGGGACUUUCA
UUCUGAAGCAUAUAAACAUCAGCAGAUGUCCCAAAUAAAAAGUCAUCAUGGAACCAGUCAAAGUGCAGGUUCUUGCUGUAGC
GGUAACUCAAGUGGCCAAGUUUACGGGUUAGAAUCUUCAUGGCAAUAUUACAGGCAAUAGAUAGAUGUUGAUUAUCAGGGGU
ACGGGACUUGGCAAAGCCUUUGAGCAGAGAGUAGGAGAAACUGGCAACCUGCAGAUCAGCCUCUUCUAGAAGGACCUCACUU
ACUACUGAAAUCAGAGCUGUGGACGGCUUGGUCUCUAGAAGAACUAUGCAGGCCAGCAUGCGGAUUUCAGCUGGUAAAUGUU
UCUGUACGAAGAGGUUUAAGACAAUAUCCUGUACACUGUGGGAGGCUCUGCUUGCAAGCAGCCUAAAUGCUUGGACUGCAGC
UCCCUGCACUCUGGUGGAAAGUUUUUCAGCUCCAUUGGAGUAUCCAGGAAGGAACUUGAGGAGAGUCUUGA <714 bp>
GGAAGUUUCCUCCCUUUACAUUGAACGGAGAGAAAUAUUGGCGCUCCUGAGCAAAUGCUUUAGUAAUCUGACCACCGUCUGC
UGUGGACUUCACUGUGUAGGUGUGUUUCACAGUGGAAACAACGCUUUCGCCUCUCUGUUUGCUAAGUUUGUCUUCAGGUGCA
AGAGCCAUACCUCUGUACAAAGAUGCUGGCUGUUGACAGUUGGUGAUAUCAACAAUUCGUGUUACUAUCAACUCUUUUGCGU
UAGAGUCUUCAUCAACAGUGUAACUGCUCUGACACAAACCAUGAAUUCCCAACUCAAUUAGUUCGUAAAAACUUUGUGUGGU
UUUGACCGUGACUUGUAAAAAUCCAAGGAUCCCCCUCACAAUAUUCACAACUGUGUUUGAGACUCCAGGUGCUGUGCGAAUG
UCAGUAAUUUGUCCUUUAGAAUAUUCAAAAAUGAUUGGCUGGCUGAUCUCGGCAGACAGAUGCUUAGUGAUGUUUUUGGAAG
GGCUGAAGACACUUUUCCCAGGUAUGCCAUUAAAAUCUUCAAAGUCUACAUUUGAGACCUGAAGGACAAAGGUGUGUGGUGA
CUCUCCAAUGAUUUUAAAAGUGCACCUCAGUUUCAGCGCUGAUUCAACCAGGUGUGGCAGUUCCCGUCCCACUUGUACCAAU
CCUUCAUAUUUAUACUCGUAUGUUUUUUUCGAGUUCAGAAAAGGCUCAUAAUUUGCCAU

E) *vtg1*-KO

>*vtg1*-KO_reverse complementary cDNA

ATGAGAGCTGTTGTGCTTGCCTTGACTGTAGCCCTCGTGGCATGTCAACAATTCAACCTTGTTCCTGAGT
TTGCCCATGATAAGACCTATGTGTACAAGTATGAGGCTCTGCTTTTGGGAGGTCTTCCTCAAGAAGGTCT
GGCCAGAGCAGGTATTAAAGTCAGCAGCAAGGTTCTCATCAGTGCCACGACAGAGAATACCTACCTGATG
AAGCTTATGGATCCTCTACTCTACGAGTATGCTGGCACTTGGCCCAAGGATCCATTTGTTCCTGCTACTA
AGCTCACCTCAGCACTGGCTGCTCAGCTTCAGATTCCCATCAAGTTTGAGTATGCTAATGGTGTGGTTGG
CAAGGTTTTTGCCCCAGCAGGAGTCTCTCCTACAGTCATGAACTTGCACAGAGGTATCCTCAACATCCTT
CAGCTCAACCTCAAGAAGACCCAGAACATCTACGAGATGCAAGAGGCTGGAGCTCAGGGAGTGTGCAGAA
CACACTATGTCATC*AATGAGGATCCAAAGGCCAACCACATTATTGTGACAAAGTCTAAAGATCTGAGCCA*
CTGCCAGGAGAGAATCATGAAGGATGTTGGCTTGGCATACACTGAGAGGTGTGCTGAATGCACAGAGAGG
GTCAAGAGTCTGATTGAAACTGCAACTTATAACTACATCATGAAACCAGCTGACAATGGTGCACTGATCG
*CTGAGGCAACAGTTGAGGAAGTGTATCAGTTCTCACCCTTCAATGAGATTCATGGT*GCTGCAATGATGGA
AGCAAAACAAACCTTGGCTTTTGTTGAGATTGAGAAGACCCCTGTCGTTCCAATCAAAGCTGATTACATG
CCCCGTGGATCCCTGCAGTACGAGTTTGCAACTGAGATTCTTCAGACCCCCATTCAACTCATGAAGATCA
GTGATGCACCTGCCCAGATTGTCGAGGTCCTGAAGCACTTGGTTTCAAACAATAAAGACATGGTCCATGA
TGATGCTCCATTCAAGTTTGTTCAGCTTGTCCAGCTCTTGCGTGTTGCCTCCTTGGAGAAAATTGAGGCT
ATCTGGTCTCAGTTCAAGGACAAACCAGTTTACAGGCGCTGGCTTCTGGATGCTCTTCCTGCTGTTGGTA
CACCAGTCATTATAAAATTCATCAAGGAGAAGTTCCTGGCTGGTGAATTTACCACTCCCGAGTTCATTCA
GACTCTTGTGATTGCTCTGCAAATGGTCACTGCTGATCCTGAAACCATTAAAATGACAGCTAGTTTGGCT
ACTCATGAGAAATTTGCCACAATCCCAGCTCTGCGTGAAGTTGTCATGCTTGGATATGGTTCCCTGATTG
CCAAATACTGTGTTGCAGTTCCCACTTGCCCTGCTGAGCTCCTCAGGCCCATCCACGAGATCGCCACAGA
GGCCATTTCTAAGAATGACATTCCTGAAATCACTTTGGCTCTGAAAGTTATGGGCAATGCTGGTCACCCT
TCAAGTCTTAAGCCAATCATGAAGCTCCTTCCTGGACTGAGAACTGCAGCTAATGCTTTGCCCATTAGAG
TCCAGGTTGATGCCAT <703 bp> ATGGCTACTGGACCCAAACCACGTGCACTGCTGAAGGAGGCTCT
TAAAGCTTTGCAGGAAGGAGTTGCCTTCCAGTATGCTAAACCTTTGCTTGCAGCTGAAGTGCGTCGCATC
TTGCCAACTGCAGTTGGTGTGCCCATGGAGTTCAGTTGGTACACTGCTGCAGTTGCTGCTGCAAGTGTCA
ATGTTCAGGCCACCATTACACCTGCTCTCCCTGAGAAATTGGAGTCCATGACTTATGAGCAACTAAAGAA
GACTGATGTTCAGTTCCAAGCTGAAGCTAGACCAAGTGTTGCTCTCCAGACATTTGCTGTGATGGGAGTT
AACACTGCCTTCATCCAAGCTGCTGTTATGGCAAGAGGAAAGATCCGTACAATTGCACCCGGAAAAGTGG
CAGCAAGAGCAGACATTCTCAAGGGCAACTACAAGGTGGAGGCTCTGCCTGTTGAACTTCCTGAACACAT
TGCTTCTGCAAGCTTTGAGACTTATGCCGTGGTCAGAAACATTGAAGATCACAGTGCTGAAAGGTCTGTT
CCCCTGGTACCTGAATTGTCTCTGCAAAACTCCCAGGCATCTTATGCTGGTGATTTGTCATCTGAGATGT
CATCTGTTGCTTCAGTAAGAGCTCCTGCTCCATTTGACAGAACCCTCTGTTATGCTGTCCCATACATTGA
AATCAAGGGATGTGTTGAGGTGCACTCTCACAATGCTGCTTTTATCAGAAATTCCACTCTTTTCTACATA
ATTGGACACCACTCAGTCCGTGCTGCAGTGGCAAGAGCTGAAGGTCCTGCAGTTGAAAGACTGGAGTTTG
AAGTTCAAGTTGGTCCTAGAGCTGCTGAGAGGCTTGTTAAGCAAATCAACATCATTGATGATGATACTCC
AGAAGGACAGGCTTTCTTGTTGAAACTGAGGGAAATCCTGGACACTGAAGCTAAAAATGCACCTGTTTCT
TCTGAAAGCAGCAGCAGTCGTAACAGTCGCAGCAGCAGCAGCCGCAGCACCAGCACTAGCACCAGCTCAA
GCTCAAGCTCAAGTTCAAGTTCAAGTTCAAGCTCAAGCTCCTCTATGTCCAGCTCTCGTATGTCTAAGAC
TGCCACCATCATTGAGCCTTTCAGGAAATTCCACAAAGATCGGTACTTGGCACACCATAGCGCCACAAAG
GATACTAGCAGTGGAAGTGCTGCAGCTAGCTTTGAACAAATGCAGAAACAGAATAGATTCCTTGGAAATG
ATATTCCACCTGTTTTTGCTATCATCGCCCGTGCTGTTAGAGCTGACCAGAAGCTTCTGGGCTACCAACT
GGCTGCTTACTTTGACAAACCAACTGCAAGAGTGCAACTGATAGTTTCCTCCATTGCTGAAAACGACAAC
ATGAAGATCTGTGCTGATGGTGCTCTGTTGAGCAAGCACAAAGTTACTGGCAAGTTTTCTTGGGGTGCGG
AGTGCAAACAGTATGCAGTCTTTGCTAAAGCTGAAGCTGGTGTCCTGGGTGAATTCCCTGCTGCACGTCT
AGAAGTGGAATGGGAGAGACTGCCAATAATTGTCACCACCTATGCCAAAAAGCTGGGTAAACACATCCTT
ACAGCAGCTTACGACACAGGATTCAGGTTTGAACGAGCAACGAACAGCGAGAAAGAGATTGAACTGACTG
CAGCCTTGCCATCTCAGAGGTCCTTGAATATCATTGCTAGGATTCCAGAGATCACAATGTCAAAAAGGGA
TATTTATCTTCCTGTCGCTGTTCCCATCAATCCAGACGGAACTTTTTCCATTGAGACCTATGAAGACTTT
CTCGCCTGGATCCAGAAATATATCAAGGAGGAATAA

RbD / RbM

F) *vtg3*-KO

>*vtg3*-KO reverse complementary cDNA

ATGGCAAATTATGAGCCTTTTCTGAACTCGAAAAAAACATACGAGTATAAATATGAAGGATTGGTACAAGT
GGGACGGGAACTGCCACACCTGGTTGAATCAGCGCTGAAACTGAGGTGCACTTTTAAAATCATTGGAGAGT
CACCACACACCTTTGTCCTTCAGGTCTCAAATGTAGACTTTGAAGATTTTAATGGCATACCTGGGAAAAGT
GTCTTCAGCCCTTCCAAAAACATCACTAAGCATCTGTCTGCCGAGATCAGCCAGCCAATCATTTTTGAATA
TTCTAAAGGACAAATTACTGACATTCGCACAGCACCTGGAGTCTCAAACACAGTTGTGAATATTGTGAGGG
GGATCCTTGGATTTTTACAAGTCACGGTCAAAACCACACAAAGTTTTTACGAACTAATTGAGTTGGGAATT
CATGGTTTGTGTCAGAGCAGTTACACTG*TTGATGAAGACTCTAACGCAAAAGAGTTGATAGTAACACGAAT*
*TGTTGATATCACC*AACTGTCAACAGCCAGCATCTTTGTACAGAGGTATGGCTCTTGCACCTGAAGACAAAC
TTAGCAAACAGAGAGGCGAAAGCGTTGTTTCCACTGTGAAACACACCTACACAGTGAAGTCCACAGCAGAC
GGTGGTCAGATTACTAAAGCATTTGCTCAGGAGCGCCAATATTTCTCTCCGTTCAATGTAAAGGGAGGAAA
CTTCC<714 bp>TCAAGACTCTCCTCAAGTTCCTTCCTGGATACTCCAATGGAGCTGAAAAACTTTCCA
CCAGAGTGCAGGGAGCTGCAGTCCAAGCATTTAGGCTGCTTGCAAGCAGAGCCTCCCACAGTGTACAGGAT
ATTGTCTTAAACCTCTTCGTACAGAAACATTTACCAGCTGAAATCCGCATGCTGGCCTGCATAGTTCTTCT
AGAGACCAAGCCGTCCACAGCTCTGATTTCAGTAGTAAGTGAGGTCCTTCTAGAAGAGGCTGATCTGCAGG
TTGCCAGTTTCTCCTACTCTCTGCTCAAAGGCTTTGCCAAGTCCCGTACCCCTGATAATCAACATCTATCT
ATTGCCTGTAATATTGCCATGAAGATTCTAACCCGTAAACTTGGCCACTTGAGTTACCGCTACAGCAAGAA
CCTGCACTTTGACTGGTTCCATGATGACTTTTTATTTGGGACATCTGCTGATGTTTATATGCTTCAGAATG
AAAGTCCCATCCCCACAAAACTTATGCTTAAGGGAAAATTTCATTTCATTGGGAGAATACTGCAATTTCTT
GAGTTTGGTATCCGTGCAGATGGACTCAAAGATCTGTTTGCTGGAAAAATCCCAGAACTCACGAAAGATTT
AGGAATCAGCGATTTGGCTTCCATATTGAAAATTCTCTCTAACTGGCAGAGCCTACCAAAAGACAAGCCTC
TTTTGACAGCTTATGCAAGAGTTTTTGGACAGGAAGCCTTTTTAATGGATGTAAGCAGAGACTCAGTTCAA
AGCATCATAAAGTCTTTCAGTCCTTCTGCAGGAAAGGAGAGTAAAGTTTGGGAAAGGATTCAAGATGTTCA
GAAAGGGACTTCATGGCACTGGACTAAGCCGCATCTTGTGTATGAGGCTCGGTTCATACAGCCGACATGTC
TGGGTCTCCCAGTTGAAATCAGCAAATATTATTCCGTAGTAAATGCTGTTACAATGAAAGCAAAAGCTGAA
ATAAATCCTCCTCCAAAGGAACATCTGGGTGAACTGCTAAGCTCAGACATTTCCATGCAGACAGATGGCTT
TATCGGCGTGACAAAGGATCATTTTCTCTTCCATGGAATCAACACTGATCTTTTTCAGTGTGGAACTGAGC
TGAAAAGTAAGGTTTCAATGGGCCTGCCGTGGGCATTTGACCTGAAAATAAATCCGAAAGAGCAAACGTAT
GAAATGAACTTGACTCCAAGCAAATCGGTCACCGAATTATTTTCAGTCAGTTCTAATGTGTATGCTGTTTT
GAGAAACATTGAAGACCCAACCTCATCTAAAATAACACCCATGATGCCTGAGACAGGGGAGTCCTGGCAGG
GTGTGCCTCTGAGAATGTTACCCCCTTTAAGGGATGAACAGACCAAAAAATCTGGAATGAAATTCAGGCAA
TGTGCTGAAGCCAAAATTTATGGAACTGCACTCTGCATTGAGGCAGAAGCCAAACGTGCACACTATCTTCA
CGAATATCCTCTGTATTACTTACTGGGTGATACTCACTTTTCATACAGTTTAGAACCAGCAAAGGATGCAA
AACCCATTGAAAAAATTCAGATTCAGGTCTCTGCCAGCAGACAACATCCTTCAGTAATGAGTGGAATGGTG
AATCTCAACCAAAGGGTATTTAAGGAGACAAGAGATGAGAACACCTCCTGTGAGGAACGCAAAACATCCAG
TTCACTCCCAGTAACTCAGGATCTAGATGTCACTCCAGACCCGGTAGTCACAGTAAAAGCACTTAGTTTAA
GTCCACAAGCAAAACCCCTTGGCTATGAAGGCGTAGCCTTTTATCTGCCAACTGCCCAAAAAGACGACATT
GAAATGATCGTCTCTGAAGTTGGTGAAGAAGCAAACTGGAAAATGTGTGCCAATGCACATTTTGATAAGAC
TCATACATCAGCAAAGGCTCATCTCAGATGGGGTGCAGAGTGTCAAACATATGATGTTTCTATGAGAGTGT
CCGCAGCGTGCCAACCAGAGTCCAAACCATCTATAAGCACAAAGATTAACTGGGGGACTCTGCCCTCAGTA
TTCACAACAGTTGGTCAAATAGTTCAAGAGTATGTACCTGGCGTGTCTTACATTATGGGTTTCTACCAGAA
AAAGGAGGAAAACCCAGAACGGCAGGCATCTGTCATCGTTGTAGCATCCTCACCAGAGACCTTTGACCTGA
AAGTGAAAATTCCAGAGCGAACTATCTACAAAAAGAAAATTCCCTCACCAATTGAACTTTTGGGGATCGAA
GCTGCAAATCTCACCATGTCAACTTAA

RbD / RbM

G) *vtg1*-KO

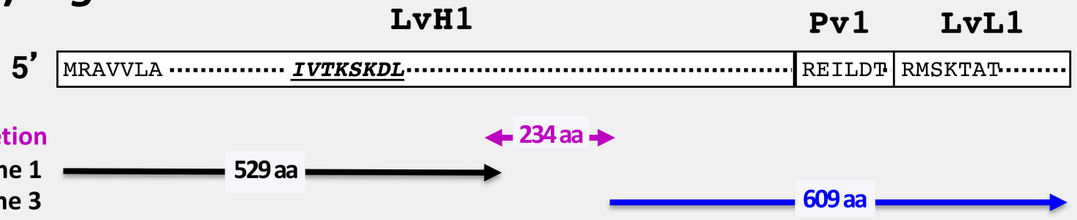

Frame 1 5′>3'

|MRAVVLALTVALVACQQFNLVPEFAHDKTYVYKYEALLLGGLPQEGLARAGIKVSSKVLISATTENTYLMKLMD
PLLYEYAGTWPKDPFVPATKLTSALAAQLQIPIKFEYANGVVGKVFAPAGVSPTVMNLHRGILNILQLNLKKTQN
IYEMQEAGAQGVCRTHYVI**NEDPKANHIIVTKSKDLSHCQERIMKDVGLAYTERCAECTERVKSLIETATYNYIM**
KPADNGALIAEATVEEVYQFSPFNEIHGAAMMEAKQTLAFVEIEKTPVVPIKADYMPRGSLQYEFATEILQTPIQ
LMKISDAPAQIVEVLKHLVSNNKDMVHDDAPFKFVQLVQLLRVASLEKIEAIWSQFKDKPVYRRWLLDALPAVGT
PVIIKFIKEKFLAGEFTTPEFIQTLVIALQMVTADPETIKMTASLATHEKFATIPALREVVMLGYGSLIAKYCVA
VPTCPAELLRPIHEIATEAISKNDIPEITLALKVMGNAGHPSSLKPIMKLLPGLRTAANALPIRVQVDAI<234aa>
WLLDPNHVHC-RRLLKLCRKELPSSMLNLCLQLKCVASCQLQLVCPWSSVGTLLQLLLQVSMFRPPLHLLSLRNW
SP-LMSN-RRLMFSSKLKLDQVLLSRHLL-WELTLPSSKLLLWQEERSVQLHPEKWQQEQTFSRATTRWRLCLLN
FLNTLLLQALRLMPWSETLKITVLKGLFPWYLNCLCKTPRHLMLVICHLRCHLLLQ-ELLLHLTEPSVMLSHTLK
SRDVLRCTLTMLLLSEIPLFST-LDTTQSVLQWQELKVLQLKDWSLKFKLVLELLRGLLSKSTSLMMILQKDRLS
C-N-GKSWTLKLKMHLFLLKAAAVVTVAAAAAAAPALAPAQAQAQVQVQVQAQAPLCPALVCLRLPPSLSLSGNS
TKIGTWHTIAPQRILAVEVLQLALNKCRNRIDSLEMIFHLFLLSSPVLLELTRSFWATNWLLTLTNQLQECN--F
PPLLKTTT-RSVLMVLC-ASTKLLASFLGVRSANSMQSLLKLKLVSWVNSLLHV-KWNGRDCQ-LSPPMPKSWVN
TSLQQLTTQDSGLNEQRTARKRLN-LQPCHLRGP-ISLLGFQRSQCQKGIFIFLSLFPSIQTELFPLRPMKTFSP
GSRNISRRN

Frame 2 5′>3'

-ELLCLP-L-PSWHVNNSTLFLSLPMIRPMCTSMRLCFWEVFLKKVWPEQVLKSAARFSSVPRQRIPT--SLWIL
YSTSMLALGPRIHLFLLLSSPQHWLLSFRFPSSLSMLMVWLARFLPQQESLLQS-TCTEVSSTSFSSTSRRPRTS
TRCKRLELRECAEHTMSSMRIQRPTTLL-QSLKI-ATARRES-RMLAWHTLRGVLNAQRGSRV-LKLQLITTS-N
QLTMVH-SLRQQLRKCISSHPSMRFMVLQ-WKQNKPWLLLRLRRPLSFQSKLITCPVDPCSTSLQLRFFRPPFNS
-RSVMHLPRLSRS-STWFQTIKTWSMMMLHSSLFSLSSSCVLPPWRKLRLSGLSSRTNQFTGAGFWMLFLLLVHQ
SL-NSSRRSSWLVNLPLPSSFRLL-LLCKWSLLILKPLK-QLVWLLMRNLPQSQLCVKLSCLDMVP-LPNTVLQF
PLALLSSSGPSTRSPQRPFLRMTFLKSLWL-KLWAMLVTLQVLSQS-SSFLD-ELQLMLCPLESRLM<234aa>PY
GYWTQTTCTAEGGS-SFAGRSCLPVC-TFACS-SASHLANCSWCAHGVQLVHCCSCCCKCQCSGHHYTCSP-EIG
VHDL-ATKED-CSVPS-S-TKCCSPDICCDGS-HCLHPSCCYGKRKDPYNCTRKSGSKSRHSQGQLQGGGSAC-T
S-THCFCKL-DLCRGQKH-RSQC-KVCSPGT-IVSAKLPGILCW-FVI-DVICCFSKSSCSI-QNPLLCCPIH-N
QGMC-GALSQCCFYQKFHSFLHNWTPLSPCCSGKS-RSCS-KTGV-SSSWS-SC-EAC-ANQHH---YSRRTGFL
VETEGNPGH-S-KCTCFF-KQQQS-QSQQQQPQHQH-HQLKLKLKFKFKFKLKLLYVQLSYV-DCHHH-AFQEIP
QRSVLGTP-RHKGY-QWKCCS-L-TNAETE-IPWK-YSTCFCYHRPCC-S-PEASGLPTGCLL-QTNCKSATDSF
LHC-KRQHEDLC-WCSVEQAQSYWQVFLGCGVQTVCSLC-S-SWCPG-IPCCTSRSGMGETANNCHHLCQKAG-T
HPYSSLRHRIQV-TSNEQRERD-TDCSLAISEVLEYHC-DSRDHNVKKGYLSSCRCSHQSRRNFFH-DL-RLSRL
DPEIYQGGI

Frame 3 5′>3'

ESCCACLDCSPRGMSTIQPCS-VCP--DLCVQV-GSAFGRSSSRRSGQSRY-SQQQGSHQCHDREYLPDEAYGSS
TLRVCWHLAQGSICSCY-AHLSTGCSASDSHQV-VC-WCGWQGFCPSRSLSYSHELAQRYPQHPSAQPQEDPEHL
RDARGWSSGSVQNTLCHQ-GSKGQPHYCDKV-RSEPLPGENHEGCWLGIH-EVC-MHREGQESD-NCNL-LHHET
S-QWCTDR-GNS-GSVSVLTLQ-DSWCCNDGSKTNLGFC-D-EDPCRSNQS-LHAPWIPAVRVCN-DSSDPHSTH
EDQ-CTCPDCRGPEALGFKQ-RHGP--CSIQVCSACPALACCLLGEN-GYLVSVQGQTSLQALASGCSSCCWYTS
HYKIHQGEVPGW-IYHSRVHSDSCDCSANGHC-S-NH-NDS-FGYS-EICHNPSSA-SCHAWIWFPDCQILCCSS
HLPC-APQAHPRDRHRGHF-E-HS-NHFGSESYGQCWSPFKS-ANHEAPSWTENCS-CFAH-SPG-CH<234aa>M
ATGPKPRALLKEALKALQEGVAFQYAKPLLAAEVRRILPTAVGVPMEFSWYTAAVAAASVNVQATITPALPEKLE
SMTYEQLKKTDVQFQAEARPSVALQTFAVMGVNTAFIQAAVMARGKIRTIAPGKVAARADILKGNYKVEALPVEL
PEHIASASFETYAVVRNIEDHSAERSVPLVPELSLQNSQASYAGDLSSEMSSVASVRAPAPFDRTLCYAVPYIEI
KGCVEVHSHNAAFIRNSTLFYIIGHHSVRAAVARAEGPAVERLEFEVQVGPRAAERLVKQINIIDDDTPEGQAFL
LKL|REILDTEAKNAPVSSESSSSRNSRSSSSRSTSTSTSSSSSSSSSSSSSSSSSMSSS|RMSKTATIIEPFRK
FHKDRYLAHHSATKDTSSGSAAASFEQMQKQNRFLGNDIPPVFAIIARAVRADQKLLGYQLAAYFDKPTARVQLI
VSSIAENDNMKICADGALLSKHKVTGKFSWGAECKQYAVFAKAEAGVLGEFPAARLEVEWERLPIIVTTYAKKLG
KHILTAAYDTGFRFERATNSEKEIELTAALPSQRSLNIIARIPEITMSKRDIYLPVAVPINPDGTFSIETYEDFL
AWIQKYIKEE-

H) *vtg3*-KO

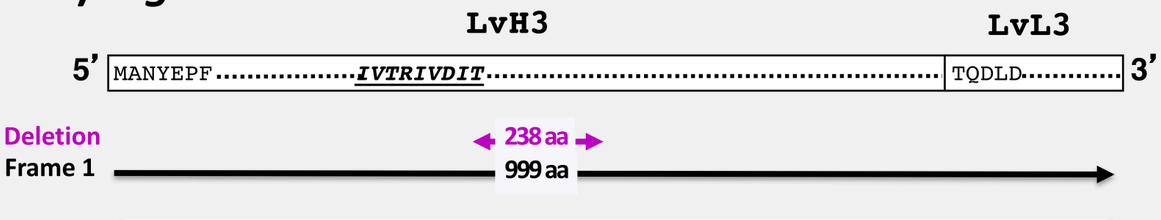

Frame 1 5′>3'

|MANYEPFLNSKKTYEYKYEGLVQVGRELPHLVESALKLRCTFKIIGESPHTFVLQVSNVDFEDFNGIPGKSVFS
PSKNITKHLSAEISQPIIFEYSKGQITDIRTAPGVSNTVVNIVRGILGFLQVTVKTTQSFYELIELGIHGLCQSS
YTV**DEDSNAKELIVTRIVDITNCQQPASLYRGMALAPEDKLSKQRGESVVSTVKHTYTVKSTADGGQITKAFAQE**
RQYFSPFNVKGGNF <238aa> LKTLLKFLPGYSNGAEKLSTRVQGAAVQAFRLLASRASHSVQDIVLNLFVQKHL
PAEIRMLACIVLLETKPSTALISVVSEVLLEEADLQVASFSYSLLKGFAKSRTPDNQHLSIACNIAMKILTRKLG
HLSYRYSKNLHFDWFHDDFLFGTSADVYMLQNESPIPTKLMLKGKFHFIGRILQFLEFGIRADGLKDLFAGKIPE
LTKDLGISDLASILKILSNWQSLPKDKPLLTAYARVFGQEAFLMDVSRDSVQSIIKSFSPSAGKESKVWERIQDV
QKGTSWHWTKPHLVYEARFIQPTCLGLPVEISKYYSVVNAVTMKAKAEINPPPKEHLGELLSSDISMQTDGFIGV
TKDHFLFHGINTDLFQCGTELKSKVSMGLPWAFDLKINPKEQTYEMNLTPSKSVTELFSVSSNVYAVLRNIEDPT
SSKITPMMPETGESWQGVPLRMLPPLRDEQTKKSGMKFRQCAEAKIYGTALCIEAEAKRAHYLHEYPLYYLLGDT
HFSYSLEPAKDAKPIEKIQIQVSASRQHPSVMSGMVNLNQRVFKETRDENTSCEERKTSSSLPV|TQDLDVTPDP
VVTVKALSLSPQAKPLGYEGVAFYLPTAQKDDIEMIVSEVGEEANWKMCANAHFDKTHTSAKAHLRWGAECQTYD
VSMRVSAACQPESKPSISTKINWGTLPSVFTTVGQIVQEYVPGVSYIMGFYQKKEENPERQASVIVVASSPETFD
LKVKIPERTIYKKKIPSPIELLGIEAANLTMST-

Frame 2 5′>3'

WQIMSLF-TRKKHTSINMKDWYKWDGNCHTWLNQR-N-GALLKSLESHHTPLSFRSQM-TLKILMAYLGKVSSAL
PKTSLSICLPRSASQSFLNILKDKLLTFAQHLESQTQL-IL-GGSLDFYKSRSKPHKVFTN-LSWEFMVCVRAVT
LLMKTLTQKS---HELLISPTVNSQHLCTEVWLLHLKTNLANREAKALFPL-NTPTQ-SPQQTVVRLLKHLLRSA
NISLRSM-REETS<238aa> SRLSSSSFLDTPMELKNFPPECRELQSKHLGCLQAEPPTVYRILS-TSSYRNIYQ
LKSACWPA-FF-RPSRPQL-FQ--VRSF-KRLICRLPVSPTLCSKALPSPVPLIINIYLLPVILP-RF-PVNLAT
-VTATARTCTLTGSMMTFYLGHLLMFICFRMKVPSPQNLCLRENFISLGEYCNFLSLVSVQMDSKICLLEKSQNS
RKI-ESAIWLPY-KFSLTGRAYQKTSLF-QLMQEFLDRKPF-WM-AETQFKAS-SLSVLLQERRVKFGKGFKMFR
KGLHGTGLSRILCMRLGSYSRHVWVSQLKSANIIP--MLLQ-KQKLK-ILLQRNIWVNC-AQTFPCRQMALSA-Q
RIIFSSMESTLIFFSVELS-KVRFQWACRGHLT-K-IRKSKRMK-T-LQANRSPNYFQSVLMCMLF-ETLKTQPH
LK-HP-CLRQGSPGRVCL-ECYPL-GMNRPKNLE-NSGNVLKPKFMELHSALRQKPNVHTIFTNILCITYWVILT
FHTV-NQQRMQNPLKKFRFRSLPADNILQ--VEW-ISTKGYLRRQEMRTPPVRNAKHPVHSQ-LRI-MSLQTR-S
Q-KHLV-VHKQNPLAMKA-PFICQLPKKTTLK-SSLKLVKKQTGKCVPMHILIRLIHQQRLISDGVQSVKHMMFL
-ECPQRANQSPNHL-AQRLTGGLCPQYSQQLVK-FKSMYLACLTLWVSTRKRRKTQNGRHLSSL-HPHQRPLT-K
-KFQSELSTKRKFPHQLNFWGSKLQISPCQL

Frame 3 5′>3'

GKL-AFSELEKNIRV-I-RIGTSGTGTATPG-ISAETEVHF-NHWRVTTHLCPSGLKCRL-RF-WHTWEKCLQPF
QKHH-ASVCRDQPANHF-IF-RTNY-HSHSTWSLKHSCEYCEGDPWIFTSHGQNHTKFLRTN-VGNSWFVSEQLH
C--RL-RKRVDSNTNC-YHQLSTASIFVQRYGSCT-RQT-QTERRKRCFHCETHLHSEVHSRRWSDY-SICSGAP
IFLSVQCKGRKLP <238aa> QDSPQVPSWILQWS-KTFHQSAGSCSPSI-AACKQSLPQCTGYCLKPLRTETFTS
-NPHAGLHSSSRDQAVHSSDFSSK-GPSRRG-SAGCQFLLLSAQRLCQVPYP--STSIYCL-YCHEDSNP-TWPL
ELPLQQEPAL-LVP--LFIWDIC-CLYASE-KSHPHKTYA-GKISFHWENTAIS-VWYPCRWTQRSVCWKNPRTH
ERFRNQRFGFHIENSL-LAEPTKRQASFDSLCKSFWTGSLFNGCKQRLSSKHHKVFQSFCRKGE-SLGKDSRCSE
RDFMALD-AASCV-GSVHTADMSGSPS-NQQILFRSKCCYNESKS-NKSSSKGTSG-TAKLRHFHADRWLYRRDK
GSFSLPWNQH-SFSVWN-AEK-GFNGPAVGI-PENKSERANV-NELDSKQIGHRIIFSQF-CVCCFEKH-RPNLI
-NNTHDA-DRGVLAGCASENVTPFKG-TDQKIWNEIQAMC-SQNLWNCTLH-GRSQTCTLSSRISSVLLTG-YSL
FIQFRTSKGCKTH-KNSDSGLCQQTTSFSNEWNGESQPKGI-GDKR-EHLL-GTQNIQFTPSNSGSRCHSRPGSH
SKST-FKSTSKTPWL-RRSLLSANCPKRRH-NDRL-SW-RSKLENVCQCTF--DSYISKGSSQMGCRVSNI-CFY
ESVRSVPTRVQTIYKHKD-LGDSALSIHNSWSNSSRVCTWRVLHYGFLPEKGGKPRTAGICHRCSILTRDL-PES
ENSRANYLQKENSLTN-TFGDRSCKSHHVNL

S1 Fig. Location and character of mutations introduced by CRISPR/Cas9 in zebrafish *vtgs*. A-B) Location on genomic DNA. Schematic representations of the intron/exon structure of zebrafish *vtg1* (representative of type-I *vtgs*) and *vtg3* are given at the top of panels A and B, respectively. Horizontal line segments indicate introns and filled gold boxes indicate exons. Exons bearing CRISPR/Cas9 target sequences are indicated by large blue arrowheads pointing upwards to the target name (sg11, sg12, and sg13 for *vtg1*; sg31, sg32, and sg33 for *vtg3*). Horizontal dashed lines bearing dual arrowheads indicate regions where mutations were introduced, with the size of deletions in bp given below the arrows (1281 bp and 1181 bp for *vtg1*-KO and *vtg3*-KO, respectively). The lower sections of panels A and B show Clustal Omega alignments for partial genomic sequences of the *vtg1* and *vtg3* genes, respectively, covering regions where Cas9 introduced targeted mutations. Sequences of undisturbed wild type alleles are labeled *vtg1*+/+ and *vtg3*+/+, and sequences of homozygous mutated alleles are labeled *vtg1*-/- and *vtg3*-/-, respectively. Dashes were introduced to illustrate regions where deletions occurred in the *vtg1*-/- and *vtg3*-/-sequences. Nucleotide positions are indicated by numbers on the right and asterisks indicate nucleotide identity. Target sequences are enclosed in blue-shaded boxes emphasized by blue arrowheads on the right. Intron sequences are given in dark gray font enclosed in light gray filled frames and are labeled by Intron on the right with the same formatting. Exons are shown in regular black font and labeled on the right with exon numbers (e.g. Exon 6, 7, 8...). Exons bearing the target sites are also labeled with the target name below in parenthesis (e.g. Exon 14 (sg12)). **C-D)** Location on mRNA**.** The deleted region of mRNA is indicated in the sequence by magenta text showing the number of deleted nucleotides (703 bp *vtg1* and 714 bp for *vtg3*) enclosed by magenta angle brackets; flanking nucleotides that come together to form a new codon are underlined in magenta. **E-F)** Location on predicted cDNA. Nucleotide sequences targeted by sgRNAs for Cas9 editing and present in the predicted transcript are framed in blue-shaded boxes. The deleted region of the transcript is indicated in the sequence by magenta text showing the number of deleted nucleotides enclosed by magenta angle brackets, with flanking nucleotides that come together to form a new codon underlined in magenta (see also **S2 Fig**). The sequence encoding the Vtg receptor-binding domain (***RbD***) on the LvH of the respective Vtg (see **G-H**, below) is shown in italic typeface with the sequence encoding its critical, short receptor-binding motif (***RbM***) being additionally underlined. **G-H)** Location on predicted polypeptide sequence. Yolk protein domain models of Vtg1 (representative of zebrafish type-I Vtgs) or Vtg3 are pictured in 5' > 3' orientation above each panel. Contiguous white horizontal bars represent lipovitellin heavy and light chain (LvH, LvL) and

phosvitin (Pv) domains of the respective Vtg (Vtg3 lacks a Pv domain) that are labeled with their abbreviation above in large bold type. Sequences within these bars set in normal type represent the N-terminus of each yolk protein domain, the starting points of which are indicated, when present, by vertical bars in the predicted polypeptide sequences shown below. Predicted sequences arising from three frames of 5' > 3' translation performed using the Expasy translate tool (available online at https://web.expasy.org/translate/) are shown. Predicted products of open reading frames are highlighted in light gray, start codon products (methionine, **M**) are shown in bold green type, and stop codons are indicated by red dashed lines (**-**). The locations of deletions are indicated by magenta text showing the number of deleted amino acids (aa) enclosed by angle brackets. Residues encoded by nucleotide sequences targeted by sgRNAs for Cas9 editing are framed in blue-shaded boxes. Short sequences that were employed as epitopes to develop Vtg domain-specific antibodies against zebrafish (zf) Vtg1-LvH (anti-zfLvH1) and Vtg3-LvL (anti-zfLvL3) are indicated by boxed text in the respective LvH and LvL sequences, with their location also highlighted by black arrows labeled with the epitope names given by vertically-oriented text in the panel margins. The 85-residue Vtg receptor-binding domain (***RbD***) and the critical 8-residue Vtg receptor-binding motif (***RbM***) located within this domain, which were identified by Li et al. (2003) in the LvH domain of blue tilapia (*Orechromis aureus*) VtgAb, are shown in the polypeptide sequences in boldface italic type, with the ***RbM*** sequence being additionally underlined and also shown in the yolk protein domain map above. The location of these sequences is also highlighted by black arrows labeled with **RbD/RbM** as vertically-oriented text in the panel margins. For *vtg1*-KO (panel G), the diagram below the yolk protein domain model shows the relative location of the 234 aa deletion introduced by CRISPR/Cas9 (double headed magenta arrow), the 529 aa sequence product of the contiguous open reading frame 1 (right pointing black arrow), which is terminated by a premature stop codon arising from a frameshift introduced by the deletion (see **Fig 2A**), and the 609 aa sequence product of the contiguous open reading frame 3 (right pointing blue arrow), which initiates just after the deletion. For *vtg3*-KO (panel H), the diagram below the yolk protein domain model employs the same symbols and color coding and shows the relative position of the in-frame 238 aa deletion introduced by CRISPR/Cas9 (see **Fig 2B**), and the remaining 999 aa sequence product of the contiguous open reading frame 1.

S1 Table. Targets, primers and probes utilized in *vtg1*-KO and *vtg3*-KO studies. Target oligo an screening primer names are given according Figure 1. CRISPR recognition NGG motifs are highlighted by bold typeface on sequences. Position of primers, target sites and probes on vitellogenin (Vtg) yolk protein (YP) domains are given on the far right columns.

Target Oligos	**Sequence**	**Vtg YP domain**
sg11_Rv	**GGT**TGAGCTGAAGGATGTTG	LvH
sg12_Rv	**GGC**AGCATCATTGATCATAT	LvH
sg13_Fw	**GGA**GGCTCTTAAAGCTTTGC	LvH
sg31_Rv	**GGG**CTGAAGACACTTTTCCC	LvH
sg32_Fw	**GGG**AGGAAACTTCCGAATGT	LvH
sg33_Fw	**GGT**CCTTGCGCTGAAGTCCT	LvH
Screening Primers	**Sequence**	**Vtg YP domain**
11_Fw	GAAGCAACACTTAATAAGCAATGG	LvH
11_Rv	CTTATTACCTCTGTGCATTCAGC	LvH
12_Fw	CTTATGAGCCGCAAACTGGA	LvH
12_Rv	TGTGAGTATCAGTCACAGTTCAA	LvH
13_Fw	AACTGGAGGAATCCATGAAGC	LvH
13_Rv	AGGTGTAATGGTGGCCTGAA	LvH
31_Fw	TATGAAGGATTGGTACAAGTGGG	LvH
31_Rv	AGGATCCCCCTCACAATATTCA	LvH
32_Fw	TGATGAAGACTCTAACGCAAAAGA	LvH
32_Rv	TTATACATCAGGTTGCCTCTGC	LvH
33_Fw	AGTAAATCCCATCCTCTCCTGTG	LvH
33_Rv	TTTAGTGCGCAACCAGATGAA	LvH
qPCR Primers (SybrGreen)	**Sequence**	**Vtg YP domain**
vtg1_Fw	GATTAAGCGTACACTGAGACCA	LvH
vtg1_Rv	AGCCACTTCTTGTCCAAATACT	
vtg2_Fw	TGCCGCATGAAACTTGAATCT	Ct
vtg2_Rv	GTTCTTACTGGTGCACAGCC	
vtg3_Fw	GGGAAAGGATTCAAGATGTTCAGA	LvH
vtg3_Rv	ATTTGCTGATTTCAACTGGGAGAC	
vtg4_Fw	TCCAGACGGTACTTTCACCA	LvL
vtg4_Rv	CTGACAGTTCTGCATCAACACA	
vtg5_Fw	ATTGCCAAGAAAGAGCCCAA	LvH
vtg5_Rv	TTCAGCCTCAAACAGCACAA	
vtg6_Fw	TTTGGTGTGAGAACTGGAGG	LvH
vtg6_Rv	CCAGTTTGTGAGTGCTTTCAG	
vtg7_Fw	TTGGTGTGAGAACTGGAGGA	LvH
vtg7_Rv	TTGCAAGTGCCTTCAGTGTA	
rpl13a_Fw	TCTGGAGGACTGTAAGAGGTATGC	N/A
rpl13a_Rv	AGACGCACAATCTTGAGAGCAG	
eif1a_Fw	CTGGAGGCCAGCTCAAACAT	N/A
eif1a_Rv	ATCAAGAAGAGTAGTACCGCTAGCATTAC	
18S_Fw	TCGCTAGTTGGCATCGTTTATG	N/A
18S_Rv	CGGAGGTTCGAAGACGATCA	
qPCR Primers and probes (TaqMan)	**Sequence**	**Vtg YP domain**
vtg1_Fw	CCATGAAGCTCTCCTAAAATCTC	LvH
vtg1_probe	[FAM]CACTGAGAGCAGTCACAAACTGGAAGG[BHQ1]	
vtg1_Rv	TAGGCTGATGCTAGTGGTTTATC	
vtg2_Fw	GGCTGATGGTTTGTCACTTTATG	Ct
vtg2_probe	[FAM]TTGCCAATGGTGACTGGAAGATCCAAG[BHQ1]	
vtg2_Rv	TGTCCCTTCATCCAGTCTGC	
vtg3_Fw	GCGTGTCTTACATTATGGGTTTC	LvL
vtg3_probe	[FAM]CGGCAGGCATCTGTCATCGTTGTAG[BHQ1]	
vtg3_Rv	TCACTTTCAGGTCAAAGGTCTC	
vtg4_Fw	TAGCTGGTGAATTTACAACTCCC	LvH
vtg4_probe	[FAM]CTCTGCAAAGGGTTTCTGCTGATCTTG[BHQ1]	
vtg4_Rv	GCATGGCAACTTCACGCAGA	
vtg5_Fw	AGGAACATTGCCAAGAAAGAGC	LvH
vtg5_probe	[FAM]AGGCTGAACCCTCAGTGGCTCTCAT[BHQ1]	
vtg5_Rv	GTCCTCAATGCTCCAGCAAG	
vtg6_Fw	GCCAAAAATTGTCACCACCTATG	LvL
vtg6_probe	[FAM]CTTAATGCAGCTTATGACACAGGATTCAGG[BHQ1]	
vtg6_Rv	TGACGGGGAGGTAAATATCCC	
vtg7_Fw	TATTCAGACTCTCGTGGTTGCTTT	LvH
vtg7_probe	[FAM]CAACGCATGAGAAGTTCACCACAATCC[BHQ1]	
vtg7_Rv	GGTAATCTCGTGGATGGGCT	

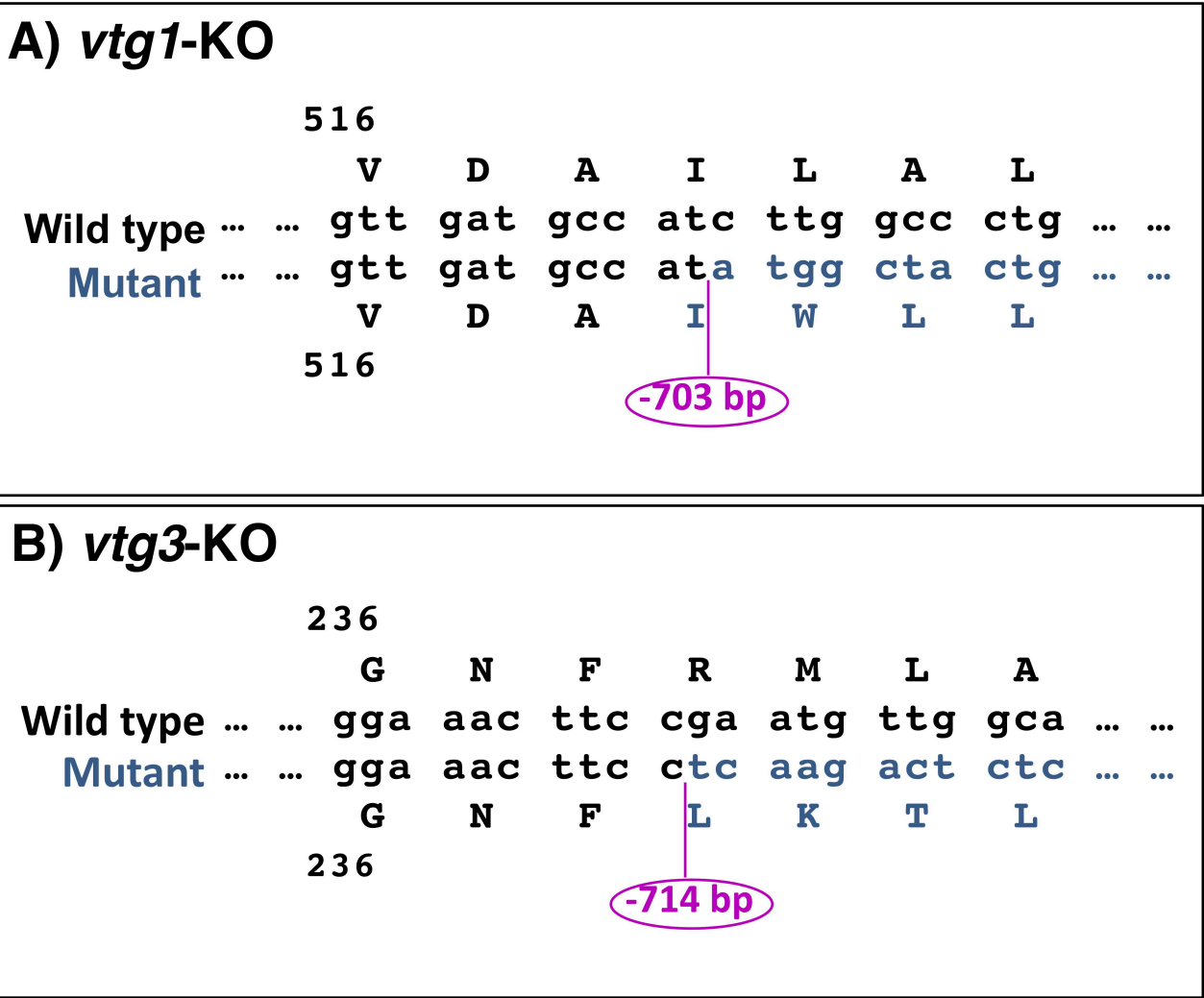
A) vtg1-KO
516
V D A I L A L
Wild type … … gtt gat gcc atc ttg gcc ctg … …
Mutant … … gtt gat gcc ata tgg cta ctg … …
V D A I W L L
516
-703 bp
B) vtg3-KO
236
G N F R M L A
Wild type … … gga aac ttc cga atg ttg gca … …
Mutant … … gga aac ttc ctc aag act ctc … …
G N F L K T L
236
-714 bp

S2 Fig. Location and consequence of deletion mutations introduced by CRISPR/Cas9 into zebrafish *vtgs*. A) *vtg1*-KO. The 703 bp deletion introduces a frame shift at residue 519, changing the codon without altering the encoded amino acid (isoleucine, I). This frame shift results in the appearance of a premature stop codon after 10 additional residues (not shown, see **Fig 2A** for details). **B) *vtg3*-KO.** The 714 bp deletion alters the codon encoding residue 239, resulting in the substitution of leucine (L) for arginine (R) at this position, but it does not otherwise alter the remainder of the Vtg3 polypeptide (see **Fig 2B**).